

Biophysical regulation of actin cytoskeleton remodeling in adherent cells

Citation for published version (APA):

Tamiello, C. (2015). *Biophysical regulation of actin cytoskeleton remodeling in adherent cells*. [Phd Thesis 1 (Research TU/e / Graduation TU/e), Biomedical Engineering]. Technische Universiteit Eindhoven.

Document status and date:

Published: 03/09/2015

Document Version:

Publisher's PDF, also known as Version of Record (includes final page, issue and volume numbers)

Please check the document version of this publication:

- A submitted manuscript is the version of the article upon submission and before peer-review. There can be important differences between the submitted version and the official published version of record. People interested in the research are advised to contact the author for the final version of the publication, or visit the DOI to the publisher's website.
- The final author version and the galley proof are versions of the publication after peer review.
- The final published version features the final layout of the paper including the volume, issue and page numbers.

[Link to publication](#)

General rights

Copyright and moral rights for the publications made accessible in the public portal are retained by the authors and/or other copyright owners and it is a condition of accessing publications that users recognise and abide by the legal requirements associated with these rights.

- Users may download and print one copy of any publication from the public portal for the purpose of private study or research.
- You may not further distribute the material or use it for any profit-making activity or commercial gain
- You may freely distribute the URL identifying the publication in the public portal.

If the publication is distributed under the terms of Article 25fa of the Dutch Copyright Act, indicated by the "Taverne" license above, please follow below link for the End User Agreement:

www.tue.nl/taverne

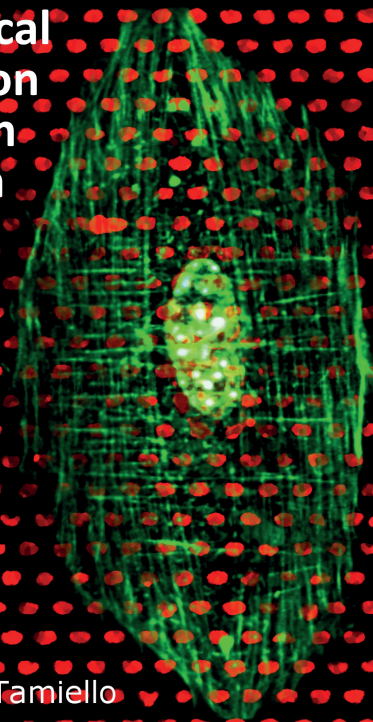
Take down policy

If you believe that this document breaches copyright please contact us at:

openaccess@tue.nl

providing details and we will investigate your claim.

Biophysical
regulation
of actin
cytoskeleton
remodeling
in
adherent
cells



Chiara Tamiello

Biophysical regulation of actin cytoskeleton remodeling in adherent cells

Chiara Tamiello

Biophysical regulation
of actin cytoskeleton remodeling
in adherent cells

Chiara Tamiello

A catalogue record is available from the Eindhoven University of Technology Library
ISBN: 978-90-386-3895-9

Copyright © by Chiara Tamiello, 2015

All rights reserved. No part of this book may be reproduced, stored in a database or retrieval system, or published, in any form or in any way, electronically, mechanically, by print, photo print, microfilm or any other means without prior permission by the author.

Cover design by Chiara Tamiello.

Printed by Proefschriftmaken.nl | | Uitgeverij BOXPress

The work described in this thesis was funded by NanoNextNL.

Financial support by the Dutch Heart Foundation for the publication of this thesis is gratefully acknowledged.

Biophysical regulation of actin cytoskeleton remodeling in adherent cells

PROEFSCHRIFT

ter verkrijging van de graad van doctor
aan de Technische Universiteit Eindhoven,
op gezag van de rector magnificus, prof.dr.ir. F.P.T. Baaijens,
voor een commissie aangewezen door het College voor Promoties
in het openbaar te verdedigen
op donderdag 3 september 2015 om 16.00 uur

door

Chiara Tamiello

geboren te Rovigo, Italië

Dit proefschrift is goedgekeurd door de promotoren en de samenstelling van de promotiecommissie is als volgt:

voorzitter:	prof. dr. P.A.J. Hilbers
1 ^e promotor:	prof. dr. ir. F.P.T. Baaijens
2 ^e promotor:	prof. dr. C.V.C. Bouten
copromotor:	dr. J.L.V. Broers (Maastricht University)
leden:	prof. dr. V.S. Deshpande (University of Cambridge)
	prof. dr. G.H. Koenderink (VU University Amsterdam)
	prof. dr. K. Ito
adviseur:	dr. C.M. Sahlgren

Contents

<i>Contents</i>	<i>i</i>
<i>Summary</i>	<i>v</i>
Chapter 1 General introduction	1
<i>Preface</i>	2
<i>Understanding cellular orientation responses to complex biophysical cues</i>	3
<i>The structural mechanotransduction pathway: a physical connection between the extracellular environment and the genome</i>	5
Interconnection between the extracellular environment and the actin cytoskeleton.....	5
Interconnection between the actin cytoskeleton and the nucleus	7
<i>Cellular orientation response to substrate anisotropy and cyclic strain</i>	10
Cellular orientation response to substrate anisotropy.....	10
Cellular orientation response to cyclic uniaxial strain	15
Cellular orientation response to combined substrate anisotropy and cyclic uniaxial strain	20
<i>Outlook and thesis outline</i>	22
<i>References</i>	25
Chapter 2 Competition between cap and basal actin fiber orientation in cells subjected to contact guidance and cyclic strain	35
<i>Introduction</i>	36
<i>Results</i>	37
Modular setup	37
Contact guidance dictates stress fiber orientation independent of micropost stiffness under static conditions	38
Competition between contact guidance and strain avoidance determines stress fiber orientation	41
Distinct responses of basal and perinuclear actin cap fibers to contact guidance and cyclic strain explain the competition between these cues	41
<i>Discussion</i>	45
<i>Materials and Methods</i>	48
Cell cultures	48
Micropost design and fabrication	48
Micro-contact printing on microposts	49
Loading protocol	49
Immunofluorescence labelling.....	50
Microscopy and image analysis	50
Quantification of cell and nuclear orientation.....	50
Quantification of stress fibers orientation.....	50
Data analysis	51
<i>Acknowledgments</i>	51
<i>References</i>	52
Chapter 3 Cellular strain avoidance is regulated by a functional actin cap	55

Contents

<i>Introduction</i>	56
<i>Results</i>	58
Topographical cues induce similar actin stress fiber alignment and focal adhesion maturation in normal and <i>Imna</i> -lacking fibroblasts.....	58
Impaired strain avoidance response of <i>Imna</i> -lacking fibroblasts.....	62
Alpha-actinin 4 does not re-localize along stress fibers in <i>Imna</i> -lacking fibroblasts but accumulates at focal adhesions upon topographical cues and cyclic uniaxial strain.....	65
Cell reorientation is facilitated by actin cap presence and rounder cell morphology.....	66
<i>Discussion</i>	68
<i>Materials and Methods</i>	70
Cell culture.....	70
Micropost design and fabrication.....	71
Fibronectin micro-contact printing on microposts.....	71
Static experiments.....	71
Loading protocol for cyclic uniaxial strain in dynamic experiments.....	71
Immunofluorescence studies.....	72
Microscopy.....	72
Quantification orientation actin stress fibers.....	72
Cap anisotropy quantification.....	73
Cell orientation and aspect ratio.....	73
Data analysis and statistics.....	73
<i>Acknowledgments</i>	74
<i>References</i>	75
Chapter 4 Soft substrates normalize nuclear morphology and prevent nuclear rupture in fibroblasts from a laminopathy patient with compound heterozygous LMNA mutations.....	79
<i>Introduction</i>	80
<i>Results</i>	81
Nuclear shape of <i>LMNAMut</i> is abnormal on stiff substrates but preserved on soft substrates.....	81
<i>LMNAMut</i> cells show a defective actin cytoskeleton on stiff substrates but not on soft substrates.....	84
Disruptions of the actin-cytoskeleton and trypsinization partially normalize nuclear abnormalities in <i>LMNAMut</i> cells.....	87
Cellular compartmentalization in <i>LMNAMut</i> cells is not compromised on soft substrates.....	89
Nuclear ruptures in <i>LMNAMut</i> cells increase with substrate stiffness, but are prevented on soft substrates.....	90
<i>Discussion</i>	93
<i>Materials and methods</i>	95
Cell cultures.....	95
Transfection for live-cell imaging.....	96
Coated polyacrylamide (PA) gels and glass substrates.....	96
Immunofluorescence labelling and imaging.....	97
Cytochalasin D treatment.....	98
Cell spreading assay.....	98
Image analysis.....	98
Live-cell imaging.....	98
Statistical Analysis.....	99

<i>Acknowledgments</i>	99
<i>References</i>	100
Chapter 5 General discussion	103
<i>Main findings of this thesis and implications for understanding interplay between cell cytoskeleton response and complex biophysical environments</i>	104
A model system capable of dissecting the effects of separate and combined topographical cues and cyclic strain	104
Cap and basal actin fibers have distinct response to combined cyclic strain and topographical cues.....	105
The actin cap is crucial for response to cyclic strain	106
Structural weakness of laminopathy cells can be rescued by soft culture substrates	108
<i>Methodological challenges</i>	109
Technological Challenges.....	109
Mimicking substrate stiffness.....	112
Biological Challenges	113
<i>Road towards the translation to tissue regeneration and therapeutic strategies</i>	114
A micropost model system for comprehensive mechanobiological studies	114
Actin cytoskeleton remodeling by biophysical cues for regenerative and therapeutic strategies.....	115
Towards an assay for laminopathy detection.....	116
<i>Outlook and future perspectives: where do we go from here?</i>	117
Studying actin cytoskeleton remodeling in 3D environments	117
Studying actin remodeling by live-cell imaging, using vital probes	118
Studying the roles of structural and biochemical mechanotransduction pathways in actin cytoskeleton remodelling.....	118
Linking actin remodeling to other sub-cellular structures.....	119
Studying actin remodeling with the support of computational models.....	119
<i>Conclusion</i>	119
<i>References</i>	121
<i>Acknowledgments</i>	125
<i>Curriculum Vitae</i>	127
<i>List of publications</i>	129

Summary

In the native environment, adherent cells are active entities exposed to a myriad of biophysical cues coming from the surrounding environment and resulting from the daily activities. Thanks to the structural continuity between the cellular interior and the extracellular environment, adherent cells are able to sense the signals coming from the biophysical cues and transduce them to the nucleus, where the cellular response is elaborated. Both cellular sensing and responding to biophysical cues are mediated by an entwined network of intracellular structures, among which the actin cytoskeleton plays a pivotal role. The actin cytoskeleton is a dynamic and well-organized network of fibers that, first, takes part in the signal transduction and, then, arranges and remodels itself to adapt to the physical and mechanical properties of the surrounding cellular environment. While a wealth of observations that describe actin cytoskeletal remodeling in response to the biophysical cellular environment is available, a deep and comprehensive understanding of actin cytoskeleton remodeling and consequent cellular behaviour is still lacking. Therefore, in this thesis, we aimed at getting a quantitative understanding of actin cytoskeleton remodeling in response to relevant biophysical cues such as topographical cues, cyclic strain and stiffness. This knowledge is of fundamental importance for regenerative strategies aimed to restore functionality of diseased or damaged tissues and organs.

For obtaining functional tissue through regenerative strategies such as biomaterial-based *in situ* tissue engineering approaches, it is crucial to achieve *in vivo*-like tissue organization and associated cellular alignment. Cellular alignment induced by the orientation of the actin cytoskeleton, has been shown to be invoked by environmental topography as well as cyclic strain. Topographical cues promote and guide actin cytoskeleton orientation along the direction of the anisotropy created by the topographical cues, a response called contact guidance. Cyclic uniaxial strain, instead, induces active reorientation of the actin cytoskeleton almost perpendicular to the strain direction, a phenomenon referred to as strain avoidance. In cardiovascular tissues both environmental topography and cyclic strain cues are presented to the cells simultaneously, while they invoke apparently competing orientation responses when applied along the same direction. In order to understand the driving cue for actin cytoskeleton remodeling, we investigated the mechanisms of actin orientation response to the combination of environmental topography and cyclic uniaxial strain. To this end, we developed a dedicated experimental model system made of elastomeric microposts capable of stimulating cells with both cues, separately and in combination. The analysis of the orientation response of myofibroblasts demonstrated that the sub-cellular organization of the actin cytoskeleton plays a discriminating role in determining the global orientation response of the cells when both topographical cues and cyclic uniaxial strain are applied along the same direction. The apical actin cytoskeleton running on top of the cell nucleus, named actin cap, responds by strain avoidance even in the presence of topographical cues, triggering a whole-cell strain avoidance response. Instead, the actin cytoskeleton present underneath the nucleus (basal actin fibers), continues to respond to the topographical cues by contact guidance only, neglecting the cyclic strain. From this, we concluded that the competition between topographical cues and cyclic uniaxial strain is due to the distinct response of actin and basal actin fibers, inducing opposed orientation responses.

Summary

Further, we explored the effects of normal and aberrant actin cytoskeleton formation in the cellular orientation response to topographical cues and cyclic uniaxial strain. For this study we considered cells without a functional actin cap (knock-out cellular models) as our experimental group and wild-type cells as our control. By studying the orientation response of the actin cytoskeleton of these cells to topographical cues and cyclic strain applied separately and in combination, we demonstrated that the presence of a functional actin cap is crucial for strain avoidance response but not for contact guidance. In the experimental group stimulated by topographical cues only, cells showed the expected response of contact guidance, indicating that absence of an intact actin cap does not compromise cellular sensing and response to environmental topography. However, cells without a functional cap showed impaired strain avoidance response in response to cyclic uniaxial strain. When both cues were applied simultaneously and along the same direction, the absence of the actin cap in the experimental group rendered knock-out cells insensitive to the cyclic strain stimulation. These cells continued to respond to topographical cues only, while wild-type cells showed tendency to respond by strain avoidance, as seen in their actin cap fibers. Importantly, the cells without a functional actin cap used in this study serve as model cells for the laminopathy diseases, a family of genetic disorders causing mechanically weakened cell phenotypes. Thus, translation of the obtained results to pathophysiological conditions is possible.

As a next step we focussed on the mechanically weakened and structurally impaired laminopathy cells. We hypothesized that the nuclear abnormalities observed in these cells could well relate to a high cytoskeletal tension and, thus, could be rescued by inducing a lower actin cytoskeleton tension, i.e. by culturing the diseased cells on soft substrates. Indeed, adherent cells develop growing cytoskeletal tension when cultured on stiff substrates due to the formation of highly organized and tensed actin stress fibers in their interior. To test our hypothesis, we examined the relationship between substrate stiffness and the development of nuclear abnormalities in dermal fibroblasts from a patient suffering from a laminopathy and healthy control cells across matrices of varying stiffness (from 3 to 80 kPa). Our data demonstrated that, in laminopathy cells, nuclear abnormalities and disruptions were only absent on the softest substrates, while in healthy cells they were absent on every substrate. The observation that nuclear abnormalities in laminopathy cells correlates with the stiffness of the culture substrate opens up new avenues for the interpretation of the pathogenesis of laminopathies, their diagnosis and potential therapeutic strategies.

In conclusion, this thesis demonstrates that accurate analysis of sub-cellular structures such as actin cap and basal actin fibers is of fundamental importance to understand and, ultimately, guide overall cell orientation response. Moreover, the relevance of a functional actin cap for normal cell orientation response to cyclic strain has been unravelled. Lastly, modulation of actin cytoskeletal tension by varying the stiffness of the culturing substrate has been shown to represent an interesting approach for protecting cells with reduced structural integrity from mechanical instability. The obtained fundamental knowledge is of particular relevance for application in (re)building and regenerating diseased or damaged tissues and for elaborating new therapeutic approaches. Key challenges for the future translation of our results to clinical research include investigating actin cytoskeleton behaviour by live-cell imaging in 3D *in vivo*-like environments and integrating the experimental knowledge with computational model of the actin cytoskeleton mechanoresponse.

Chapter 1

General introduction

The contents of this chapter are based on:

Tamiello,C., Buskermolen,A.B., Baaijens,F.P., Broers,J.L., & Bouten,C.V. Understanding cellular orientation responses to complex biophysical cues – the need for systematic, combinatorial approaches. *In preparation*.

Preface

Advances in tissue regeneration and therapeutic strategies rely on the comprehensive understanding of the interplay between cellular responses and the properties of the surrounding cellular environment. For cardiovascular regeneration, achieving controlled cellular organization is of utmost importance as this dictates biological and mechanical functioning of the whole tissue. To recapitulate the *in vivo* cellular organization, it is therefore crucial to have an in-depth understanding of the mechanisms regulating cell orientation, being this at the basis of a well-structured tissue organization. Recent advances in the understanding of cellular mechanotransduction have demonstrated that cellular orientation response is the result of the interaction between the cell and its complex biophysical environment. In particular, the anisotropy of the substrate and the cyclic strain exerted on the cells, have been demonstrated to influence cell orientation. However, despite a wealth of observations linking cellular orientation to the anisotropy or to the cyclic straining of the cellular environment, surprisingly little is known about the mechanisms governing cellular orientation responses to these cues.

Biophysical cues from the environment are continuously detected and transduced to the nucleus through entwined mechanotransduction pathways. Next to the signalling cascades capable of translating mechanical stimuli into biochemical signals, the structural mechanotransduction pathway made of an interconnected network of intracellular structures, can quickly pass information such as mechanical signals directly to the nucleus. This pathway is made of focal adhesions and the actin cytoskeleton. The ability of the actin cytoskeleton to continuously reorganize in response to biophysical stimuli renders it an important structure for numerous cellular processes, e.g. cellular organization and orientation.

This chapter provides the state-of-the-art knowledge on the structural mechanotransduction pathway of adhesive cells, followed by an overview of the current understanding of cellular orientation responses to environmental anisotropy and strain. Finally, we present the outline of the research reported in this thesis that aims at understanding and modulating actin cytoskeleton response in physiological and pathophysiological conditions.

Understanding cellular orientation responses to complex biophysical cues

Cardiovascular regenerative medicine has emerged as a promising approach to replace or regenerate damaged or diseased cardiovascular tissues. This interdisciplinary field, at the cross-section of engineering and life sciences, has the potential to restore normal cardiovascular function by using (the properties of) living cells in combination with biomaterials, genes, or drugs. Novel *in situ* tissue engineering approaches build on the regenerative potential of the body itself by guiding and controlling cell behaviour inside the human body with tailored biomaterials.

The premise of this approach is that, to recapitulate tissue function, an in-depth understanding of native cell behaviour under physiological conditions and in response to a biomaterial environment is needed. Only then, strategies for controlling cell behaviour can be designed towards the restoration of tissue functionality and mechanical integrity¹.

One crucial, but often overlooked, aspect of mimicking native tissue functioning is obtaining and retaining cellular organization. The importance of cellular organization is demonstrated by the fact that biological and mechanical functioning of most tissues is dictated by the cellular arrangement². The tissues of the cardiovascular system are highly organized. For instance, the myocardial wall³, heart valves⁴ and larger arteries⁵ are characterized by a layered structure with a well-defined cellular arrangement conferring the tissues their native unique anisotropic mechanical behaviour needed to perform their function. Given the correlation between structural organization and function, it becomes clear that the loss of cellular organization is indicative of tissue malfunctioning, which can eventually lead to pathophysiological conditions. The disorganized arrangement of cardiac cells, for example, is a histological hallmark of cardiac dysfunction in hypertrophic cardiomyopathy⁶⁻⁹.

Cellular organization in cardiovascular tissues depends on the complex interactions between cells, the properties of the microenvironment and the cyclic strains resulting from the hemodynamic environment. Living adherent cells actively interact, respond, and adapt to biochemical and biophysical perturbations. These perturbations trigger intracellular signalling events leading to specific cellular mechanoreponse capable of directing biological relevant processes such as cell differentiation, proliferation and contractility. The mechanisms employed by cells to respond and adapt to the biochemical and biophysical cues of the micro-environment consist of a myriad of distinct but interconnected pathways whose details remain to be unravelled. The outside-in and inside-out feedback loop, referred to as mechanotransduction, is traditionally regarded as the process of converting mechanical stimuli into biochemical signals. Recently, it has been suggested that the structural pathway connecting the extracellular environment to the nucleus¹⁰, here defined as “the structural mechanotransduction pathway”, might be as important as the biochemical transduction pathway for conducting biophysical signal to the nuclear interior. This new concept is supported by the fact that the long-range force propagation into the cell, resulting in deformations deep inside the cytoskeleton and nucleus, occurs 40 times faster than biochemical signalling¹¹. The structural mechanotransduction pathway consists of structural load bearing elements, such as integrins and focal adhesion complexes at the cellular membrane, and actin cytoskeleton stress fibers connected to the nucleus via so-called LINC (Linkers of the Nucleoskeleton and Cytoskeleton) complexes. Experimental evidence for this direct interconnection arises from studies where forces

were applied directly to a small spot on the cell surface and consequently induced deformations and movements in the cellular interior^{12,13}. Clearly, defects in the complex and delicate interplay between the cell and its micro-environment resulting, for instance, from aberrations of the structural mechanotransduction pathway, may result in altered cellular mechanoresponse in case no compensatory mechanisms signalling arises.

The recent development of micro-fabricated devices capable of effectively mimicking controlled biophysical cues has triggered numerous studies aiming at unravelling cellular responses to the properties of the micro-environment. It has become clear that cell orientation is actively determined by the actin stress fibers¹⁴. Stress fiber orientation and, consequently, cellular alignment can be induced by two important biophysical cues of the cellular environment, such as those occurring during hemodynamic loading: i) the anisotropy of the environment, e.g. the substrate on which cells are cultured and ii) cyclic uniaxial strain^{15,16}. These cues induce rapid and specific orientation of the intracellular elements of the structural mechanotransduction pathway, i.e. the focal adhesions, the actin cytoskeleton and the nucleus, suggesting that the direct structural mechanotransduction pathway plays a fundamental role in the cellular orientation response^{17,18}.

Although a wealth of information is obtained by recent mechanotransduction studies, our understanding of cellular mechanobiological response is still far from being comprehensive. Integrating the results of different investigations is a difficult task because of the complexity of the cellular response, which is not only highly dependent on the choice of the physical and mechanical experimental parameters, but also dependent on the cell-type. Moreover, the effects of combined biophysical cues on the cellular orientation response have just begun to be explored.

In this chapter we present a state-of-the-art review on the complex interplay between cells, topographical and cyclic strains cues of the extracellular environment, with a focus on cells of the cardiovascular system. First, we introduce the structural mechanotransduction pathway, i.e. the connected cellular components forming the physical link between the extracellular environment and the nuclear genome. Then, we continue our discussion with a review of experimental observations regarding cellular orientation response to anisotropy of the substrate and cyclic uniaxial strain in two-dimensional (2D) environments. We conclude with a brief outlook on future research directions for improving our current knowledge of cellular mechanoresponse and we present the outline of the chapters of this thesis.

The structural mechanotransduction pathway: a physical connection between the extracellular environment and the genome

In this section we provide background information on the cellular structural components forming the structural mechanotransduction pathway, i.e. the physical connection between the extracellular matrix (ECM) and the genome contained by the nucleus.

The structural components are represented by the focal adhesion complexes situated at the cell membrane, the cytoskeletal filaments and, at last, the nucleus (**Figure 1.1**). Among the cytoskeletal elements we concentrate on the actin filaments, since these structures are directly connected to the focal adhesions and play an important role in determining cell orientation^{19,20}. Moreover their behaviour is relatively easy to analyse and quantify from microscopy imaging as they form anisotropic networks when cells are aligned^{20,21}.

Interconnection between the extracellular environment and the actin cytoskeleton

In vivo adhesive cells are embedded in a filamentous network called extracellular matrix (ECM). The integrins are the first components that physically link the ECM (outside of a cell) with the actin cytoskeleton (inside of the cell). Integrins are transmembrane $\alpha\beta$ heterodimeric receptors that mediate cell adhesion to various ECM ligands such as collagen, fibronectin and laminin. The integrin family consists of approximately 25 members which are composed of combinations of α and β subunits, where the α subunit determines the ligand specificity for cell adhesion to the ECM²² (**Figure 1.1a**). During cell adhesion, conformational changes in the integrins are induced by bidirectional (inside-out and outside-in) signalling of mechanical and biochemical signals across the cell membrane²³⁻²⁵. Ligand binding to the integrins leads to clustering of integrin molecules at the cell membrane and recruitment of actin filaments inside the cell. The result of this process is the formation of the so called nascent focal adhesion complexes, multi-molecular complexes that consist of a large number of different proteins, including talin, vinculin, paxillin and tensin.

Focal adhesion complex formation initially starts with immature, small structures (approximately 100 nm in diameter²⁶). These structures reside at the leading edge in protrusions of the cells and provide the structural links between the ECM and the actin cytoskeleton. Strikingly, the maturation of the small focal adhesion complexes into bigger, mature focal adhesions is dependent on the actin cytoskeleton bundling and the generation of mechanical force. The actin cytoskeleton spans the whole cytoplasm of eukaryotic cells, continuously remodels and reorganizes to perform specific cellular functions^{27,28}. It is made of globular actin (G-actin) which continuously polymerizes into semi-flexible actin filaments, the filamentous actin (F-actin). F-actin assembles into bundles of fibers interconnected by actin crosslinkers (such as alpha-actinin and filamin) and motor proteins such as myosin II²⁹. These bundles of F-actin fibers are referred to as stress fibers. The presence of myosin II within the stress fibers is responsible for their contractility. The newly formed focal adhesions (FAs) reside in both central and peripheral regions of the cell. During this process the morphology of the FAs changes from a dot-like structure to a bigger and more elongated structure (2-10 μm)^{30,31}. This happens also as a consequence of the recruitment at the adhesion complex of several other proteins, for instance zyxin and alpha-actinin³². A critical molecule for both maturation of FAs and mechanosensing is focal adhesion kinase (FAK). This molecule is involved in the transmission of external signals to the cytoskeleton by phosphorylation³³.

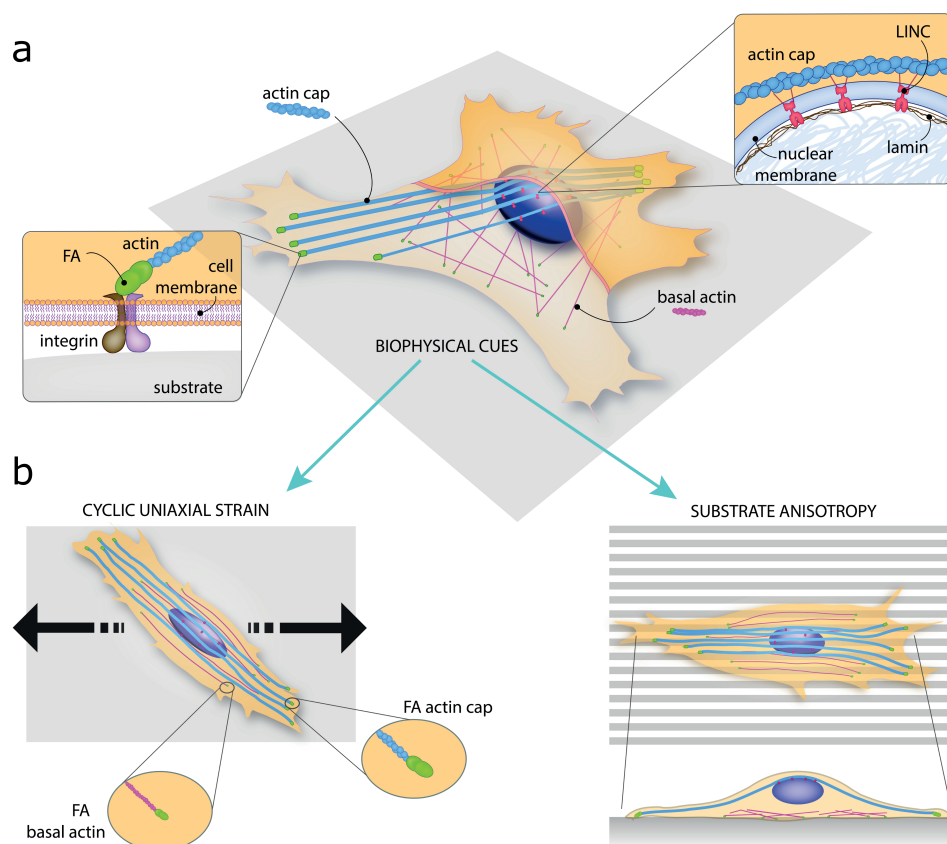


Figure 1.1. Cellular structural mechanotransduction pathway and orientation response to cyclic uniaxial strain and anisotropy of the substrate. a) Schematic illustration highlighting the (protein) structural elements forming the structural mechanotransduction pathway. Integrins at the cell membrane connect the extracellular environment (substrate) to the actin cytoskeleton. The connection is realized, in the cellular interior, by the focal adhesion complex (FA). Within the actin cytoskeleton filaments, two kinds of fibers can be distinguished. i) The basal actin fibers (pink) that can be found underneath the nucleus and ii) the actin cap fibers running on top of the nucleus (cyan). Actin cap fibers are connected to the nuclear interior via the LINC complex and lamins, a group of proteins underlying the nuclear membrane. This network of components forms a direct connection between the extracellular environment and the nuclear interior and functions as a fast passing system for the biophysical stimuli. b) Schematic illustration of the cellular response to cyclic uniaxial strain and substrate anisotropy. Upon cyclic uniaxial strain (left), the cell responds by strain avoidance. The focal adhesions and the actin cytoskeleton align at an angle with respect to the straining direction (black arrows, horizontal direction). Overall cell orientation coincides with the actin cytoskeleton orientation. Note that the focal adhesions associated with the actin cap fibers are bigger than those associated with the basal actin fibers. When plated on anisotropic substrate (right), the cell tends to align in the direction of the anisotropy. Focal adhesions as well as the actin cytoskeleton align accordingly. The side view shows the arrangements of the actin cap and basal actin fibers. Figure by Anthal Smits.

The maturation of FAs provides stable adhesive interconnections between the stress fibers and the ECM. This allows the cell to probe its complex biophysical environment in various directions and over large temporal and spatial scales³⁴. Focal adhesions do not actively generate forces, but rather serve to regulate force transmission between the cytoskeleton and ECM³⁵. The actin cytoskeleton is the intracellular structure able to impose increasing forces when facing growing resistance. This

confers the actin cytoskeleton intrinsic mechanosensing and the ability to adapt to developing mechanical cues of the cellular environment. However, to which extent stress fibers participate in sensing and transducing environmental signals has not been fully elucidated yet.

Interconnection between the actin cytoskeleton and the nucleus

In the surrounding of the nucleus, a subset of actin stress fibers have been found to organize in thick parallel and well-ordered bundles of fibers, physically anchored to the apical surface of the nucleus^{36,37} (Figure 1.1a). Wirtz and co-workers have made an effort to characterize these fibers (actin cap) which are strikingly terminated by wide, long and dynamic focal adhesions^{36,38,39}. First, they have demonstrated that the actin cap stress fibers differ from the conventional stress fibers found below the nucleus (basal actin layer). By containing more myosin II and the actin bounding protein alpha-actinin, actin cap stress fibers are very contractile and highly dynamic⁴⁰. Furthermore, these fibers not only play a major role in shaping and positioning the nucleus^{36,38,40-43}, but they are also involved in mechanosensing of substrate elasticity. For instance, cells without an actin cap were observed to be less responsive to changes in matrix elasticity. Finally, fast mechanotransduction also seems to be enabled by this subset of stress fibers. In their study, Chambliss *et al.*⁴⁴ showed that, in response to shear stress stimulation, cells without the actin cap build up thick stress fibers in a short time span as compared to in response to biochemical stimulation. From these findings it has become clear that the perinuclear actin cap is a key component of the physical pathway from the ECM to the nuclear interior for mechanosensing and mechanotransduction.

The coupling between the perinuclear actin cap and the nucleus (nucleo-cytoskeletal connection) is mediated by a group of recently discovered proteins, referred to as the LINC complex (Linker of Nucleoskeleton and Cytoskeleton)⁴⁵⁻⁴⁷. Hooking at the cytoplasmic side of the nucleus, on the outer nuclear membrane (ONM), we find the nesprins (KASH domain proteins), which are connected to the various cytoskeletal filaments^{48,49}. Among the four variants of nesprins, nesprin-1 and -2 bind to actin filaments⁵⁰. Nesprins, in turn, bind to SUN domain proteins spanning the whole nuclear envelope reaching the nuclear interior. SUN proteins then bind to lamins, a family of type V intermediate filaments underlying the inner nuclear membrane (INM)⁵¹. Lamins, in turn, physically connect to chromatin. Thus, a physical bridge is formed between the cellular exterior and the nuclear interior.

The nucleus is wrapped by the nuclear envelope, a double lipid bilayer (ONM and INM) with multiple pores (nuclear pore complexes), and contains the nuclear interior with the genome. Since its main role is to regulate gene expression and cellular function through protein synthesis, the nucleus is referred to as the 'brain' of the cell. Below the INM, the lamins form an elastic meshwork called nuclear lamina^{52,53}. Lamins fall into two categories, A- and B-type lamins (encoded by the gene LMNA or LMNB1 and LMNB2 respectively)⁵⁴. While B-type lamins are essential for cell survival, A-type lamins are thought to contribute significantly to the maintenance of mechanical integrity of the nucleus⁵⁵⁻⁵⁸. The nuclear lamina interacts also with the chromatin of the nucleoplasm, and therefore plays a major role in gene expression, DNA replication and repair, chromatin organization and transcriptional response⁵⁹⁻⁶².

The role of the nucleo-cytoskeletal connection in force transmission has been examined recently by many groups. The results of various experimental approaches based on two- and three-dimensional

substrates or application of mechanical load, have shown that the structural integrity of this connection is indeed needed for propagation of forces to the nucleus. Indirect demonstration has come from studies employing LMNA-depleted cells. By using this model, it has been shown that nuclear deformations in response to local cellular membrane stretch are completely abolished¹². These cells present also abnormal nuclear morphology⁴³, altered nuclear mechanics and defective cytoskeletal organization around the nucleus⁶³. In addition, the studies by Poh *et al.*⁶⁴ and Zweger *et al.*⁶⁵ have provided direct evidence that forces are not transmitted to the nucleus when LMNA is depleted from cells, thus when the nucleo-cytoskeletal connection is lost. Recently, it has emerged as well that the tension exerted by the actin on the nucleus directly mediates the spatial polarization of nuclear lamina and the intranuclear architecture⁶⁶. In cells lacking A-type lamins, the formation of a nuclear actin cap is partially abolished⁶⁷. A number of other studies in which either the LINC complex was disrupted or a loss of lamins was induced, support these findings adding that also other cellular functions such as migration, polarization and developmental processes become affected^{68,69}.

Although the role of the LINC complex in force propagation to the nucleus has been clarified, controversy remains about its impact on the activation of mechanotransduction pathways. The impaired activation of mechanosensitive genes has been reported in studies with cells lacking A-type lamins^{70,71}. At the same time, it has been suggested that the biochemical signals coming from the cytoplasm might take over or compensate the lack of the physical nucleo-cytoskeletal interconnection^{12,68}. A study by Lombardi *et al.*¹² showed that disruption of the LINC-complex (by dominant-negative nesprin and SUN construct) did not invoke nuclear deformation under substrate strain, but still the tested mechanosensitive genes were activated normally. Most probably the explanation of these distinct observations comes from the integration of the two major hypotheses about the role of the nucleus in mechanosensing and mechanotransduction. The first hypothesis is that the nucleus is the last element of an entirely physical force propagation network capable of activating gene expression via nuclear deformations. The other scenario supports the idea that a cascade of biochemical reactions, initiated by changes in the actin cytoskeleton in response to extracellular biophysical cues, influences cell mechanoreponse. Recently, Swift and co-workers have proposed that the nucleus might act directly as a mechanosensor⁷². To exclude the interference of the biochemical signalling, they have carried out investigations with isolated nuclei. They observed that the quantity of A-type lamins in the nuclear interior scales with the stiffness of the culture substrate, indicating that the nuclear lamins could act as shock absorber for the cell and protect the genome. Still, it remains to be elucidated how the nuclear lamina is directly involved in mechanosensing or whether the regulation of lamin levels is the result of other signalling pathways. Also it cannot be excluded that altered gene expression in cells with impaired nucleo-cytoskeletal connection is the result of the loss of the interaction between lamins, LINC-complex proteins and transcriptional regulators. Moreover, it remains to be understood how the activation of certain genes at spatial location within the nucleus is induced by conversion of the mechanical stimuli.

Altogether, the examples above demonstrate that several structural components of the mechanotransduction pathway connecting the cellular micro-environment and the nuclear interior have been identified. While we do not know the degree of completeness of our understanding, we can confidently state that the structural interconnection is crucial for determining the cellular mechanoreponse.

Laminopathies, diseases arising from a compromised nucleo-cytoskeletal connection

Mutations in the LMNA gene encoding for A-type lamins in the nuclear lamina cause a broad spectrum of genetic diseases, collectively referred to as laminopathies⁷³. Over two hundred mutations in the gene have been discovered and most of them have tissue-specific phenotypes. Twelve different diseases are included into this group: those affecting striated muscle (ranging from Emery/Dreifuss muscular dystrophy (EDMD) to dilated cardiomyopathy with conduction system defects (DCM-CD) and Limb-girdle muscular dystrophy (LGDM), those affecting the adipose tissue (partial lipodystrophy of Dunningan type (FPLD)) and those affecting the nervous system (Autosomal recessive Charcot-Marie-Tooth type 2 and Autosomal dominant axonal Charcot-Marie-Tooth disease). However, primary laminopathies can also affect tissues in a systemic fashion and cause premature-ageing syndromes like Restrictive Dermopathy (RD) and Hutchinson-Gilford progeria syndrome (HGPS)⁷⁴. Strikingly, there is a high variability in disease symptoms between individual patients carrying an identical LMNA mutation. The genotype/phenotype correlations in laminopathies remain unclear and, consequently, classical mutation screening alone is not sufficient to diagnose the disease or to predict clinical outcome. The mechanisms underlying tissue-specific effects observed in laminopathies are still not known. However, three major hypotheses have been formulated to explain how mutation in A-type lamins could yield pathology.

1. Gene regulation hypothesis: since A-types lamins play a pivotal role in specific DNA transcription by activating mechanosensitive genes, mutations in LMNA gene can alter the interaction between nuclear lamina and transcription factors resulting in altered gene expression, which can interfere with normal tissue functioning^{63,75,76}.
2. The "structural hypothesis" states that lamins are involved in the maintenance of the integrity of the nucleus and thus, of the whole cell. Mechanical balance of the cells can be therefore disturbed by lamina changes and renders cells more susceptible to mechanical stress - especially in cells continuously challenged by mechanical strain^{55,77-79}.
3. The third hypothesis states that premature aging and failure to regenerate in cells and tissue result from impaired DNA repair caused by mutation in the LMNA gene, resulting in affected maintenance of cell cycle and/or stem cell⁸⁰.

These hypotheses, most probably, do not exclude each other and are closely related⁸¹. Especially in the most diffuse laminopathies, the muscular dystrophies and cardiomyopathies⁸², it might well be that the lack of structural integrity, thus the susceptibility to mechanical stress could result in altered chromatin organization which, on its turn, results in altered gene expression. Recently it was observed that not only mutations in the LMNA gene but also those of other components of nucleo-cytoskeleton linker (e.g. emerin, nesprin-1, nesprin-2, etc.) can give rise to the same EDMD disease pathology⁸³⁻⁸⁶. Next to this, combinations of mutations in the nucleo-cytoskeletal system have been shown to lead to more severe diseases than the individual component mutations⁸⁷⁻⁸⁹. Altogether, these results suggest that mechanical instability of the cells, consistent with cellular structural integrity both at the nuclear and cytoskeletal level, might play a key role in the onset of the diseases.

Cellular orientation response to substrate anisotropy and cyclic strain

In the previous section we introduced the components of the structural mechanotransduction pathway interconnecting the extracellular environment with the nucleus in order to appreciate the inside-in part of the cellular mechanotransduction, i.e. how environmental signals are transmitted to the nucleus. To get a comprehensive understanding of the interplay between cellular responses and complex biophysical environments, it is also necessary to have a deep understanding of the inside-out signalling used for cellular mechanoreponse, i.e. how cells respond to environmental cues and which are the mechanisms employed by cells for mechanoreponse. In this section we will report the knowledge we have acquired about the cellular orientation response to substrate anisotropy and cyclic uniaxial strain, focussing on the main components of the structural mechanotransduction pathway, i.e. the focal adhesions, the actin cytoskeleton and the nucleus (**Figure 1.1b**).

Cellular orientation response to substrate anisotropy

Various biophysical cues such as topography, cyclic strain and the mechanical properties of the extracellular environment (e.g. stiffness, ligand density) can induce the alignment of adherent cells by promoting an anisotropic arrangement of structural components at the subcellular level (**Figure 1.1b**). Early in 1912, Harrison⁹⁰ reported for the first time that the topography of a substrate could influence cell behaviour. Weiss⁹¹ confirmed this phenomenon in 1945 with the observation that cells preferentially orient and migrate along fibers, an organization principle he named 'contact guidance'. Today the connotation of this term is slightly different. Contact guidance is now regarded as the ability of cells to sense and align with the anisotropy of the surrounding micro-environment. Recent developments in microfabrication technologies have led to the manufacturing of a variety of substrates with different geometries and length scales, which can induce contact guidance. In order to elucidate the exact mechanisms behind contact guidance, distinction needs to be made between anisotropy by biochemical features (e.g. geometrical features created by microcontact printing of extracellular matrix protein), here referred to as two-dimensional (2D) environments, and topographical features (e.g. pillars, posts, microgrooves, fibers), here named two-and-a-half-dimensional environments (2.5D).

Nowadays, microengineered substrates covered with arrays of parallel micrometer sized grooves and ridges with a certain height (2.5 D environments) are often used to study the mechanisms behind contact guidance. To date, a large number of studies using microgrooved topography have indicated that a variety of tissue cells, ranging from endothelial cells⁹²⁻⁹⁴, to fibroblasts⁹⁵⁻⁹⁹, and smooth muscle cells¹⁰⁰ align along the direction of the anisotropy of the substrate. A summary of illustrative studies showing the response of cells of the cardiovascular system to anisotropic features of the culture substrate in the sub-micrometer to micrometer scale is reported in **Table 1.1**.

At the subcellular level it is observed that actin fibers and the focal adhesions follow cellular orientation, but the specific response of these structural cellular components depends on many parameters such as groove height^{93,99,101-103}, surface treatment⁹², groove width^{92,94,96,99,104}, and ridge width^{92,94-96,101,103}. The observed general trend is that, when either the grooves' width decreases or its height increases, the cell forms focal adhesions on top of the ridges and consequently orients in their direction.

There have been several attempts to understand the mechanisms behind contact guidance, such as the theories proposed by Dunn and Heath¹⁰⁵ (mechanical restriction theory), Ohara and Buck¹⁰⁶ (focal adhesion theory) and Curtis and Clark¹⁰² (discontinuity theory). The mechanical restriction theory¹⁰⁵ focuses on the relative inflexibility of cytoskeletal structures as a primary regulator to cellular alignment. The shape of the substrate is demonstrated to impose mechanical restrictions for the formation of cytoskeletal protrusions, called filopodia. Recently, there has been renewed interest in the role of filopodia in cellular alignment. For example, Zimerman *et al.*¹⁰⁷ and Ventre *et al.*¹⁰⁸ studied the influence of filopodia on cell orientation by geometrically confining cells in 2D and 2.5D environments, respectively. They reported that when either the distance between ridges or printed adhesive lines inhibits single filopodia to cross the step, cells become highly polarized and elongated in the direction of the anisotropy of the substrate. Next to the alignment of the actin filaments, long focal adhesions in the direction of the lines or grooves were observed, which were anchored to thick stress fibres. These long structures were presumably the focal adhesions of the actin cap. However, one limitation of the mechanical restriction theory is that the role of microtubules is not taken into consideration. These cytoskeletal structures appear indeed to align earlier than actin filaments to substrate topography⁹⁷. Next to this, the mechanical restriction theory is closely connected to the focal adhesion theory, because of the relationship between focal adhesions and the cytoskeleton. In the focal adhesion theory, it is proposed that the orientation of cells is caused by the tendency of focal adhesions to maximize their contact area. In this way, ridge width comparable to focal adhesion size can induce cell alignment along the ridge. However, other studies^{97,107} observed that focal adhesions can develop both perpendicular and parallel to the same ridge, which argues against the focal adhesion theory. More recently Clark and Curtis¹⁰² proposed the idea that sharp discontinuities in the substrate induce alignment of actin filaments and focal adhesions leading to cell alignment. Although this theory includes both the alignment of actin filaments and focal adhesions, it raises the question of how cells sense discontinuity.

An easy approach to investigate the influence of the actin cytoskeleton in cellular alignment to grooves consists in inhibiting the actin cytoskeleton via disrupting agents, such as performed by Walboomers *et al.*⁹⁸ and Gerecht *et al.*¹⁰⁹ On one hand, Walboomers *et al.*⁹⁸ observed that fibroblasts can still align along the microgrooves even if the polymerization of actin is inhibited with the use of cytochalasin-B. Contrarily, Gerecht *et al.*¹⁰⁹ found that, by adding actin disrupting agents to human embryo stem cells on sub-micrometer sized grooves, the morphology of the cells becomes rounder. These results demonstrate that there is no consensus yet on the role played by the actin cytoskeleton in the cellular response to substrate anisotropy.

Our view is that a systematic approach is needed to dissect the various aspects of the environment (e.g. height, edges, biochemical patterning) in such a way that the importance of each of the structural cellular components can be unravelled. The first step towards this systematic approach, is neglecting the influence of the height of topographic features (e.g. discontinuity) and create anisotropy in a solely biochemical way (2D environment). This kind of anisotropic features can be fabricated with microcontact printing. According to this methodology, an elastomeric stamp of polydimethylsiloxane (PDMS) incubated with an extracellular matrix protein (e.g. fibronectin) can be used to create adhesive patterns on flat surfaces, such as glass or PDMS. The bare regions are then backfilled with a non-adhesive protein or polymer, to avoid non-specific cell adhesion. Microcontact printing has proven to be a useful technique to adhere cells to single or multiple islands^{110,111}. In this

way one can geometrically control cell adhesion to regulate cell functions. However, there are only limited studies^{107,112,113} where this technique has been used to induce cellular alignment via printed lines whose width is in the order of micrometers. Thus, the precise mechanisms behind cellular alignment by pure biochemical anisotropy still remain to be uncovered.

Table 1.1. Experimental investigations on cell response induced by anisotropy of the substrate.

Cell type	Method	Parameters	Main results	Source
Fibroblasts (REF52 cells)	Parallel microcontact printed fibronectin lines Glass	Lines: 2 μm wide separated by 4, 6, 10 or 12 μm wide stripes	Focal adhesions are formed at the adhesive lines. If spacing is larger than 6 μm , focal adhesions orient either perpendicular to the lines or orient in the direction of the lines. Actin stress fibres can cross several stripes when the non-adhesive spacing is smaller than 6 μm . With wider spacing stress fibres form between adjacent adhesive stripes or along single stripes	107
Chick heart fibroblasts	Parallel grooves Quartz	Ridge width from 1.65 to 8.96 μm Groove width from 3 to 32 μm Constant depth: 0.69 μm	Focal adhesions observed on the floor of the grooves and at the ridges. The actin bundle associated with a focal contact on the floor of a groove is parallel to the groove axis and hardly ever nearly perpendicular to this axis. No such restriction is found on the ridges	96
Human gingival fibroblasts	Parallel grooves Silicon Titanium coating	Ridge and groove width of 15 μm Constant depth: 3 μm	Microtubules located at the bottom of the grooves are the first component to align along the grooves. Subsequently, focal adhesions and focal adhesions and actin microfilaments align. At a single groove or ridge, focal adhesions are oriented both parallel and perpendicular to the groove direction.	97
Rat dermal fibroblasts	Parallel grooves PDMS RFGD treatment	Ridge and groove width from 1 to 10 μm Depth: 0.45 or 1 μm Ridge and groove width from 1 to 20 μm Depth: 0.5, 1, 1.5, 1.8, 5.4 μm	Cells at surfaces with a ridge width smaller than 10 μm elongate along the surface grooves. If the ridge width is larger than 4 μm , cellular orientation was random and the shape of the cells became more circular. The ridge width is the most important parameter, since varying the groove width and groove depth does not affect cell size, shape, nor the angle of cellular orientation	95
Rat dermal fibroblasts	Parallel grooves PDMS	Ridge and groove width from 1 to 20 μm Depth: 0.5, 1, 1.5, 1.8, 5.4 μm	The cells always elongate in the groove direction without any significant difference in behaviour between a 2–20 μm wide grooves, but the cellular orientation is affected by the groove depth	99
Myofibroblasts (HVSCs)	Elastomeric microposts PDMS Plasma Fibronectin on top of microposts	Ridge and groove width from 1 to 10 μm Constant depth: 0.5 μm Elliptical microposts: a= 1.5 μm , b= 0.87 μm Circular microposts: d = 2 μm	Actin fibers orient in direction of the grooves. This happens more rapidly on the narrow grooves. The addition of cytochalasin-B only causes delay in cell attachment and spreading, thus a well-formed cellular actin cytoskeleton is no prerequisite for the occurrence of contact guidance.	98
Myofibroblasts (HVSCs)	Elastomeric microposts PDMS Plasma Fibronectin on top of microposts	Ridge and groove width from 1 to 10 μm Constant depth: 0.5 μm Elliptical microposts: a= 1.5 μm , b= 0.87 μm Circular microposts: d = 2 μm	Elliptical microposts: orientation in the direction of the major axis of the ellipse, even for very stiff microposts. Topographical cues induce cellular alignment.	114

Cell type	Method	Parameters	Main results	Source
Vascular smooth muscle cells	Parallel grooves PDMS Fibronectin coating	Ridge width: 12 μm Groove width: 20, 50, and 80 μm Constant depth: 5 μm	For all groove widths investigated, cells align in the direction of the grooves. The actin filaments are highly aligned and parallel to the grooves on the smallest groove widths. As the groove width is increased to 50 and 80 μm , there is a clear decrease in the number of highly aligned fibers.	104
	Parallel microcontact printed fibronectin or laminin lines PDMS	Lines width from 20 to 100 μm , separated by 100 μm wide stripes	Actin cytoskeleton aligns along all patterns.	112
Aortic smooth muscle cells	Parallel grooves PDMS Gelatine, fibronectin, vitronectin or poly-D-lysine coating	A PDMS sheet was stretched uniaxially using a custom-made stretcher to produce a fixed amount of prestretch. The stretched sheet was treated with oxygen plasma for a fixed period of time. This resulted in substrates with or without parallel grooves.	Focal adhesions are more prone to become mature when they run along microgrooves, causing mature focal adhesions to align in the direction of the microgrooves. These adhesions have straighter actin bundles oriented parallel to the microgrooves.	100
	Parallel grooves PDMS Fibronectin coating	Ridge width from 3 to 5.5 μm Groove width from 3 to 4 μm Depth: 200 nm, 500 nm, 1 μm , 5 μm	Majority of the focal adhesions and actin fibers oriented in direction of the ridges. Focal adhesions localized at the ridge edges and along the sidewalls of 1 μm deep grooves. No focal adhesions on the bottom of the 5 μm deep grooves.	93
Bovine aortic endothelial cells	Parallel grooves Silicone Human Plasma Fibronectin coating	Ridge and groove width of 2, 5, and 10 μm Constant depth: 5 μm	On 2 μm surfaces the vast majority of focal contacts are deposited on the ridges. On the 5 μm and 10 μm surfaces, cells are increasingly able to form these contacts also in the grooves.	94
	Parallel grooves PDMS Serum-free medium and without protein coating	Ridge and groove width from 200 to 2000 nm Constant depth: 300 nm	HUVECs oriented parallel to the long axis of underlying ridges, even in the absence of added protein. The actin stress fibers aligned parallel to the ridges and grooves on patterned substrates.	92
Endothelial cells (HUVECs)	Elastomeric microposts PDMS	Elliptical microposts: a=0.95 μm , b=0.55 μm Elliptical adhesive islands: a=0.95 μm , b=0.55 μm	Elliptical posts: orientation of the focal adhesions and actin cytoskeleton in the direction of the major axis of the ellipse Elliptical islands: no preferential orientation of the focal adhesions and actin cytoskeleton. Alignment is induced by differential stiffness of elliptical microposts.	115
	Microcontact printed fibronectin on top of microposts and microcontact printed fibronectin elliptical islands glass			

HUVECs = Human Umbilical Vein Endothelial Cells; MDCK = Madin-Darby canine kidney; PDMS = polydimethylsiloxane; RFGD= radio frequency glow discharge

Cellular orientation response to cyclic uniaxial strain

Cellular response to cyclic uniaxial strain is demonstrated by the dynamic reorganization and reorientation of cells and stress fibers (**Figure 1.1b**). It has become clear that stress fibers do play a crucial role in cell ability to remodel and respond appropriately to cyclic strain. Indeed, stress fiber disruption causes inhibition of cellular reorientation¹¹⁶⁻¹¹⁸. In the 80's, the response of tissue cell to strain was for the first time observed and interpreted as an avoidance response to the strain of the substrate on which the cells were cultured, the so called strain avoidance response¹¹⁹. Since then, further studies have highlighted that, on 2D substrates, cell reorientation occurs at angles (nearly) perpendicular to the stretch direction, i.e. the direction of minimal substrate deformation. In the last decades, several studies have been carried out in order to quantify and unravel the mechanisms of this phenomenon. Stretch avoidance appears to be a behaviour belonging to many kinds of tissue cells, ranging from endothelial cells^{18,116,120-128}, to fibroblasts¹²⁹⁻¹³¹ and smooth muscle cells¹³²⁻¹³⁴. However, the dependence of such response on the spatiotemporal parameters of the cyclic stimulation, such as frequency^{16,122,130}, magnitude^{18,122,126,127,129,132,134}, strain rate^{124,131,135,136}, duration^{128,137,138}, or even the combination of some of those¹³⁹, makes any attempt to correlate the effects of these factors with cellular response unsuccessful. Moreover stretch avoidance response seems to be cell type-dependent and a minimal strain amplitude^{120,131,132}, frequency^{122,130,135} or cell contractile status¹⁴⁰ may be required for the response to occur. Summary of studies about cells of the cardiovascular system (fibroblasts, tissue cells, endothelial and progenitor cells) and stress fiber response to cyclic uniaxial stretch are reported in **Table 1.2**.

Most of these studies are carried out with custom-built devices for which an accurate and rigorous strain characterization is needed, but often overlooked. These devices are made of motorized stages capable of stretching silicone membranes coated with extracellular matrix proteins such as fibronectin or collagen. Given the mechanical properties of the elastomeric materials, once the membrane is stretched along one direction, it contracts in the perpendicular direction (Poisson's effect). New commercially available devices have been designed to avoid this drawback (FlexCell^{16,133,141} and STREX¹³⁶). Nevertheless, the use of such diverse instrumentations cannot help to distinguish between the impacts of the different factors. Moreover, the interference of signalling mechanisms cannot be excluded when different coatings are employed. Altogether, controlled experimental conditions are needed towards a comprehensive understanding of cell reorientation.

Efforts to unravel the spatiotemporal dynamics of cellular adaptations, especially at the level of stress fibers, are still limited. Most of the observations come from a state-to-state like manner, making use of fixed cells that do not allow observations of subcellular dynamics. The technological challenges that must be overcome include the use of actin stress fiber probes that do not interfere with the dynamics of actin polymerization and the mechanical properties¹⁴². Moreover, the timescale of actin reorganization pushes further the experimental limits.

From time-lapse studies, it has been established that cells become nearly round in the first phases of reorientation and, subsequently elongate along the strain avoidance direction^{117,125,130}. During this second phase, a process of reinforcement and repair of the stress fiber strain sites occurs. Zyxin is recruited at strain-induced damage sites of stress fibers and subsequently activates actin cytoskeleton repair and reinforcement¹⁴³⁻¹⁴⁷. In terms of temporal dynamics, stress fibers significantly anticipate cell overall reorientation. Stress fiber reorganization response occurs within the first minutes from the onset of the cyclic strain stimulation, while complete cell reorientation is

seen in the time range of hours^{117,132}. In 2001, Hayakawa *et al.*¹⁴⁸ observed in rat smooth muscle cells the breakdown of stress fibers aligned along the stretching direction soon after the start of the mechanical stimulation, followed by stress fiber reorientation at an oblique angle with respect to the axis of stretching. Similar observations were reported by Ngu *et al.* in bovine endothelial aortic cells¹²⁵. Also, the investigation of Lee *et al.*¹²⁴ pointed out that bovine aortic endothelial cell reorientation involved the disassembly of the stress fiber proximal section (far from the focal adhesions) and *de novo* formation of stress fiber at a reoriented angle with comparatively little focal adhesion turnover. These studies suggest that reorientation of stress fiber takes place through stress fiber turnover and re-assembly. However, there is also another line of evidence which suggests that stress fiber turnover might occur via focal adhesion sliding and consequent stress fiber rotation. Deibler *et al.*¹⁴² demonstrated that rat embryonic fibroblasts reorient by realigning pre-existing stress fiber while Goldyn *et al.*¹⁴⁹ tracked the dramatical sliding of focal adhesions induced by cyclic uniaxial strain in NIH3T3 fibroblasts. Most probably, the aforementioned mechanisms are not mutually exclusive. Still, the challenge for the future remains to uncover the precise mechanisms of stress fiber and cell reorientation, by focusing on the heterogeneity observed not only on subcellular locations but also along the same stress fiber^{124,150}.

A number of theoretical models have been elaborated in the endeavour to describe the relationship between the actin cytoskeleton reorganization and the cyclic uniaxial strain acting on cells. In 2000, Wang *et al.*¹⁵¹ proposed that stress fibers tend to orient in the direction of minimal normal strain, where the unperturbed state is maintained. Other models, mostly based on the molecular aspects of stress fiber assembly¹⁵²⁻¹⁵⁴, were developed based on the same approach. Instead, the work of De *et al.*¹⁵⁵ predicts stress fiber orientation in the minimal matrix stress direction using a coarse-grained model of cells approximated as single force dipoles. While consistency between the predictions of these models and experimental results was proven in many studies, recently, Livne *et al.*¹⁵⁶ have found significant deviation between their results and the theoretical predictions proposed by the existing models. By investigating strain avoidance response over a wide range of stretch configurations, they demonstrated that stress fiber reorganization does not coincide with the direction of minimal strain or stress of the substrate. Therefore, they developed a new theoretical approach based on the molecular and physical properties of the stress fiber-focal adhesion system. Yet, it remains to be tested whether this model is cell type-independent.

Table 1.2. Experimental investigations on cell and stress fiber orientation response upon cyclic uniaxial strain.

Cell type	Method	Parameters	Main results	Source
	Custom-built device Silicone membranes ProNectin-F coating. ¹³⁹	10% at 0.5 Hz for 3 h 5 and 10% at 0.5 and 1 Hz for 3.5 h	Reorientation is inhibited by stress fiber disruption. Reorientation depends on stretch magnitude.	116 126
Human Aortic Endothelial Cells	Custom-built device Silicone membranes Fibronectin coating	10% at 10%/s for 3 h For time lapse: 5% at a constant rate of 5%/s for 6 h	Reorientation depends on stretch magnitude. Cell reorientation is independent of SFs presence. Cytoskeletal reorganization within few seconds from onset of stretching. SFs break and disassemble. FAs loosen and cells become nearly round.	157 125
Human Umbilical Vein Endothelial Cells	Custom-built device Silicon membranes Plasma treated Custom-built device Silicon membranes Collagen type I coating	10% at 1 Hz for 3 h 10% at 0.5 Hz for 0 to 20 h	Threshold for reorientation 1.8% strain magnitude. The variance of actin fiber orientation became smaller after 2 h of stretch. Actin fiber density increased within 30 min of stretching and decreased after 10 h of stretching.	120 128
Gottinger Minipigs Aorta Endothelial Cells	Custom-built device Silicon membranes Collagen type I coating. ¹³²	15% at 1 Hz for 3 days	Strain avoidance observed both in SFs and cells.	121
Bovine Aortic Endothelial Cells (BAECs)	Custom-built device Silicon membranes Fibronectin coating	10% at 1 Hz for 6 h 10% at 1 Hz for 8 h 0 to 20% at 0.01 to 1 Hz for 4 h	SFs reorientation depends on interplay between Rho pathway activity and the stretch magnitude. Stretch-induced remodeling of the actin cytoskeleton modulates JNK signalling in response to cyclic stretch. Reorientation depends on frequency (optimal at 1 Hz).	18 123 122
BAECs and U2OS Osteosarcoma cells Stably expressing GFP-actin	Custom-built device Silicon membranes Fibronectin coating	10% at 0.01 to 1 Hz for 4 h 10% at 0.1 and 1 Hz for 2 h	SF reorientation depends on strain rate. FAs and SFs distal ends do not disassemble. SFs exhibit heterogeneous behaviour within the cell, but also along the length of individual SFs.	135 124
Rabbit Aortic Smooth muscle cells	Custom-built device Silicon membranes Collagen type I coating	2 to 20% at 1 Hz for 3 to 12 h 2 to 10% at 1.2 Hz for 14 days	Threshold 2% for reorientation. Reorientation depends on stretch amplitude. SF reorient prior to the reorientation of the cell bodies. Reorientation depends on stretch amplitude.	132 158

Cell type	Method	Parameters	Main results	Source
a7r5 Rat Aortic Smooth Muscle Cells	FlexCell Collagen I-coated plates	100 to 124% of cell resting length at 1 Hz for 48 h	Cellular reorientation is independent of stretch-activated calcium channels. Alignment is reversible after 48 h from stretch cessation. Reorientation depends on stretch amplitude.	133
Rat Aortic Smooth Muscle Cells		10% at 0.5 to 2.0 Hz for 24 h 20% at 1 Hz for 3 h	SFs are needed for reorientation. 1.25 Hz, the most effective frequency for reorientation. SFs reorient within 15 min after the onset of stretching. Cells reorient within 1-3 h.	16 117
A10 Rat aortic Smooth Muscle Cells	Custom-built device Silicone membranes Collagen type I coating	1.2 times cell original length at 1 Hz for 3 h	Cell orientation but not SF reorientation depends on stretch-activated calcium channels. Rapid withdrawal of the cell periphery located in the direction of stretching and gradual extension toward the direction oblique to the stretching axis.	148
A10 Rat Aortic Smooth Muscle Cells Transfected EGFP-tagged moesin (fragments with actin-binding ability)			SFs aligned along the stretching direction are torn into pieces soon after stretching, and then reorient obliquely to the direction of stretching.	148
Earle's Fibroblast	Custom-built device Silicon membrane	Elongation and recoil at 15 s intervals for 18 to 24 h 4 to 12% at 1 Hz for 24 h	Pioneering study: strain avoidance is observed.	119
Human Dermal Fibroblasts	Custom-built device Silicone membranes ProNectin-F coating		Reorientation depends on combination of strain rate and amplitude. Threshold for reorientation is 4.2% for fibroblasts.	131
Human Dermal Fibroblasts		8% at 1 Hz for 24 h	Reorientation starts within 2-3 h from stretch onset and is complete at 24 h.	159
MRC5 Lung Human Fibroblasts	Instron 5564 testing Instrument Silicone sheets Fibronectin coating	1 to 25% at 0.5 Hz and 2% at 0.25 to 3 Hz for 3 h	Reorientation depends on strain amplitude. Rapid response of cytoskeleton to strain.	129
Primary Human Umbilical Cord Fibroblasts	Custom-built device PDMS membranes of 1 kPa, 3 kPa, 11 kPa and 50 kPa Fibronectin coating	4.9 to 32% at 9 to 52 mHz for 16 h	Threshold in amplitude. On very soft substrates no reorientation occurs, even for high strain. Changes in cell shape follow cytoskeletal reorientation with a significant temporal delay.	140
REF-52 Rat Embryonic Fibroblasts and Human Dermal Fibroblasts	Custom-built device Silicon membranes Fibronectin coating	1% to 15% at 0.0001 to 20 s ⁻¹ for 8 h	Reorientation depends on strain frequency (from 1 to 5 h).	130
NIH3T3 Fibroblasts Transfected with GFP-Vinculin	Custom-built device Silicon membranes Fibronectin coating	8% at 1 Hz for 3 h	FAs reorient by sliding, without turnover and reassembly. Reorientation is independent of microtubules but dependent of actin stress fiber presence.	149

Cell type	Method	Parameters	Main results	Source
Monkey Kidney Fibroblasts Transfected with GFP-Actin	Custom-built device PDMS membranes Fibronectin coating	16% and 28% for 3 h ca.	Reorientation occurs by dynamic rotation of intact actin stress fibers in fibroblasts. Subcellular reorganization begins within minutes from strain application. SFs at cell center region rotate, while SFs at cell periphery remain stable.	150
NIH3T3 Fibroblasts Transfected with EGFP-actin	Custom-built device Silicon membranes Fibronectin coating	6 to 32% in 2 s and kept stretched for 10 m, relaxation membrane within 2 s	SFs disassemble during stretching. New filament bundling occurs after stretch.	160
REF-52 Rat Embryonic Fibroblasts Transfected with Life Act		8% at 4 Hz for 90 m	Cell reorient by realigning pre-existing SFs. GFP-actin fusion proteins influence the mechanical behaviour of cells.	142
NIH3T3 Fibroblasts Transfected with GFP-LifeAct and mCherry-Vinculin	Custom-built device Silicon membranes Fibronectin coating ¹³⁰	8% at 0.1 to 3 Hz	Increasing frequency induces less spreading. Above 1 Hz level of perpendicular cell reorientation is not further increased. Disruption of contractility affects cells reorientation. SFs rather form <i>de novo</i> in the perpendicular direction where low mechanical forces are acting on the cell.	161
REF-52 Fibroblasts Stably expressing YFP-paxillin		4 to 24% at 1.2 Hz wide range of stretch configurations	Cell and SF orientation deviate from the zero strain and zero stress prediction.	156
UZOS Osteosarcoma cells Stably expressing GFP-Actin	STREX Silicon chambers Fibronectin coating	different waves for 10.5 h	Reorientation depends on strain rate.	136
Rat Bone Marrow Mesenchymal Stem Cells (BMSCs)	Custom-built device Silicon membranes Gelatine coating	10% at 1 Hz for 0 to 36 h	Cell reorientation depends on strain duration. Cell reorganization depends on the duration of the stretching.	137

SF, stress fiber; FA, focal adhesion; PDMS, polydimethylsiloxane; JNK, c-Jun N-terminal kinase

Live cell imaging and study of SFs reorientation dynamic

Cellular orientation response to combined substrate anisotropy and cyclic uniaxial strain

From the previous paragraphs it appears that cell and stress fiber orientation can be influenced by anisotropic cues or by imposing cyclic uniaxial strain on cell substrates. This legitimates to ask what the influence of anisotropic cues and cyclic strain is when these cues are applied in combination and along the same direction. This simultaneous stimulation, theoretically, would lead to competing stimuli for cell reorientation. An overview of the studies conducted applying anisotropic cues and cyclic uniaxial strain are reported in **Table 1.3**. We have considered all cell types, as the number of these studies is limited.

By using microgrooves integrated in a custom-built stretching device, Wang and Grood¹⁶² demonstrated that micro-topography generally overrules strain avoidance. E.g., tissue cells maintain the original orientation imposed by the microgrooves, even if strain stimulation occurs along the same direction¹⁶²⁻¹⁶⁴. Prodanov *et al.*¹⁶⁵ have added to this evidence that cellular response might be influenced by the dimension of the anisotropic textures. They showed that osteoblasts plated on nanogrooves and subjected to cyclic strain responded by strain avoidance, while on micro-sized features they remained aligned with the anisotropy of the substrate. Next to this, it has been observed by Ahmed *et al.*¹⁶⁶ that topographical cues combined with cyclic strain can have distinct impact on stress fibers as compared to cell body reorientation response. In their study, myoblasts were confined on substrates patterned with parallel fibronectin lines (widths comparable to cell size) and exposed to cyclic uniaxial stretch. It appeared that, while cell bodies remained confined on the micropatterned lines, stress fiber succeeded in reorganizing perpendicular to the strain direction. This points to different mechanisms involved in strain and anisotropy sensing.

Recently, a study from our group has provided further insight on the mechanisms underlying stress fiber response to combined cyclic strain and anisotropic cues. It was observed that distinct responses occur at the actin cap and basal layer. The actin cap stress fibers clearly tend to neglect the topographical cues and respond to strain, while the basal actin fibers remain aligned with the topography of the substrate¹⁶⁷. These findings provided evidence that cellular response to anisotropy of the substrate and cyclic strain is the complex integration of subcellular structural responses. Nevertheless, most of the mentioned studies reported on cell and stress fiber orientation but neglected the response of crucial structures such as focal adhesions.

In summary, although general indication exists that anisotropic cues modulate cell and stress fiber orientation response to cyclic uniaxial strain, a deeper understanding of the phenomenon is still needed. Detailed quantification of stress fiber reorientation dynamics at the subcellular level upon presentation of simultaneous anisotropic and cyclic strain cues would be of great benefit for unravelling the temporal dynamics of the processes involved in cellular adaptation.

Table 1.3. Experimental studies about cell and stress fiber orientation response to combined substrate anisotropy and cyclic uniaxial strain.

Cell type	Anisotropic cues	Stretching method and parameters	Main results	Source
MC3T3-E1 osteoblasts	Parallel microgrooves: 1.6 µm depth and varying groove/ridge widths from 1 to 6 µm ProNectin-F coating Parallel to stretching direction	Custom-built device ¹³⁹ Silicon membranes 4% at 1 Hz for 20 days	Cells align with grooves independently of topographic features. SFs highly aligned and elongated after stretch.	¹⁶³
Human Skin Fibroblasts	Parallel microgrooves: 1.6 µm depth, with widths from 1 to 6 µm (2 to 6 µm wide ridge) ProNectin-F coating Parallel to stretching direction	Custom-built device ¹³⁹ Silicon membranes 4 to 12% at 1 Hz for 24 days	Until 8% stretch, cells maintain the alignment imposed by the microgrooves, regardless of their dimensions. For high strain (12%) and small microgrooves (1 µm width and 2 ridge width) cells change orientations. Dimension of the microgrooves and the strain magnitude are two important factors in determining cell alignment.	¹⁶²
Human Patellar Tendon Fibroblasts	Parallel microgrooves: 3 µm depth and 10 µm width ProNectin-F coating Parallel to stretching direction	Custom-built device ¹³⁹ Silicon membranes 8% at 0.5 Hz for 72 h	Cells do not change alignment, regardless of the alignment to stretching direction.	¹⁶⁴
Mesenchymal Stem Cells	Parallel microgrooves: 10 µm width and 3 µm height Parallel and perpendicular to strain direction	Custom-built device Silicone membranes Rat tail collagen I coating 5% at 1 Hz for 2-4 days	Cells and SFs remain well aligned with the microgrooves in both parallel and perpendicular microgrooves. Distinct effects on gene expression in parallel and perpendicular microgrooves.	¹⁶⁸
Bovine Vascular Smooth Muscle Cells	Parallel microgrooves of varying widths Human plasma fibronectin coating Parallel or perpendicular to the direction of strain	Custom-built device Elastomeric membranes 10% at 1 Hz for 24 h	Strain parallel to microgrooves limit cell orientation response, small (15 µm) and large (70 µm) grooves are more favourable for reorientation than average size (40 µm). Strain perpendicular to microgrooves: enhanced cellular alignment.	¹⁶⁹
C2C12 Skeletal Myoblasts	Parallel microcontact printed fibronectin lines: 30 µm width, 40 µm spacing on hydrogels Arranged parallel, horizontal and 45° to strain direction	Custom-built device ¹³⁰ Elastomeric membranes 7% at 0.5 Hz for 4 days	SFs reorient while cell are geometrically constrained to the lines Parallel lines: SFs reorient at 48°, with a large scatter. Perpendicular lines: SFs reorient at 91°. Lines at 45°: SFs reorient at 52°.	¹⁶⁶
Rat Bone Marrow Mesenchymal Stem Cells	Parallel nano- and micro-grooves: 300 nm width and 60 nm depth (600 nm pitch) and 1 µm wide, and 500 nm deep (pitch 2 µm) RFGD treatment Parallel to strain direction	Custom-built device ¹³¹ Elastomeric membranes 1 to 8% at 1 Hz with intermittent stretch duration (15 min stretch/15 min rest for 16 h, followed by 8 h of rest)	Nanodimensions induce less alignment than microdimensions in static conditions. Cells have strain avoidance response on nanotextured surface but not on micrometer-sized textures.	¹⁶⁵
Human Vena Saphena Cells (Myofibroblasts)	Elastomeric microposts Elliptical cross-section (major semi-axis 1.5 µm, minor semi-axis 0.87 µm) 1, 3 and 6 µm height Human Plasma Fibronectin microcontact printed coating on top of microposts	FlexCell 7% at 0.5 Hz for 19 h	Competition between contact guidance and strain avoidance results from distinct behaviour of actin cap and basal actin layer.	¹⁶⁷

SF = stress fiber; RFGD = radio frequency glow discharge

Outlook and thesis outline

A deep understanding of the mechanisms by which biophysical cues regulate cellular behaviours is of fundamental importance for cardiovascular regeneration strategies. For instance, in biomaterial-based *in situ* engineering approaches that need to guide and control cell and tissue organization for proper tissue functioning, it is crucial to know how cellular orientation can be modulated. Achieving controlled cellular organization is a primary aim of regeneration of cardiovascular tissues because it allows matching native tissue micro architecture and functionality¹⁷⁰.

In this chapter, we have provided an overview of the knowledge obtained in the last decades about the components of the structural mechanotransduction pathway, an interconnected chain of proteins implicated in force propagation from the extracellular environment to downstream targets such as the nucleus and gene expression regulation. We also reported on the current understanding of cellular orientation response induced by the application of substrate anisotropy and cyclic uniaxial strain. The development of *in vivo*-like micro-devices has enabled researchers to perform experimental studies under controlled conditions, in the effort to identify the link between applied biophysical cues and cellular response. These studies have demonstrated that an intact structural mechanotransduction pathway plays a crucial role in the control of normal cellular functionality. Still, the large body of knowledge generated by using such diverse approaches and the cell-type dependence of the results complicate the attempt of unifying the available knowledge. Therefore, further research is required to achieve an in-depth understanding of the role of structural mechanotransduction pathway in biophysical signal transduction.

In this thesis, we will focus on the actin cytoskeleton, a crucial component of the structural mechanotransduction pathway. By transferring and responding to the signals coming from the biophysical cues of the extracellular environment, the actin cytoskeleton filaments play a major role in cellular mechanoreponse and, thus, in numerous cellular processes (**Figure 1.2**). In particular, the actin cytoskeleton is responsible for cellular alignment, in response to topographical or cyclic strain cues, and for the developed intracellular tension, in response to changes in substrate stiffness.

In view of achieving relevant knowledge for attaining control over actin cytoskeleton behaviours by modulating the cues of the extracellular environment in physiological and pathophysiological conditions, in this thesis, we will perform experimental investigations of the actin cytoskeleton mechanoreponse upon stimulation by relevant biophysical cues, such as topographical cues, cyclic uniaxial strain and stiffness.

In order to obtain functional tissue through regenerative strategies, it is crucial to mimic the structural organization of living tissues, which ultimately results from controlled cellular alignment. In **chapter 2**, with the help of a dedicated experimental modular model system, we will investigate the influence on actin cytoskeleton orientation of two apparently competing stimuli for cellular alignment: topographical cues and cyclic uniaxial strain.

Furthermore, in **chapter 3**, we will explore the effects of normal and aberrant actin cytoskeleton formation in the orientation response to topographical cues and cyclic uniaxial strain. To investigate the relevance of an intact structural mechanotransduction pathway in the cellular orientation response, we consider cells with defected actin cytoskeleton (knock-out cellular models). This allows

getting deeper insights in the different subcellular actin structures relevant for cellular mechanoreponse to topographical cues and cyclic uniaxial strain. Moreover, translation to pathophysiological conditions is possible since the cells used in this study represent a model for a family of diseases called laminopathies characterized by mechanically weakened cell phenotypes.

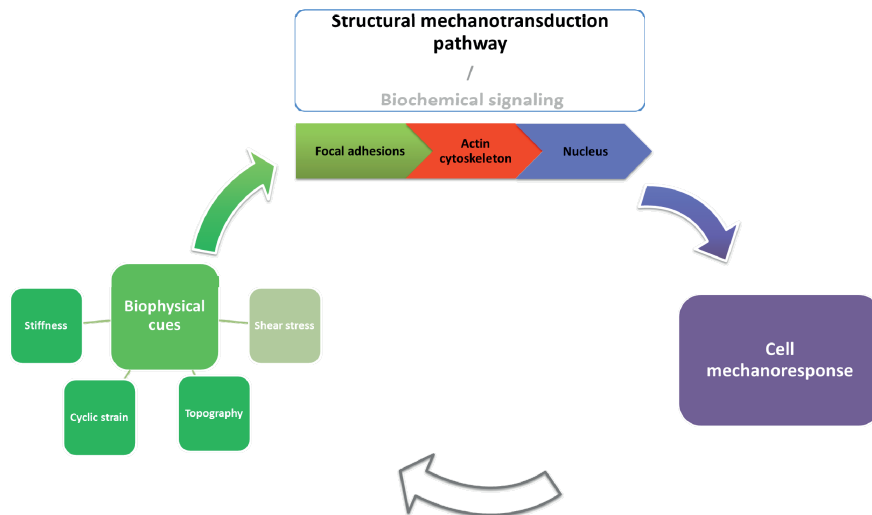


Figure 1.2. Schematic overview of the interplay between the biophysical cues of the cellular environment and cellular mechanoreponse. The biophysical cues considered in this thesis are i) topography ii) cyclic uniaxial strain and iii) substrate stiffness (all dark green). These stimuli are transmitted (green arrow) through an interconnected network of structural elements in the cellular interior (focal adhesions (light green), actin cytoskeleton (red) and nucleus (blue)). Alternatively, these stimuli can initiate a cascade of biochemical signals. In both cases, the signals ultimately reach the nucleus, where cellular mechanoreponse (purple) is regulated. In this thesis we focus on the structural mechanotransduction pathway for the transmission of biophysical cues to the nuclear interior. Cell mechanoreponse may eventually result in changes in the biophysical properties of the surrounding environments (white arrow). However, this part of the mechanotransduction loop is not considered in this thesis.

In **chapter 4** we will focus on mechanically weakened and structurally impaired cells. We consider substrate stiffness as a cue for modulating the actin cytoskeleton remodeling, and, overall, cellular processes. Adherent cells anchor to the substrate via focal adhesions and pulls on it through the actin-myosin cytoskeleton. This allows for probing the stiffness (resistance to deformation) of the surrounding microenvironment^{171,172}. Through mechanotransduction processes, tissue cells respond to the sensed resistance by adjusting their adhesion sites and reorganizing the cytoskeleton¹⁷³. In general, on soft substrates cells have reduced adhesion strength resulting from a disorganized and barely tensed actin cytoskeleton and dynamic focal adhesions^{171,174}. On stiffer substrates, instead, adherent cells, such as fibroblasts, develop organized and the tensed actin stress fibers and stable focal adhesions¹⁷⁵⁻¹⁷⁷. The intracellular stiffness and tension vary accordingly. Based on such observations, it becomes clear that actin cytoskeletal tension can be modulated by modifying the substrate stiffness on which cells are cultured.

In our study, we employ this property of adherent cells and we investigate whether variations in stiffness of the culture substrate influence the onset of cellular structural abnormalities in mechanically weakened cells.

Finally, **chapter 5** discusses the results obtained in this thesis. Next to this, we review future perspectives towards a comprehensive understanding of actin cytoskeleton remodeling, which can eventually be exploited for developing new strategies for repairing or regenerating cellular organization in diseased/damaged tissues, as well as for elaborating new therapies for rescuing mechanically weakened cells.

References

1. Grenier,G. *et al.* Tissue reorganization in response to mechanical load increases functionality. *Tissue Eng* **11**, 90-100 (2005).
2. Feinberg,A.W. *et al.* Controlling the contractile strength of engineered cardiac muscle by hierarchal tissue architecture. *Biomaterials* **33**, 5732-5741 (2012).
3. Sands,G., Goo,S., Gerneke,D., LeGrice,I., & Loiselle,D. The collagenous microstructure of cardiac ventricular trabeculae carneae. *J. Struct. Biol.* **173**, 110-116 (2011).
4. Schoen,F.J. Aortic valve structure-function correlations: role of elastic fibers no longer a stretch of the imagination. *J. Heart Valve Dis.* **6**, 1-6 (1997).
5. Tranquillo,R.T., Girton,T.S., Bromberek,B.A., Triebes,T.G., & Mooradian,D.L. Magnetically orientated tissue-equivalent tubes: application to a circumferentially orientated media-equivalent. *Biomaterials* **17**, 349-357 (1996).
6. Harvey,P.A. & Leinwand,L.A. The cell biology of disease: cellular mechanisms of cardiomyopathy. *J. Cell Biol.* **194**, 355-365 (2011).
7. Chung,A.S. & Ferrara,N. Developmental and pathological angiogenesis. *Annu. Rev. Cell Dev. Biol.* **27**, 563-584 (2011).
8. Hinton,R.B., Jr. *et al.* Extracellular matrix remodeling and organization in developing and diseased aortic valves. *Circ. Res.* **98**, 1431-1438 (2006).
9. Niwa,K. *et al.* Structural abnormalities of great arterial walls in congenital heart disease: light and electron microscopic analyses. *Circulation* **103**, 393-400 (2001).
10. Wang,N., Tytell,J.D., & Ingber,D.E. Mechanotransduction at a distance: mechanically coupling the extracellular matrix with the nucleus. *Nat. Rev. Mol. Cell Biol.* **10**, 75-82 (2009).
11. Na,S. *et al.* Rapid signal transduction in living cells is a unique feature of mechanotransduction. *Proc. Natl. Acad. Sci. U. S. A* **105**, 6626-6631 (2008).
12. Lombardi,M.L. *et al.* The interaction between nesprins and sun proteins at the nuclear envelope is critical for force transmission between the nucleus and cytoskeleton. *J. Biol. Chem.* **286**, 26743-26753 (2011).
13. Maniotis,A.J., Chen,C.S., & Ingber,D.E. Demonstration of mechanical connections between integrins, cytoskeletal filaments, and nucleoplasm that stabilize nuclear structure. *Proc. Natl. Acad. Sci. U. S. A* **94**, 849-854 (1997).
14. Tomasek,J.J. & Hay,E.D. Analysis of the role of microfilaments and microtubules in acquisition of bipolarity and elongation of fibroblasts in hydrated collagen gels. *J. Cell Biol.* **99**, 536-549 (1984).
15. Bettinger,C.J., Langer,R., & Borenstein,J.T. Engineering substrate topography at the micro- and nanoscale to control cell function. *Angew. Chem. Int. Ed Engl.* **48**, 5406-5415 (2009).
16. Liu,B. *et al.* Role of cyclic strain frequency in regulating the alignment of vascular smooth muscle cells in vitro. *Biophys. J.* **94**, 1497-1507 (2008).
17. Dalby,M.J. Topographically induced direct cell mechanotransduction. *Med. Eng Phys.* **27**, 730-742 (2005).
18. Kaunas,R., Nguyen,P., Usami,S., & Chien,S. Cooperative effects of Rho and mechanical stretch on stress fiber organization. *Proc. Natl. Acad. Sci. U. S. A* **102**, 15895-15900 (2005).

19. Tojkander,S., Gateva,G., & Lappalainen,P. Actin stress fibers - assembly, dynamics and biological roles. *Journal of Cell Science* **125**, 1855-1864 (2012).
20. Weichsel,J., Herold,N., Lehmann,M.J., Krausslich,H.G., & Schwarz,U.S. A Quantitative Measure for Alterations in the Actin Cytoskeleton Investigated with Automated High-Throughput Microscopy. *Cytometry Part A* **77A**, 52-63 (2010).
21. Borejdo,J. & Burlacu,S. Measuring Orientation of Actin-Filaments Within A Cell - Orientation of Actin in Intestinal Microvilli. *Biophysical Journal* **65**, 300-309 (1993).
22. Humphries,M.J. Integrin structure. *Biochem. Soc. Trans.* **28**, 311-339 (2000).
23. Alon,R. & Dustin,M.L. Force as a facilitator of integrin conformational changes during leukocyte arrest on blood vessels and antigen-presenting cells. *Immunity*. **26**, 17-27 (2007).
24. Puklin-Faucher,E., Gao,M., Schulten,K., & Vogel,V. How the headpiece hinge angle is opened: New insights into the dynamics of integrin activation. *J. Cell Biol.* **175**, 349-360 (2006).
25. Puklin-Faucher,E. & Sheetz,M.P. The mechanical integrin cycle. *J. Cell Sci.* **122**, 179-186 (2009).
26. Geiger,B. & Yamada,K.M. Molecular architecture and function of matrix adhesions. *Cold Spring Harb. Perspect. Biol.* **3**, (2011).
27. Vogel,V. & Sheetz,M. Local force and geometry sensing regulate cell functions. *Nat. Rev. Mol. Cell Biol.* **7**, 265-275 (2006).
28. Mogilner,A. & Oster,G. Cell motility driven by actin polymerization. *Biophys. J.* **71**, 3030-3045 (1996).
29. Nobes,C.D. & Hall,A. Rho GTPases control polarity, protrusion, and adhesion during cell movement. *J. Cell Biol.* **144**, 1235-1244 (1999).
30. Geiger,B., Spatz,J.P., & Bershadsky,A.D. Environmental sensing through focal adhesions. *Nat. Rev. Mol. Cell Biol.* **10**, 21-33 (2009).
31. Choi,C.K. *et al.* Actin and alpha-actinin orchestrate the assembly and maturation of nascent adhesions in a myosin II motor-independent manner. *Nat. Cell Biol.* **10**, 1039-1050 (2008).
32. Zaidel-Bar,R., Ballestrem,C., Kam,Z., & Geiger,B. Early molecular events in the assembly of matrix adhesions at the leading edge of migrating cells. *J. Cell Sci.* **116**, 4605-4613 (2003).
33. Gregor,M. *et al.* Mechanosensing through focal adhesion-anchored intermediate filaments. *FASEB J.* **28**, 715-729 (2014).
34. Schwarz,U.S. & Gardel,M.L. United we stand: integrating the actin cytoskeleton and cell-matrix adhesions in cellular mechanotransduction. *J. Cell Sci.* **125**, 3051-3060 (2012).
35. Oakes,P.W. & Gardel,M.L. Stressing the limits of focal adhesion mechanosensitivity. *Curr. Opin. Cell Biol.* **30**, 68-73 (2014).
36. Khatau,S.B. *et al.* A perinuclear actin cap regulates nuclear shape. *Proc. Natl. Acad. Sci. U. S. A* **106**, 19017-19022 (2009).
37. Khatau,S.B., Kim,D.H., Hale,C.M., Bloom,R.J., & Wirtz,D. The perinuclear actin cap in health and disease. *Nucleus*. **1**, 337-342 (2010).
38. Hotulainen,P. *et al.* Defining mechanisms of actin polymerization and depolymerization during dendritic spine morphogenesis. *J. Cell Biol.* **185**, 323-339 (2009).

39. Burridge,K. & Wittchen,E.S. The tension mounts: Stress fibers as force-generating mechanotransducers. *Journal of Cell Biology* **200**, 9-19 (2013).
40. Nagayama,K., Yamazaki,S., Yahiro,Y., & Matsumoto,T. Estimation of the mechanical connection between apical stress fibers and the nucleus in vascular smooth muscle cells cultured on a substrate. *J. Biomech.* **47**, 1422-1429 (2014).
41. Kim,D.H., Cho,S., & Wirtz,D. Tight coupling between nucleus and cell migration through the perinuclear actin cap. *J. Cell Sci.* **127**, 2528-2541 (2014).
42. Vishavkarma,R. *et al.* Role of actin filaments in correlating nuclear shape and cell spreading. *PLoS. One.* **9**, e107895 (2014).
43. Chancellor,T.J., Lee,J., Thodeti,C.K., & Lele,T. Actomyosin tension exerted on the nucleus through nesprin-1 connections influences endothelial cell adhesion, migration, and cyclic strain-induced reorientation. *Biophys. J.* **99**, 115-123 (2010).
44. Chambliss,A.B. *et al.* The LINC-anchored actin cap connects the extracellular milieu to the nucleus for ultrafast mechanotransduction. *Sci. Rep.* **3**, 1087 (2013).
45. Crisp,M. *et al.* Coupling of the nucleus and cytoplasm: role of the LINC complex. *J. Cell Biol.* **172**, 41-53 (2006).
46. Starr,D.A. KASH and SUN proteins. *Current Biology* **21**, R414-R415 (2011).
47. Padmakumar,V.C. *et al.* The inner nuclear membrane protein Sun1 mediates the anchorage of Nesprin-2 to the nuclear envelope. *Journal of Cell Science* **118**, 3419-3430 (2005).
48. Zhong,Z., Wilson,K.L., & Dahl,K.N. Beyond lamins other structural components of the nucleoskeleton. *Methods Cell Biol.* **98**, 97-119 (2010).
49. Sosa,B.A., Rothbaler,A., Kutay,U., & Schwartz,T.U. LINC complexes form by binding of three KASH peptides to domain interfaces of trimeric SUN proteins. *Cell* **149**, 1035-1047 (2012).
50. Gundersen,G.G. & Worman,H.J. Nuclear positioning. *Cell* **152**, 1376-1389 (2013).
51. Haque,F. *et al.* SUN1 interacts with nuclear lamin A and cytoplasmic nesprins to provide a physical connection between the nuclear lamina and the cytoskeleton. *Mol. Cell Biol.* **26**, 3738-3751 (2006).
52. Pajerowski,J.D., Dahl,K.N., Zhong,F.L., Sammak,P.J., & Discher,D.E. Physical plasticity of the nucleus in stem cell differentiation. *Proc. Natl. Acad. Sci. U. S. A* **104**, 15619-15624 (2007).
53. Dahl,K.N., Ribeiro,A.J., & Lammerding,J. Nuclear shape, mechanics, and mechanotransduction. *Circ. Res.* **102**, 1307-1318 (2008).
54. Gruenbaum,Y., Margalit,A., Goldman,R.D., Shumaker,D.K., & Wilson,K.L. The nuclear lamina comes of age. *Nat. Rev. Mol. Cell Biol.* **6**, 21-31 (2005).
55. Broers,J.L. *et al.* Decreased mechanical stiffness in LMNA-/- cells is caused by defective nucleo-cytoskeletal integrity: implications for the development of laminopathies. *Hum. Mol. Genet.* **13**, 2567-2580 (2004).
56. Ho,C.Y. & Lammerding,J. Lamins at a glance. *J. Cell Sci.* **125**, 2087-2093 (2012).
57. Lammerding,J. *et al.* Lamins A and C but not lamin B1 regulate nuclear mechanics. *J. Biol. Chem.* **281**, 25768-25780 (2006).

Chapter 1

58. Versaevel,M., Grevesse,T., & Gabriele,S. Regulation of Nuclear Shape and Function with Cell Elongation. *Biophysical Journal* **104**, 151A (2013).
59. Simon,D.N. & Wilson,K.L. The nucleoskeleton as a genome-associated dynamic 'network of networks'. *Nat. Rev. Mol. Cell Biol.* **12**, 695-708 (2011).
60. Dechat,T. *et al.* Nuclear lamins: major factors in the structural organization and function of the nucleus and chromatin. *Genes Dev.* **22**, 832-853 (2008).
61. Zuela,N., Bar,D.Z., & Gruenbaum,Y. Lamins in development, tissue maintenance and stress. *Embo Reports* **13**, 1070-1078 (2012).
62. Gonzalez-Suarez,I., Redwood,A.B., & Gonzalo,S. Loss of A-type lamins and genomic instability. *Cell Cycle* **8**, 3860-3865 (2009).
63. Houben,F., Ramaekers,F.C., Snoeckx,L.H., & Broers,J.L. Role of nuclear lamina-cytoskeleton interactions in the maintenance of cellular strength. *Biochim. Biophys. Acta* **1773**, 675-686 (2007).
64. Poh,Y.C. *et al.* Dynamic force-induced direct dissociation of protein complexes in a nuclear body in living cells. *Nat. Commun.* **3**, 866 (2012).
65. Zwerger,M. *et al.* Myopathic lamin mutations impair nuclear stability in cells and tissue and disrupt nucleocytoskeletal coupling. *Hum. Mol. Genet.* **22**, 2335-2349 (2013).
66. Kim,D.H. & Wirtz,D. Cytoskeletal tension induces the polarized architecture of the nucleus. *Biomaterials* **48**, 161-172 (2015).
67. Khatau,S.B. *et al.* A perinuclear actin cap regulates nuclear shape. *Proc. Natl. Acad. Sci. U. S. A* **106**, 19017-19022 (2009).
68. Brosig,M., Ferralli,J., Gelman,L., Chiquet,M., & Chiquet-Ehrismann,R. Interfering with the connection between the nucleus and the cytoskeleton affects nuclear rotation, mechanotransduction and myogenesis. *Int. J. Biochem. Cell Biol.* **42**, 1717-1728 (2010).
69. Lee,J.S. *et al.* Nuclear lamin A/C deficiency induces defects in cell mechanics, polarization, and migration. *Biophys. J.* **93**, 2542-2552 (2007).
70. Lammerding,J. *et al.* Lamin A/C deficiency causes defective nuclear mechanics and mechanotransduction. *J. Clin. Invest* **113**, 370-378 (2004).
71. Ho,C.Y., Jaalouk,D.E., Vartiainen,M.K., & Lammerding,J. Lamin A/C and emerin regulate MKL1-SRF activity by modulating actin dynamics. *Nature* **497**, 507-511 (2013).
72. Swift,J. *et al.* Nuclear lamin-A scales with tissue stiffness and enhances matrix-directed differentiation. *Science* **341**, 1240104 (2013).
73. Broers,J.L., Ramaekers,F.C., Bonne,G., Yaou,R.B., & Hutchison,C.J. Nuclear lamins: laminopathies and their role in premature ageing. *Physiol Rev.* **86**, 967-1008 (2006).
74. Worman,H.J. Nuclear lamins and laminopathies. *J. Pathol.* **226**, 316-325 (2012).
75. Vlcek,S. & Foisner,R. Lamins and lamin-associated proteins in aging and disease. *Current Opinion in Cell Biology* **19**, 298-304 (2007).
76. Schirmer,E.C. & Foisner,R. Proteins that associate with lamins: many faces, many functions. *Experimental Cell Research* **313**, 2167-2179 (2007).

77. Lammerding, J. *et al.* Lamin A/C deficiency causes defective nuclear mechanics and mechanotransduction. *J. Clin. Invest* **113**, 370-378 (2004).
78. Hutchison, C.J., Alvarez-Reyes, M., & Vaughan, O.A. Lamins in disease: why do ubiquitously expressed nuclear envelope proteins give rise to tissue-specific disease phenotypes? *Journal of Cell Science* **114**, 9-19 (2001).
79. Hutchison, C.J. & Worman, H.J. A-type lamins: Guardians of the soma? *Nature Cell Biology* **6**, 1062-1067 (2004).
80. Liu, B.H. *et al.* Genomic instability in laminopathy-based premature aging. *Nature Medicine* **11**, 780-785 (2005).
81. Meinke, P., Makarov, A.A., Lê Thành, P., Sadurska, D., Schirmer, E.C. Nucleoskeleton dynamics and functions in health and disease. *Cell Health and Cytoskeleton* **7**, 55-69 (2015).
82. Burke, B. & Stewart, C.L. The laminopathies: the functional architecture of the nucleus and its contribution to disease. *Annu. Rev. Genomics Hum. Genet.* **7**, 369-405 (2006).
83. Meinke, P. *et al.* Muscular dystrophy-associated SUN1 and SUN2 variants disrupt nuclear-cytoskeletal connections and myonuclear organization. *PLoS Genet.* **10**, e1004605 (2014).
84. Liang, W.C. *et al.* TMEM43 Mutations in Emery-Dreifuss Muscular Dystrophy-Related Myopathy. *Annals of Neurology* **69**, 1005-1013 (2011).
85. Bione, S. *et al.* Identification of A Novel X-Linked Gene Responsible for Emery-Dreifuss Muscular-Dystrophy. *Nature Genetics* **8**, 323-327 (1994).
86. Zhang, Q.P. *et al.* Nesprin-1 and -2 are involved in the pathogenesis of Emery-Dreifuss muscular dystrophy and are critical for nuclear envelope integrity. *Human Molecular Genetics* **16**, 2816-2833 (2007).
87. Li, P., Meinke, P., Huong, L.T.T., Wehnert, M., & Noegel, A.A. Contribution of SUN1 Mutations to the Pathomechanism in Muscular Dystrophies. *Human Mutation* **35**, 452-461 (2014).
88. Taranum, S. *et al.* LINC complex alterations in DMD and EDMD/CMT fibroblasts. *European Journal of Cell Biology* **91**, 614-628 (2012).
89. Muntoni, F. *et al.* Disease severity in dominant Emery Dreifuss is increased by mutations in both emerin and desmin proteins. *Brain* **129**, 1260-1268 (2006).
90. Harrison, R.G. The cultivation of tissues in extraneous media as a method of morphogenetic study. *The Anatomical Record* **6**, 181-193 (1912).
91. WEISS, P. Experiments on cell and axon orientation in vitro; the role of colloidal exudates in tissue organization. *J. Exp. Zool.* **100**, 353-386 (1945).
92. Dreier, B. *et al.* Early responses of vascular endothelial cells to topographic cues. *Am. J. Physiol Cell Physiol* **305**, C290-C298 (2013).
93. Uttayarat, P., Toworfe, G.K., Dietrich, F., Lelkes, P.I., & Composto, R.J. Topographic guidance of endothelial cells on silicone surfaces with micro- to nanogrooves: orientation of actin filaments and focal adhesions. *J. Biomed. Mater. Res. A* **75**, 668-680 (2005).
94. van Kooten, T.G. & von Recum, A.F. Cell adhesion to textured silicone surfaces: the influence of time of adhesion and texture on focal contact and fibronectin fibril formation. *Tissue Eng* **5**, 223-240 (1999).
95. den Braber, E.T., de Ruijter, J.E., Ginsel, L.A., von Recum, A.F., & Jansen, J.A. Quantitative analysis of fibroblast morphology on microgrooved surfaces with various groove and ridge dimensions. *Biomaterials* **17**, 2037-2044 (1996).

96. Dunn,G.A. & Brown,A.F. Alignment of fibroblasts on grooved surfaces described by a simple geometric transformation. *J. Cell Sci.* **83**, 313-340 (1986).
97. Oakley,C. & Brunette,D.M. The sequence of alignment of microtubules, focal contacts and actin filaments in fibroblasts spreading on smooth and grooved titanium substrata. *J. Cell Sci.* **106 (Pt 1)**, 343-354 (1993).
98. Walboomers,X.F., Ginsel,L.A., & Jansen,J.A. Early spreading events of fibroblasts on microgrooved substrates. *J. Biomed. Mater. Res.* **51**, 529-534 (2000).
99. Walboomers,X.F., Monaghan,W., Curtis,A.S., & Jansen,J.A. Attachment of fibroblasts on smooth and microgrooved polystyrene. *J. Biomed. Mater. Res.* **46**, 212-220 (1999).
100. Saito,A.C., Matsui,T.S., Ohishi,T., Sato,M., & Deguchi,S. Contact guidance of smooth muscle cells is associated with tension-mediated adhesion maturation. *Exp. Cell Res.* **327**, 1-11 (2014).
101. Britland,S. *et al.* Synergistic and hierarchical adhesive and topographic guidance of BHK cells. *Exp. Cell Res.* **228**, 313-325 (1996).
102. Clark,P., Connolly,P., Curtis,A.S., Dow,J.A., & Wilkinson,C.D. Topographical control of cell behaviour: II. Multiple grooved substrata. *Development* **108**, 635-644 (1990).
103. Teixeira,A.I., Abrams,G.A., Bertics,P.J., Murphy,C.J., & Nealey,P.F. Epithelial contact guidance on well-defined micro- and nanostructured substrates. *J. Cell Sci.* **116**, 1881-1892 (2003).
104. Sarkar,S., Dadhania,M., Rourke,P., Desai,T.A., & Wong,J.Y. Vascular tissue engineering: microtextured scaffold templates to control organization of vascular smooth muscle cells and extracellular matrix. *Acta Biomater.* **1**, 93-100 (2005).
105. Dunn,G.A. & Heath,J.P. A new hypothesis of contact guidance in tissue cells. *Exp. Cell Res.* **101**, 1-14 (1976).
106. Ohara,P.T. & Buck,R.C. Contact guidance in vitro. A light, transmission, and scanning electron microscopic study. *Exp. Cell Res.* **121**, 235-249 (1979).
107. Zimerman,B. *et al.* Formation of focal adhesion-stress fibre complexes coordinated by adhesive and non-adhesive surface domains. *IEE. Proc. Nanobiotechnol.* **151**, 62-66 (2004).
108. Ventre,M., Natale,C.F., Rianna,C., & Netti,P.A. Topographic cell instructive patterns to control cell adhesion, polarization and migration. *J. R. Soc. Interface* **11**, 20140687 (2014).
109. Gerecht,S. *et al.* The effect of actin disrupting agents on contact guidance of human embryonic stem cells. *Biomaterials* **28**, 4068-4077 (2007).
110. Chen,C.S., Mrksich,M., Huang,S., Whitesides,G.M., & Ingber,D.E. Geometric control of cell life and death. *Science* **276**, 1425-1428 (1997).
111. Chen,C.S., Alonso,J.L., Ostuni,E., Whitesides,G.M., & Ingber,D.E. Cell shape provides global control of focal adhesion assembly. *Biochem. Biophys. Res. Commun.* **307**, 355-361 (2003).
112. Alford,P.W., Nesmith,A.P., Seywerd,J.N., Grosberg,A., & Parker,K.K. Vascular smooth muscle contractility depends on cell shape. *Integr. Biol. (Camb.)* **3**, 1063-1070 (2011).
113. Williams,C., Xie,A.W., Yamato,M., Okano,T., & Wong,J.Y. Stacking of aligned cell sheets for layer-by-layer control of complex tissue structure. *Biomaterials* **32**, 5625-5632 (2011).
114. Tamiello,C., Bouten,C.V., & Baaijens,F.P. Competition between cap and basal actin fiber orientation in cells subjected to contact guidance and cyclic strain. *Sci. Rep.* **5**, 8752 (2015).

115. Saez,A., Ghibaudo,M., Buguin,A., Silberzan,P., & Ladoux,B. Rigidity-driven growth and migration of epithelial cells on microstructured anisotropic substrates. *Proc. Natl. Acad. Sci. U. S. A* **104**, 8281-8286 (2007).
116. Wang,J.H., Goldschmidt-Clermont,P., & Yin,F.C. Contractility affects stress fiber remodeling and reorientation of endothelial cells subjected to cyclic mechanical stretching. *Ann. Biomed. Eng* **28**, 1165-1171 (2000).
117. Hayakawa,K., Hosokawa,A., Yabusaki,K., & Obinata,T. Orientation of Smooth Muscle-Derived A10 Cells in Culture by Cyclic Stretching: Relationship between Stress Fiber Rearrangement and Cell Reorientation. *Zoolog. Sci.* **17**, 617-624 (2000).
118. Goldyn,A.M., Kaiser,P., Spatz,J.P., Ballestrem,C., & Kemkemer,R. The kinetics of force-induced cell reorganization depend on microtubules and actin. *Cytoskeleton (Hoboken.)* **67**, 241-250 (2010).
119. Buck,R.C. Reorientation response of cells to repeated stretch and recoil of the substratum. *Exp. Cell Res.* **127**, 470-474 (1980).
120. Barron,V. *et al.* The effect of physiological cyclic stretch on the cell morphology, cell orientation and protein expression of endothelial cells. *J. Mater. Sci. Mater. Med.* **18**, 1973-1981 (2007).
121. Dartsch,P.C. & Betz,E. Response of cultured endothelial cells to mechanical stimulation. *Basic Res. Cardiol.* **84**, 268-281 (1989).
122. Hsu,H.J., Lee,C.F., & Kaunas,R. A dynamic stochastic model of frequency-dependent stress fiber alignment induced by cyclic stretch. *PLoS. One.* **4**, e4853 (2009).
123. Kaunas,R., Usami,S., & Chien,S. Regulation of stretch-induced JNK activation by stress fiber orientation. *Cell Signal.* **18**, 1924-1931 (2006).
124. Lee,C.F., Haase,C., Deguchi,S., & Kaunas,R. Cyclic stretch-induced stress fiber dynamics - dependence on strain rate, Rho-kinase and MLCK. *Biochem. Biophys. Res. Commun.* **401**, 344-349 (2010).
125. Ngu,H. *et al.* Effect of focal adhesion proteins on endothelial cell adhesion, motility and orientation response to cyclic strain. *Ann. Biomed. Eng* **38**, 208-222 (2010).
126. Wang,J.H., Goldschmidt-Clermont,P., Wille,J., & Yin,F.C. Specificity of endothelial cell reorientation in response to cyclic mechanical stretching. *J. Biomech.* **34**, 1563-1572 (2001).
127. Wille,J.J., Ambrosi,C.M., & Yin,F.C. Comparison of the effects of cyclic stretching and compression on endothelial cell morphological responses. *J. Biomech. Eng* **126**, 545-551 (2004).
128. Yoshigi,M., Clark,E.B., & Yost,H.J. Quantification of stretch-induced cytoskeletal remodeling in vascular endothelial cells by image processing. *Cytometry A* **55**, 109-118 (2003).
129. Boccafoschi,F., Bosetti,M., Gatti,S., & Cannas,M. Dynamic fibroblast cultures: response to mechanical stretching. *Cell Adh. Migr.* **1**, 124-128 (2007).
130. Jungbauer,S., Gao,H., Spatz,J.P., & Kemkemer,R. Two characteristic regimes in frequency-dependent dynamic reorientation of fibroblasts on cyclically stretched substrates. *Biophys. J.* **95**, 3470-3478 (2008).
131. Neidlinger-Wilke,C., Grood,E.S., Wang,J.H.C., Brand,R.A., & Claes,L. Cell alignment is induced by cyclic changes in cell length: studies of cells grown in cyclically stretched substrates. *J. Orthop. Res.* **19**, 286-293 (2001).
132. Dartsch,P.C. & Hammerle,H. Orientation response of arterial smooth muscle cells to mechanical stimulation. *Eur. J. Cell Biol.* **41**, 339-346 (1986).

133. Standley,P.R., Cammarata,A., Nolan,B.P., Purgason,C.T., & Stanley,M.A. Cyclic stretch induces vascular smooth muscle cell alignment via NO signaling. *Am. J. Physiol Heart Circ. Physiol* **283**, H1907-H1914 (2002).
134. Kakisis,J.D., Avgerinos,E.D., & Liapis,C.D. Analysis of the evidence behind the ESVS guidelines for the invasive treatment of carotid stenosis. *Acta Chir Belg.* **109**, 574-580 (2009).
135. Hsu,H.J., Lee,C.F., Locke,A., Vanderzyl,S.Q., & Kaunas,R. Stretch-induced stress fiber remodeling and the activations of JNK and ERK depend on mechanical strain rate, but not FAK. *PLoS. One.* **5**, e12470 (2010).
136. Tondon,A., Hsu,H.J., & Kaunas,R. Dependence of cyclic stretch-induced stress fiber reorientation on stretch waveform. *J. Biomech.* **45**, 728-735 (2012).
137. Zhang,L., Kahn,C.J., Chen,H.Q., Tran,N., & Wang,X. Effect of uniaxial stretching on rat bone mesenchymal stem cell: orientation and expressions of collagen types I and III and tenascin-C. *Cell Biol. Int.* **32**, 344-352 (2008).
138. Yamane,M. *et al.* Rac1 activity is required for cardiac myocyte alignment in response to mechanical stress. *Biochem. Biophys. Res. Commun.* **353**, 1023-1027 (2007).
139. Wang,H., Ip,W., Boissy,R., & Grood,E.S. Cell orientation response to cyclically deformed substrates: experimental validation of a cell model. *J. Biomech.* **28**, 1543-1552 (1995).
140. Faust,U. *et al.* Cyclic stress at mHz frequencies aligns fibroblasts in direction of zero strain. *PLoS. One.* **6**, e28963 (2011).
141. Banes,A.J., Gilbert,J., Taylor,D., & Monbureau,O. A new vacuum-operated stress-providing instrument that applies static or variable duration cyclic tension or compression to cells in vitro. *J. Cell Sci.* **75**, 35-42 (1985).
142. Deibler,M., Spatz,J.P., & Kemkemer,R. Actin fusion proteins alter the dynamics of mechanically induced cytoskeleton rearrangement. *PLoS. One.* **6**, e22941 (2011).
143. Yoshigi,M., Hoffman,L.M., Jensen,C.C., Yost,H.J., & Beckerle,M.C. Mechanical force mobilizes zyxin from focal adhesions to actin filaments and regulates cytoskeletal reinforcement. *J. Cell Biol.* **171**, 209-215 (2005).
144. Smith,M.A., Hoffman,L.M., & Beckerle,M.C. LIM proteins in actin cytoskeleton mechanoresponse. *Trends Cell Biol.* **24**, 575-583 (2014).
145. Smith,M.A. *et al.* LIM domains target actin regulators paxillin and zyxin to sites of stress fiber strain. *PLoS. One.* **8**, e69378 (2013).
146. Lele,T.P. *et al.* Mechanical forces alter zyxin unbinding kinetics within focal adhesions of living cells. *J. Cell Physiol* **207**, 187-194 (2006).
147. Guo,W.H. & Wang,Y.L. Retrograde fluxes of focal adhesion proteins in response to cell migration and mechanical signals. *Mol. Biol. Cell* **18**, 4519-4527 (2007).
148. Hayakawa,K., Sato,N., & Obinata,T. Dynamic reorientation of cultured cells and stress fibers under mechanical stress from periodic stretching. *Exp. Cell Res.* **268**, 104-114 (2001).
149. Goldyn,A.M., Rioja,B.A., Spatz,J.P., Ballestrem,C., & Kemkemer,R. Force-induced cell polarisation is linked to RhoA-driven microtubule-independent focal-adhesion sliding. *J. Cell Sci.* **122**, 3644-3651 (2009).
150. Ahmed,W.W., Kural,M.H., & Saif,T.A. A novel platform for in situ investigation of cells and tissues under mechanical strain. *Acta Biomater.* **6**, 2979-2990 (2010).
151. Wang,J.H. Substrate deformation determines actin cytoskeleton reorganization: A mathematical modeling and experimental study. *J. Theor. Biol.* **202**, 33-41 (2000).

152. Wei,Z., Deshpande,V.S., McMeeking,R.M., & Evans,A.G. Analysis and interpretation of stress fiber organization in cells subject to cyclic stretch. *J. Biomech. Eng* **130**, 031009 (2008).
153. Kaunas,R. & Hsu,H.J. A kinematic model of stretch-induced stress fiber turnover and reorientation. *J. Theor. Biol.* **257**, 320-330 (2009).
154. Obbink-Huizer,C. *et al.* Computational model predicts cell orientation in response to a range of mechanical stimuli. *Biomech. Model. Mechanobiol.* **13**, 227-236 (2014).
155. De,R. & Safran,S.A. Dynamical theory of active cellular response to external stress. *Phys. Rev. E. Stat. Nonlin. Soft. Matter Phys.* **78**, 031923 (2008).
156. Livne,A., Bouchbinder,E., & Geiger,B. Cell reorientation under cyclic stretching. *Nat. Commun.* **5**, 3938 (2014).
157. Wille,J.J., Ambrosi,C.M., & Yin,F.C. Comparison of the effects of cyclic stretching and compression on endothelial cell morphological responses. *J. Biomech. Eng* **126**, 545-551 (2004).
158. Dartsch,P.C., Hammerle,H., & Betz,E. Orientation of cultured arterial smooth muscle cells growing on cyclically stretched substrates. *Acta Anat. (Basel)* **125**, 108-113 (1986).
159. Neidlinger-Wilke,C., Grood,E., Claes,L., & Brand,R. Fibroblast orientation to stretch begins within three hours. *J Orthop. Res.* **20**, 953-956 (2002).
160. Wang,D. *et al.* A stretching device for imaging real-time molecular dynamics of live cells adhering to elastic membranes on inverted microscopes during the entire process of the stretch. *Integr. Biol. (Camb.)* **2**, 288-293 (2010).
161. Greiner,A.M., Chen,H., Spatz,J.P., & Kemkemer,R. Cyclic tensile strain controls cell shape and directs actin stress fiber formation and focal adhesion alignment in spreading cells. *PLoS. One.* **8**, e77328 (2013).
162. Wang,J.H. & Grood,E.S. The strain magnitude and contact guidance determine orientation response of fibroblasts to cyclic substrate strains. *Connect. Tissue Res.* **41**, 29-36 (2000).
163. Wang,J.H., Grood,E.S., Florer,J., & Wenstrup,R. Alignment and proliferation of MC3T3-E1 osteoblasts in microgrooved silicone substrata subjected to cyclic stretching. *J. Biomech.* **33**, 729-735 (2000).
164. Wang,J.H., Yang,G., Li,Z., & Shen,W. Fibroblast responses to cyclic mechanical stretching depend on cell orientation to the stretching direction. *J. Biomech.* **37**, 573-576 (2004).
165. Prodanov,L. *et al.* The interaction between nanoscale surface features and mechanical loading and its effect on osteoblast-like cells behavior. *Biomaterials* **31**, 7758-7765 (2010).
166. Ahmed,W.W. *et al.* Myoblast morphology and organization on biochemically micro-patterned hydrogel coatings under cyclic mechanical strain. *Biomaterials* **31**, 250-258 (2010).
167. Tamiello,C., Bouten,C.V., & Baaijens,F.P. Competition between cap and basal actin fiber orientation in cells subjected to contact guidance and cyclic strain. *Sci. Rep.* **5**, 8752 (2015).
168. Kurpinski,K., Chu,J., Hashi,C., & Li,S. Anisotropic mechanosensing by mesenchymal stem cells. *Proc. Natl. Acad. Sci. U. S. A* **103**, 16095-16100 (2006).
169. Houtchens,G.R., Foster,M.D., Desai,T.A., Morgan,E.F., & Wong,J.Y. Combined effects of microtopography and cyclic strain on vascular smooth muscle cell orientation. *J. Biomech.* **41**, 762-769 (2008).
170. Papadaki,M. *et al.* Tissue engineering of functional cardiac muscle: molecular, structural, and electrophysiological studies. *Am. J. Physiol Heart Circ. Physiol* **280**, H168-H178 (2001).

Chapter 1

171. Discher,D.E., Janmey,P., & Wang,Y.L. Tissue cells feel and respond to the stiffness of their substrate. *Science* **310**, 1139-1143 (2005).
172. Bischofs,I.B. & Schwarz,U.S. Cell organization in soft media due to active mechanosensing. *Proceedings of the National Academy of Sciences of the United States of America* **100**, 9274-9279 (2003).
173. Yeung,T. *et al.* Effects of substrate stiffness on cell morphology, cytoskeletal structure, and adhesion. *Cell Motil. Cytoskeleton* **60**, 24-34 (2005).
174. Engler,A.J. *et al.* Myotubes differentiate optimally on substrates with tissue-like stiffness: pathological implications for soft or stiff microenvironments. *Journal of Cell Biology* **166**, 877-887 (2004).
175. Georges,P.C. & Janmey,P.A. Cell type-specific response to growth on soft materials. *Journal of Applied Physiology* **98**, 1547-1553 (2005).
176. Engler,A. *et al.* Substrate compliance versus ligand density in cell on gel responses. *Biophysical Journal* **86**, 388A (2004).
177. Pelham,R.J. & Wang,Y.L. Cell locomotion and focal adhesions are regulated by substrate flexibility. *Proceedings of the National Academy of Sciences of the United States of America* **94**, 13661-13665 (1997).

Chapter 2

Competition between cap and basal actin fiber orientation in cells subjected to contact guidance and cyclic strain

In vivo, adhesive cells continuously respond to a complex range of physical cues coming from the surrounding microenvironment by remodeling their cytoskeleton. Topographical and mechanical cues applied separately have been shown to affect the orientation of the actin stress fibers. Here we investigated the combined effects of contact guidance by topographical cues and cyclic uniaxial strain on actin cytoskeleton orientation of vascular derived cells. We devised a modular setup of stretchable circular and elliptic elastomeric microposts, capable to expose the cells to both contact guidance and cyclic uniaxial strain. A competition occurs between these cues when both contact guidance and strain are oriented along the same direction. For the first time we show that this competition originates from the distinct response of perinuclear basal and actin cap fibers: while basal fibers follow the contact guidance cue, actin cap fibers respond to the cyclic strain by strain avoidance. We also show that nuclear orientation follows actin cap fiber orientation, suggesting that actin cap fibers are responsible for cellular reorientation. Taken together, these findings may have broad implications in understanding the response of cells to combined topographical and mechanical cues.

The contents of this chapter are based on:

Tamiello, C., Bouten, C.V., & Baaijens, F.P. Competition between cap and basal actin fiber orientation in cells subjected to contact guidance and cyclic strain. *Sci. Rep.* **5**, 8752 (2015).

Introduction

The implication of topographical and mechanical cues in physiological behaviours of adhesive cells such as proliferation, migration and differentiation has become increasingly evident¹⁻⁴. Consequently, the potential to manipulate cell behaviour by modulating physical cues of the surrounding microenvironment has raised great interest for tissue engineering purposes.

The effects of singular topographical and mechanical cues on the behaviour of adhesive cells have extensively been studied. Cells actively recognize topographical cues ranging from sub-micrometer to ten micrometers in size. As a consequence, cells organize their cytoskeleton in order to align and migrate along the topographical cue. This phenomenon is known as contact guidance⁵⁻⁸. Furthermore, the impact of mechanical loading on cellular behaviour has also been of broad attention. For instance, epithelial cells, endothelial cells and adjacent fibroblasts withstand and respond to strains in the surrounding microenvironment resulting from physiological processes such as embryonic development⁹, blood pulsation^{10,11} and muscular contraction respectively¹². *In vitro* investigations revealed that cyclic uniaxial strain has an effect on the alignment of cells. Most types of adhesive cells respond to cyclic uniaxial strain with a strain avoidance response, thus by reorienting almost perpendicular to the strain direction¹³⁻¹⁶. Taken together, the results of these studies suggest that topographical and mechanical cues might act as competitive cues for cellular alignment. However, investigations and understanding of the influence and interplay of topographical and mechanical cues on cell behaviour are currently lacking. This kind of studies would give insight on cell adaptation in the native cellular microenvironment, which includes a combination of topographical as well as mechanical cues. Furthermore, findings from these studies would be of great benefit for the area of (*in situ*) tissue engineering of load-bearing tissues. In micro structural scaffolds, cell organization and subsequent neo-tissue formation are indeed a function of both topographical cues and (cyclic) strain imposed on the tissue.

The ability of adhesive cells to sense and respond to the physical properties of their microenvironment lies in the interaction and communication between the cells and the surrounding environment, which results in the translation of physical stimuli into biochemical signals (mechanotransduction)¹⁷. Key cellular components for mechanotransduction are focal adhesions and actin stress fibers. These elements are responsible for cellular mechanosensing and propagation of the signals to the nucleus. By the transduction of the signals to the genome, the final adaptation of the cell to the developing microenvironment occurs¹⁸. However, recent studies report on the existence of a direction transduction mechanism going from the surrounding mechanical stimuli of the extracellular environment to the nucleus¹⁹. This physical interconnection is the perinuclear actin cap, a subset of actin stress fibers running on top of the nucleus and directly interacting with it via nuclear membrane proteins. The perinuclear actin cap has been shown to dominate the (early) mechanoreponse of adherent cells, as opposed to basal fibers which do not have a direct connection to the nucleus¹⁹⁻²³.

In this study, we concentrate on the combined effects of topographical and mechanical cues, namely contact guidance and cyclic uniaxial strain, on the actin cytoskeleton of vascular derived cells (HVSC). In particular, we aim at understanding which cue dominates the response of stress fiber orientation, when cyclic uniaxial strain and contact guidance are applied together. We cultured HVSC on top of a

modular setup of arrays of elastomeric microposts of different lengths (1, 3 and 6 μm), cross sections (circular and elliptical) and bound to a stretchable membrane. By analyzing stress fiber orientation, we were able to dissect between the effects of stiffness, contact guidance and cyclic strain. We observed that stress fiber orientation does not depend on the stiffness. Instead, stress fiber orientation is correlated with the presence of contact guidance and the relative angle between it and the cyclic uniaxial strain. We demonstrate that a competition between contact guidance and strain arises when both cues were applied along the same direction. Further examination of the actin architecture pointed out that such effect involves the distinct response of the perinuclear actin cap fibers and the basal stress fibers. While actin cap fibers are prone to a strain avoidance response, basal actin fiber orientation remains dominated by the contact guidance of the underlying microposts.

Results

Modular setup

The developed modular setup for investigating the combined effects of contact guidance, stiffness and strain on stress fiber orientation consisted of microfabricated elastomeric micropost arrays characterized by different cross sections and lengths, incorporated into a stretching device.

By changing the cross sections we fabricated anisotropic and isotropic microposts, which respectively do and do not induce cellular contact guidance. The geometrical anisotropy was given by an elliptic cross section, which directed cell alignment along the major axis of the ellipse. On the other hand, random cell alignment was obtained with isotropic microposts, which were characterized by a circular cross section (Figure 2.1a).

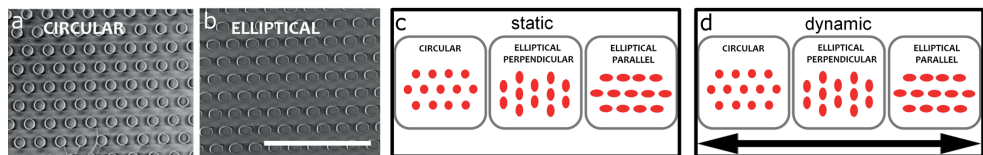


Figure 2.1. Modular setup of elastomeric micropost arrays and experimental conditions. Representative scanning electron micrographs (top view) of hexagonally arranged elastomeric microposts forming a dense hexagonal lattice. Both circular cross section microposts (circular, a) and elliptic cross section microposts (elliptical, b) are shown. Scale bar: 20 μm . Overview of static (c) and dynamic (d) experimental conditions. Schematic representation of neighbouring arrays of elastomeric microposts representing the three experimental conditions in red. 1) Circular microposts, 2) elliptical perpendicular microposts characterized by elliptic cross section which major axis is perpendicular to the strain direction and 3) elliptical parallel microposts characterized by elliptic cross section which major axis is parallel to the strain direction. The double-arrow headed line represents the strain direction for the dynamic condition.

The choice of three microposts lengths (1, 3 and 6 μm) allowed mimicking different substrate stiffnesses (Table 2.1). In fact, the bending stiffness of each micropost depends on its length when the cross section is kept unchanged^{47,48}. Finally, the micropost arrays were designed in array clusters that represent different experimental conditions. As a result, we could study the response to several topographical conditions in one experiment. The experimental conditions studied are referred to as

circular, elliptical perpendicular and elliptical parallel, where perpendicular (parallel) means that the major axis of the elliptic cross section is perpendicular (parallel) to the strain direction (**Figure 2.1b**). For control studies in static conditions (static), the micropost arrays were bound to glass coverslips. Instead, for studying the effects of cyclic uniaxial strain (dynamic), the arrays were bound to commercially available flexible-bottomed culture wells. The cyclic uniaxial strain applied to the membrane bound to the microposts was transferred to the micropost tops and, therefore, was able to exert strains to the adherent cells attached to the micropost tops²⁴.

Table 2.1. Library of microposts used for the modular setup

micropost array type	radius/semi-axis (μm)	c.t.c. dist. (μm)	L (μm)	micropost bending stiffness k (nN/ μm)
circular	$r = 1$	4	1	774
	$r = 1$	4	3	94
	$r = 1$	4	6	16
elliptical	$a = 1.5$ $b = 0.87$	4	1	$k(a) = 1252$ $k(b) = 895$
	$a = 1.5$ $b = 0.87$	4	3	$k(a) = 215$ $k(b) = 98$
	$a = 1.5$ $b = 0.87$	4	6	$k(a) = 41$ $k(b) = 16$
	$a = 1.5$ $b = 0.87$	4	6	$k(a) = 41$ $k(b) = 16$
	$a = 1.5$ $b = 0.87$	4	6	$k(a) = 41$ $k(b) = 16$
	$a = 1.5$ $b = 0.87$	4	6	$k(a) = 41$ $k(b) = 16$

In addition to the geometrical factors (radius/semi-axis (r , a , b), center to center distance (c.t.c.) and length (L)), also the corresponding micropost spring constants (k) are shown.

Contact guidance dictates stress fiber orientation independent of micropost stiffness under static conditions

To validate our modular setup, HVSC were cultured in static conditions on circular and elliptical microposts coated with rhodamine labelled fibronectin. After 33 hours cells were fixed and observed for stress fiber orientation. While no preferred orientation was observed on circular microposts (**Figure 2.2 a, c, e, g, i and k**), stress fibers aligned with the major axis of the elliptical perpendicular microposts (**Figure 2.2 b, d, f, h, j and l**).

Examination of stress fiber orientations on micropost lengths of 1, 3 and 6 μm , respectively, showed similar stress fiber distributions for the circular and elliptical perpendicular cases indicating that the stress fiber distributions are independent of the micropost bending stiffness (**Figure 2.2 and Figure 2.3**).

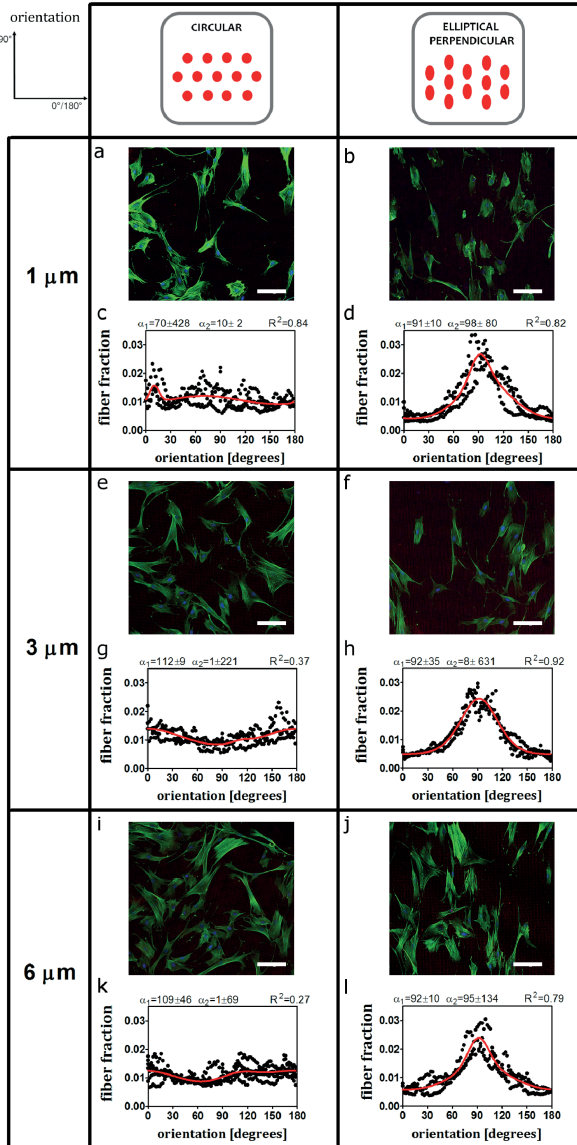


Figure 2.2. Stress fiber orientation follows contact guidance prescribed by the major axis of elliptical microposts while it is random on circular microposts. Representative fluorescent images (actin stress fibers in green, nucleus in blue, rhodamine conjugated fibronectin coated on top of microposts in red) and bimodal fits of the stress fiber orientation (including the first and the second dominant fiber angle with standard deviations and R-squared value). (a, c, e, g, i and m) For circular microposts stress fibers do not show a preferred orientation. (b, d, f, h, j and n) For elliptical perpendicular, stress fibers align with the micropost major axis (about 90°). Scale bars represent 100 μm . The data reported are results from $n = 3$ independent experiments, at least 40 cells were considered per each condition. Results for elliptical horizontal microposts were omitted.

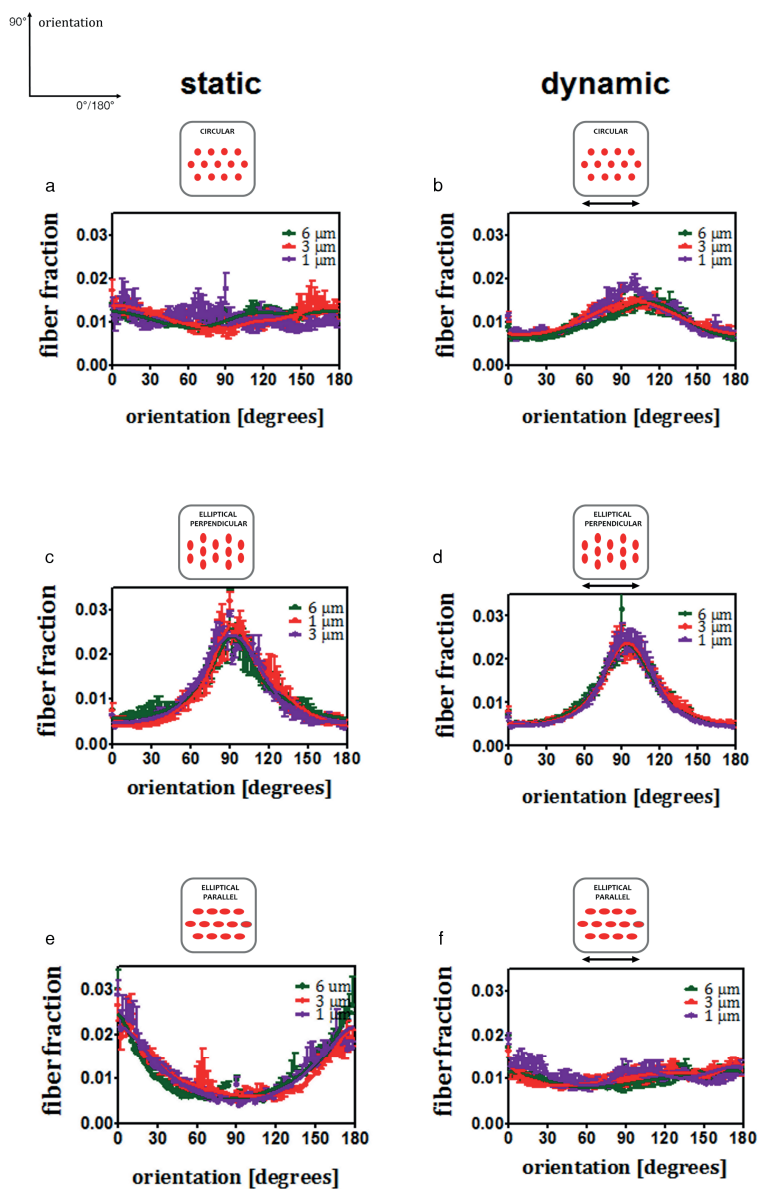


Figure 2.3. Stress fiber distribution is independent of micropost bending stiffness. Bimodal fits of the stress fiber orientation for each experimental condition. On each graph the stress fiber distributions for 1 μm , 3 μm and 6 μm microposts are reported. Data are represented by mean \pm SEM. In static condition, 3 experiments were performed; in dynamic condition, 3 experiments were performed with 1 μm microposts, while 7 experiments were performed in the other experimental conditions.

Competition between contact guidance and strain avoidance determines stress fiber orientation

To study the relative impact of contact guidance and cyclic uniaxial straining on stress fiber orientation, we exposed HVSC seeded onto elastomeric microposts to cyclic uniaxial straining in the horizontal direction at 0.5 Hz in frequency and 6.8 % in amplitude for 19 hours. The stress fiber distribution was analysed after cell fixation (**Figure 2.4**). On circular microposts, stress fibers displayed a strain avoidance response, as they oriented toward the (near) perpendicular alignment with respect to the strain direction (**Figure 2.4** a, d, g, j, m and p). On elliptical perpendicular microposts, in dynamic conditions, stress fibers exhibited alignment with the major axis of the elliptical microposts (**Figure 2.4** b, e, h, k, n and q). This result was comparable to the stress fiber orientation in static conditions and shows that stress fibers remained perpendicular to the strain direction. In contrast, on elliptical parallel microposts, we observed a change in the stress fiber distributions compared to the static conditions. The lack of a preferred orientation pointed to a competition between strain avoidance and contact guidance due the cyclic uniaxial straining and contact guidance invoked by the elliptic cross section of the microposts (**Figure 2.4** c, f, i, l, o and r). In summary, these results show that stress fiber reorientation is affected by the orientation of the elliptical microposts compared to the straining direction. Indeed, on the elliptical parallel microposts the application of strain results in hindered strain avoidance when compared to circular microposts. In agreement with our findings under static conditions, stress fiber orientation under cyclic uniaxial straining did not show any correlation with the bending stiffness of the (**Figure 2.3** and **Figure 2.4**).

Distinct responses of basal and perinuclear actin cap fibers to contact guidance and cyclic strain explain the competition between these cues

We investigated whether the stress fiber organization within the cell itself can explain the results of the combined effects of contact guidance and cyclic uniaxial strain. Therefore, we acquired z-stacks of confocal images of actin fibers stained of HVSC cultured on 1 μm micropost arrays in static and dynamic conditions. We subsequently quantified the mean orientation of the perinuclear stress fibers both at the basal and actin cap levels (**Figure 2.5a**).

In all static experimental conditions, the preferred orientation of basal and actin cap fibers was similar (**Figure 2.5** o, p and q (static)) indicating that in both zones of the cell, actin fibers ran invariably parallel to each other in HVSC adhered to circular and elliptical microposts. However, under dynamic conditions, the combination of cyclic uniaxial strain and contact guidance had distinct effects on basal and actin cap fiber orientation depending on the experimental condition. On circular microposts, cyclic uniaxial strain elicited reorientation of both basal and actin cap fibers to a mean orientation of $\langle\alpha\rangle\approx 59^\circ$. The shift between the mean orientation at the basal and actin cap levels was not significant ($\langle\alpha\rangle\approx 60^\circ$ and $\langle\alpha\rangle\approx 59^\circ$ for basal and actin cap respectively), indicating that both basal and actin cap fibers showed a similar strain avoidance response (**Figure 2.5** c, d and o). In case of elliptical perpendicular microposts the mean orientations of basal and actin cap fibers were not significantly different compared to the static condition (**Figure 2.5p**). The mean direction was $\langle\alpha\rangle\approx 85^\circ$ and $\langle\alpha\rangle\approx 81^\circ$ for basal and actin cap fibers respectively.

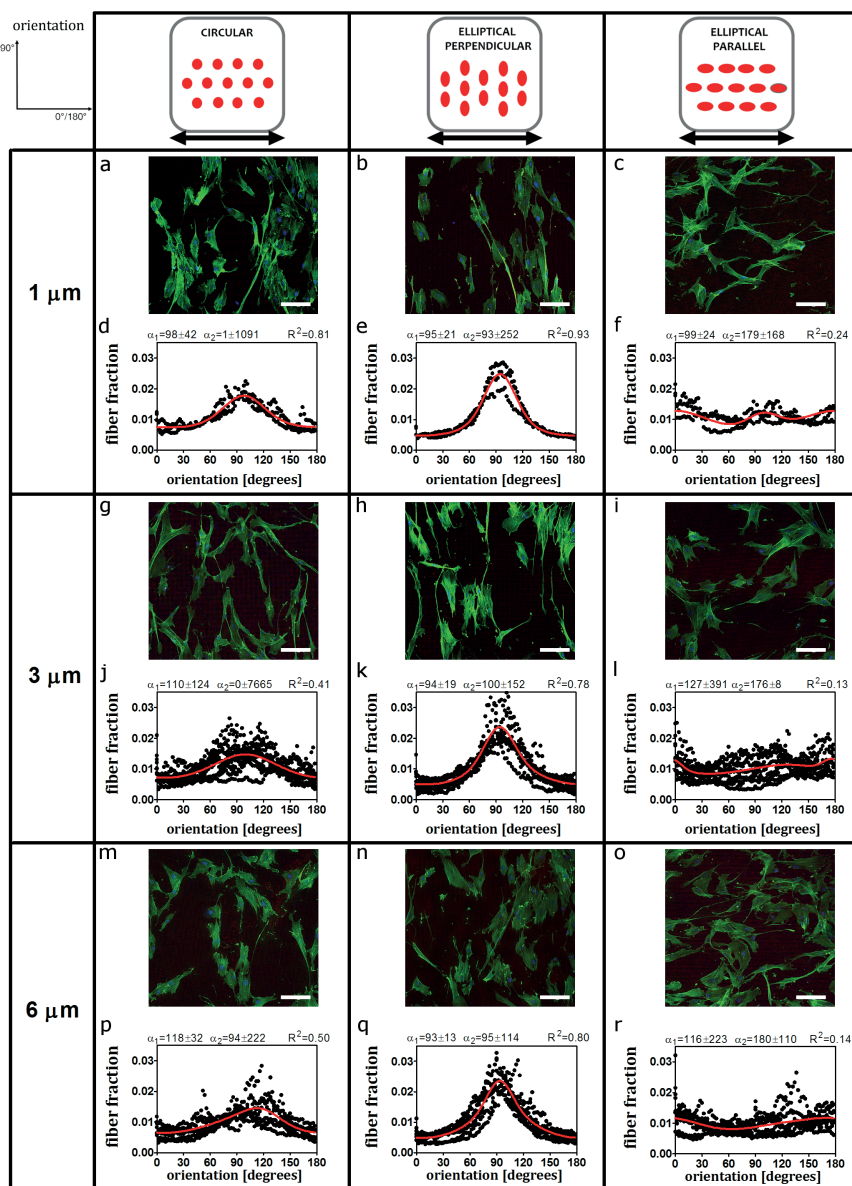


Figure 2.4. Stress fiber orientation shows strain avoidance response on circular and elliptical perpendicular microposts, but not on elliptical parallel microposts after cyclic uniaxial strain. Outcomes of stress fiber orientation upon cyclic uniaxial strain for circular, elliptical perpendicular and elliptical parallel microposts. Representative fluorescent images (actin stress fibers in green, nucleus in blue, rhodamine conjugated fibronectin coated on top of microposts in red) and bimodal fits of the stress fiber orientation (including the first and the second dominant fiber angle with standard deviations and R-squared value) after 19 hours of cyclic uniaxial strain prescribed in the horizontal direction corresponding to a 0°/180° angle. (a, d, g, l, o and r) For circular microposts subjected to dynamic loading, stress fibers reorient shows strain avoidance (perpendicular to the strain direction). (b, e, h, m, p and s) For elliptical perpendicular, stress fibers align with the micropost major axis which is also perpendicular to the mechanical load. (c, f, i, n, q and t) For elliptical parallel microposts, no preferred stress fiber alignment was observed. Scale bars represent 100 μm . The data reported come from $n = 3$ independent experiments in case of 1 μm microposts, $n = 7$ independent experiments in the other cases.

This indicates that stress fibers remained almost perpendicular to the strain direction, which is also the direction of the contact guidance provided by the microposts (**Figure 2.5 f and g**). In contrast, on elliptical parallel microposts we measured a significant shift between the mean orientation of basal and actin cap fibers. While the basal fibers had a mean orientation of $\langle\alpha\rangle\approx 4^\circ$ and thus were mainly oriented along the micropost major axis, the actin cap fiber mean orientation shifted to $\langle\alpha\rangle\approx 19^\circ$ (** $p<0.01$), reflecting the tendency of the basal fibers to remain aligned with the micropost major axis, thus with the contact guidance (**Figure 2.5q**). Instead, actin cap fibers were sensitive to the cyclic uniaxial strain cue and, consequently, they tended to orient away from the strain direction, neglecting the contact guidance cue.

We also assessed cell orientation in HVSC adhered to elliptical parallel microposts in dynamic conditions, as we observed that about half of the cells remained parallel to the microposts while about half reoriented in a different direction. We classified as “reoriented” the cells which orientation angle was $\theta>20^\circ$ (relative to the micropost major axis and strain direction) and as “remaining” the ones which orientation angle was $\theta<20^\circ$ (**Figure 2.5b**). In reoriented cells the difference between actin cap and basal fibers was $\approx 20^\circ$ ($\langle\alpha\rangle\approx 6^\circ$ for basal and $\langle\alpha\rangle\approx 26^\circ$ for actin cap, *** $p<0.001$) (**Figure 2.5 i, j and r** (left)). Instead, for the remaining cells, the shift was not significant $\approx 10^\circ$ ($\langle\alpha\rangle\approx 3^\circ$ for basal and $\langle\alpha\rangle\approx 13^\circ$ for actin cap) (**Figure 2.5 l, m and r** (right)). Summarizing, these data demonstrate a zone-based response to contact guidance and cyclic uniaxial straining due to the basal fibers and actin cap fibers independently.

Z-stacks were also studied to determine the impact of contact guidance and cyclic uniaxial straining on nuclear orientation. Since the actin cap is physically connected to the nucleus, we hypothesized that the actin cap orientation would mediate nuclear reorientation²⁰. To test this hypothesis we measured the nuclear orientation and compared it with the mean actin cap fiber orientation. Under static conditions, nuclei were oriented in the direction of actin cap fibers, which ran parallel to the basal fibers (**Figure 2.5 o, p and q** (static)). Upon cyclic uniaxial straining, the nucleus was oriented in the same direction as actin cap fibers in all the experimental conditions (**Figure 2.5 e, h, k, n, o, p, q and r**). These results indicate that a correlation exists between nuclear and actin cap orientation.

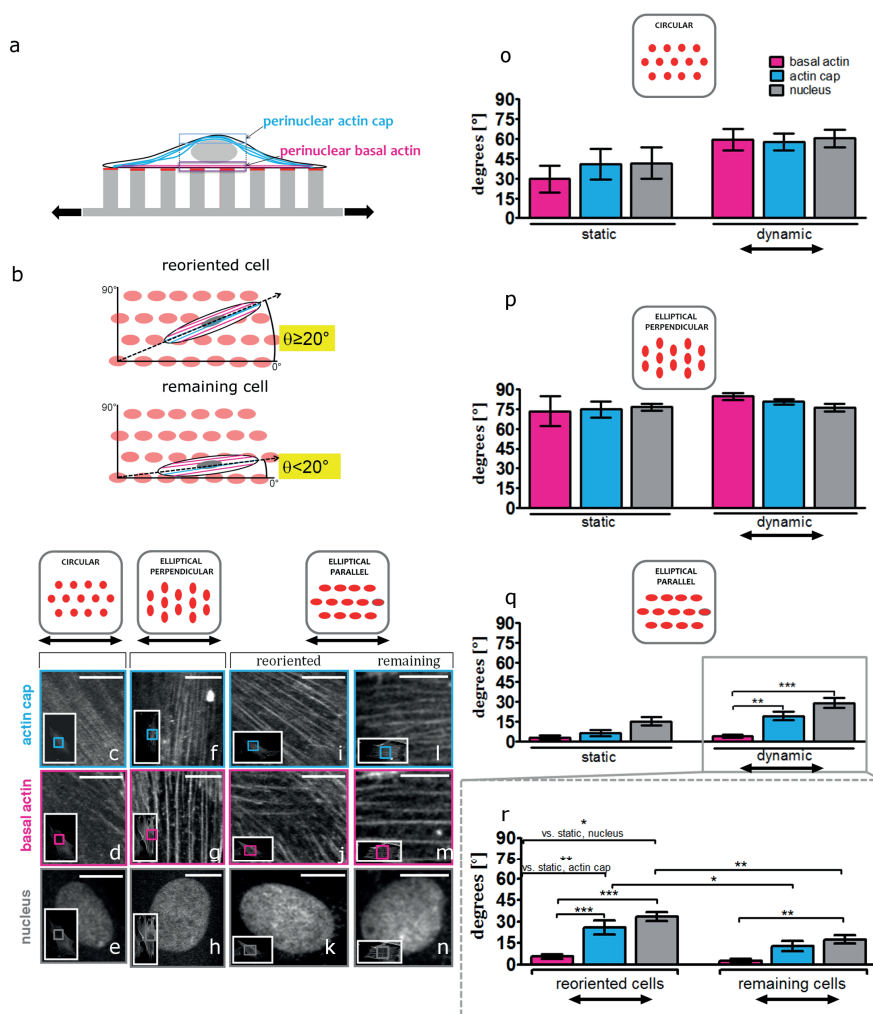


Figure 2.5. Basal stress fibers follow contact guidance, while actin cap stress fibers and nucleus display strain avoidance.

(a) Schematic of an adhesive cell cultured on top of stretchable microposts coated with rhodamine conjugated fibronectin (red). Status of actin organization at the perinuclear actin cap (light blue) and basal (magenta) is examined by confocal microscopy. (b) Schematic representation of the classification of reoriented (top) and remaining (bottom) cells on top the elliptical parallel microposts. The orientation angle θ between the micropost major axis and the major axis of a cell determined by fitting an ellipse to the cell's outer boundary. If $\theta \geq 20^\circ$, the cell is categorized as reoriented, while, if $\theta < 20^\circ$, the cell is categorized as remaining. (c-n) Representative confocal fluorescent micrographs of perinuclear actin cap fibers, basal fibers and nucleus of HVSC cultured on circular, elliptical perpendicular and elliptical parallel microposts (reoriented (left column) and remaining cell (right column)) after 19 hours of cyclic uniaxial strain applied in the horizontal direction corresponding to a 0° angle. Insets show the whole imaged cell, with inner boxes framing the zoomed regions shown in the main panels. For all images in this figure actin stress fibers are visualized with FITC-Phalloidin. Scale bars represent $10 \mu\text{m}$ (o-q) Mean orientation of basal and actin cap fibers and nucleus in static conditions (left side) and after 19 hours of cyclic uniaxial strain (dynamic) (right side) for circular (o), elliptical perpendicular (p) and elliptical parallel microposts (q). In panel o, 5 cells in static and 12 cells in dynamic conditions were analyzed. In panel p, 6 cells in static and 14 cells in dynamic conditions were analyzed. In panel q, 6 cells in static and 24 cells in dynamic conditions were analyzed. (r) Mean orientation of basal and actin cap fibers and nucleus in dynamic conditions for reoriented ($n = 13$) and remaining ($n = 11$) cells on elliptical parallel microposts. For all graphs, values represent means \pm SEM. ***, **, * indicate p value <0.001, <0.01, <0.05 respectively.

Discussion

The main objective of this investigation was to gain insight on the stress fiber orientation in vascular derived cells subjected to contact guidance and cyclic uniaxial strain. To do this we devised a modular setup made of stretchable elastomeric microposts capable to invoke cellular contact guidance. Analysis of stress fiber orientation at the cell level revealed that neither contact guidance nor strain avoidance dominates when contact guidance and strain are prescribed along the same direction. Our findings at actin fiber level give further explanation for this observation: two distinct responses are observed in perinuclear basal and actin cap fibers. Within the experimental timeframe (19 hours) and the strain regime considered, perinuclear actin cap fibers predominantly respond to cyclic uniaxial strain and not to contact guidance, while basal stress fiber orientation is dictated by contact guidance only.

Our study also shows that the modular setup of stretchable elastomeric microposts can be used to study the independent and combined effects of contact guidance and strain on stress fiber orientation of adhesive cells. Since in static conditions we observed stress fiber alignment along the major axis of the elliptical microposts, we show evidence that our system can impose contact guidance.

We were also able to simulate a range of substrate stiffnesses, by changing the micropost length (**Table 2.1**). However, we did not detect any difference in stress fiber orientation, in both static and dynamic conditions. Presumably, in the range of the stiffnesses studied, the arrangement of stress fibers, which correlates with the arrangement and maturation of focal adhesions, could be regulated by the topographical cues only and not by stiffness. This observation is consistent with the results of Seo *et al.*, who reported regulation of focal adhesions localization by topographical variations in micro patterns, independently of the substrate stiffness²⁵. Yet, the cellular stiffness sensing mechanism is a subject of intensive debate because conflicting evidences have emerged from recent studies trying to elucidate whether bulk substrate stiffness or extracellular matrix protein tethering regulates the mechanosensitive cellular response²⁶⁻³¹.

Our observations about stress fiber reorientation on circular microposts are consistent with studies on flat, isotropic, 2D substrates subjected to cyclic uniaxial strain^{14-16, 32, 33}. We show indeed that stress fiber orientation follows a strain avoidance response. The effects on cellular orientation upon simultaneous stimulation by contact guidance and mechanical loading was topic of previous studies. However, in these investigations, micro-structures such as grooves³³⁻³⁵ or micro-patterned lines^{36, 37} were employed. The spatial confinement of focal adhesions and stress fibers in the z-direction resulting from the use of grooves could be critical for stress fiber reorientation³⁸. In case of micro-patterned lines used to impose cell alignment, stress fiber reorientation is restricted to the width of the lines. To avoid these concerns, and in order to allow free cell and stress fiber reorientation, we have used contact guidance invoked by elliptical micropost cross sections. The perpendicular and parallel arrangement of the elliptical microposts enabled us to show the direct effects on stress fiber reorientation of cyclic uniaxial strain combined with contact guidance. We demonstrated that the combination of the two cues does not affect stress fiber reorientation in case of elliptical microposts oriented perpendicular to the strain direction. In this case, both basal and actin cap fibers remained oriented perpendicularly to the strain direction. Thus, it is likely that cells grown perpendicularly to

the strain direction become insensitive to strain, as they can maintain their orientation³⁹. Conversely, cyclic uniaxial strain and contact guidance resulted in antagonistic responses when we exposed the cells to both cues applied along the same direction. In this case the strain avoidance response was only partly seen; about half of the cells remain aligned with the micropost and half of the cells reorient away from the strain direction. When looking at the whole group of cells, we found that the perinuclear actin cap fibers reoriented at about 19° to the strain/micropost major axis direction, while the perinuclear basal fibers remained aligned with the underlying microposts. This observation can probably be attributed to two reasons. Firstly, the enhanced mechanosensing characterizing the actin cap associated focal adhesions make them more sensitized for mechanical loading. Actin cap associated focal adhesions have indeed been shown to differ from basal actin fiber associated conventional focal adhesions, e.g. they dominate cell mechanosensing over a wide range of matrix stiffness²⁰. Secondly, each actin cap fiber is anchored to the microposts only at the two actin cap associated focal adhesions. This makes the actin cap less entangled to the underlying microposts as compared to the basal stress fibers, which instead contact the microposts in numerous conventional focal adhesions. As a consequence, the response of actin cap fibers mechanical loading can be more dynamic. Being both explanations not mutually exclusive, we suggest that the peculiarity of the actin cap focal adhesions and the structural organization of the actin cap itself might both play a role in triggering the strain avoidance response of actin cap fibers.

Additionally, we revealed a correlation between actin cap fiber orientation and nuclear orientation both in static and dynamic conditions. In particular, even when cyclic uniaxial strain was applied along the same direction of contact guidance, we observed that actin cap fibers and nucleus oriented at the same angle. These observations lead us to hypothesize that the reorientation of the actin cap brings along nuclear reorientation. We relate this phenomenon to the fact that the actin cap is directly anchored to the nucleus²³ through linkers of nucleoskeleton and cytoskeleton complexes⁴⁰. In support to this, a recent study by Kim *et al.* also demonstrates the direct involvement of actin cap fibers in controlling nuclear rotation and translocation⁴¹.

Taken all the results into consideration, within the experimental conditions of this study, we speculate the following mechanistic model for vascular derived cells grown on elastomeric microposts exposed to cyclic uniaxial strain. In absence of contact guidance, actin cap fibers respond to cyclic uniaxial strain by reorienting towards a direction almost perpendicular to the strain. Therewith, the physical anchorage of the actin cap to the nucleus results in the reorientation of the nucleus co-aligned with actin cap fibers. While being reoriented, the nucleus and, thus, the genome receive the signals coming from the actin cap mechanosensing. This leads the nucleus to orchestrate the reorientation of the whole cell, including the reorientation of basal stress fibers, and thus the reorientation of the whole cell. If contact guidance and cyclic uniaxial strain are applied in the same direction, an active competition between the cues arises resulting in half cell population remaining aligned with the contact guidance cue and half reorienting at an angle $\geq 20^\circ$ from the contact guidance cue (**Figure 2.6**). Noticeably, in reoriented cells, actin cap fibers and the nucleus reorient at an angle to the strain direction, while the perinuclear basal actin fibers remain aligned with the contact guidance cue.

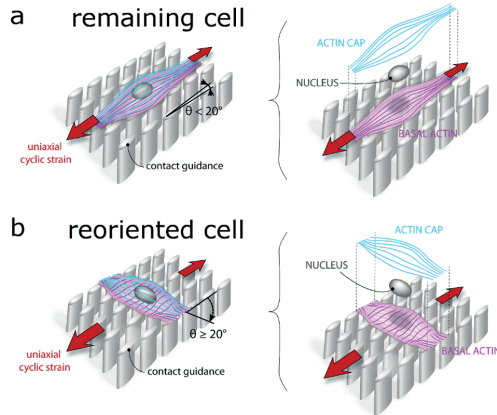


Figure 2.6. Schematic drawing of the effects of cyclic uniaxial strain on actin stress fiber orientation of vascular derived cells cultured on elliptical microposts aligned with the direction of strain. Our results revealed two kinds of cellular responses: remaining and reoriented cells. (a) The remaining cells remain aligned with the contact guidance cue provided by the micropost elliptical cross section. The perinuclear basal and actin cap fibers run parallel to each other. (b) Reoriented cells orient themselves at an angle $\geq 20^\circ$. This orientation is mainly given by actin cap fibers orientation. These fibers have a strain avoidance response. Perinuclear basal actin fibers instead do not reorient but remain aligned with the contact guidance cue. The nuclear orientation is similar to the actin cap orientation. Figure by Anthal Smits.

Clearly it needs to be further investigated whether such cell behaviour is dependent on the straining regime and the experimental time frame. Moreover, it will be important to consider the influence of cell density, as the formation of a confluent cell sheet might alter the actin cap fiber behaviour.

In conclusion, this study sheds light on the response of the actin cytoskeleton and the nucleus of vascular derived cells subjected to a combination of topographical and mechanical cues such as contact guidance and cyclic uniaxial strain on planar substrates. We show that the combination of these cues can result in competing effects on the stress fiber orientation response. We demonstrated that actin cap fibers have a pronounced response to strain and are responsible for nuclear strain avoidance response. On the other hand, the perinuclear basal actin fibers appear to be more sensitized to the contact guidance cue. These findings have implications for tissue engineering where contact guidance and cyclic uniaxial strain are involved.

Materials and Methods

Cell cultures

The cells used in this study are human vascular-derived cells (HVSC) harvested from the vena Saphena magna from the Catharina Hospital Eindhoven. The tissues are considered surgical rest material, whereby the patient has been informed on potential use of rest material for scientific research purposes⁴². Verbal informed consent was obtained from patients and tissues were handed over anonymously, without any patient-specific information except for gender. Procedures for secondary use of patient material were followed as described in the Dutch code of conduct for responsible use of patient material. According to the Dutch medical scientific research with human subjects act (WMO), secondary use of patient material does not need review by a Medical Ethics Examination Committee. HVSC have previously been characterized as myofibroblasts⁴³. The HVSC were cultured in advanced Dulbecco Modified Eagle's Medium (DMEM, Invitrogen) supplemented with 10% Fetal Bovine Serum (Greiner Bio-one), 1% penicillin/streptomycin (Lonza), 1% GlutaMax (Invitrogen). Only cells at passage 7 were used in this study. Myofibroblasts have been shown to be sensitive and respond to mechanical cues^{44,45}. This makes this cell type interesting for our study.

Micropost design and fabrication

The elastomeric microposts arrays were fabricated via standard photolithography processes, according to previous protocols⁴⁶. Briefly, silicon wafers were patterned with an array of cylindrical pits. Afterwards, poly(dimethylsiloxane) (PDMS, Sylgard 184, Dow Corning), was poured over the silicon template, spincoated 30 seconds at 1000 rpm and cured at 110° C for 20 minutes to reach a Young's Modulus of 1.8 MPa. The micropost arrays were then peeled off the wafer. Our microposts were characterized by a radius r of 1 μm in case of circular cross section (circular microposts) and semi-major axis a of 1.50 μm and semi-minor axis b of 0.87 μm in case of elliptic cross section (elliptical microposts). The densely packed microposts (center to center distance, c.t.c. of 4 μm) formed arrays of 1.0 x 1.0 mm with spaces of 150 μm between them. The micropost lengths used in this study were (L) of 1, 3 and 6 μm . Together, we created a library of microposts for our modular setup. As the bending stiffness of each micropost is solely determined by its geometry, we modulated substrate stiffness by varying micropost length^{47, 48}. Finite element analysis was used to calculate the force–displacement relationship, leading to the micropost bending stiffnesses reported in **Table 2.1 (Figure 2.7)**. Micropost arrays were bonded to glass coverslips (Menzel) or six-well plates (Uniflex Series Culture Plates, Flexcell FX 5000, Flexcell International, Hillsborough, NC, USA) using a corona discharger. To promote irreversible bonding, the sample was kept in oven at 60° overnight.

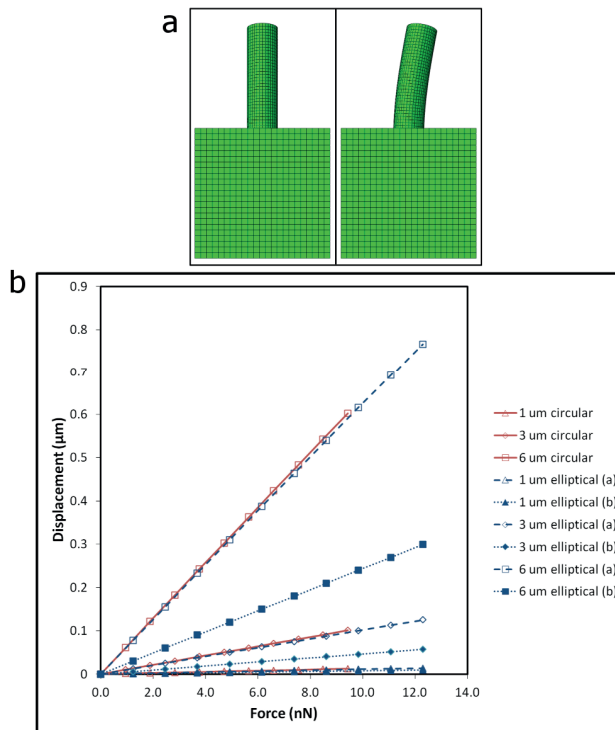


Figure 2.7. Micropost bending properties. (A) Finite element model of the micropost in its initial (left) and deformed shape (right). A thick layer of PDMS substrate underlying the micropost was taken under consideration in the FE simulations. (B) Plot of force vs. displacement as calculated from the finite element model for each micropost type.

Micro-contact printing on microposts

A flat PDMS stamp was cleaned and then incubated with 50 $\mu\text{g}/\text{ml}$ rhodamine fibronectin (Cytoskeleton, Denver, CO, USA) in deionized water for 1 hour. The stamp was dried under sterile airflow and deposited gently on the micropost array, previously subjected to UV ozone treatment. A gentle pressure was applied to the stamp. The contact between the microposts and the stamp was ensured for at least 1 minute. Subsequently the substrates were sterilized in 70% ethanol and immersed in 0.4% Pluronic F127 (Sigma-Aldrich, St. Louis, MO) in PBS for 1 hour to prevent non-specific protein absorption to the non-functionalized surface of the PDMS microposts. Finally the substrates were rinsed with sterile MilliQ water and kept in PBS before use⁴⁶.

Loading protocol

Mechanical straining experiments were performed using FX-5000 Flexcell system (Flexcell Corp. (McKeesport, PA)). Cells were seeded on the microposts at a density of 2500 cells/cm² and were allowed to adhere overnight before the strain experiment (24 hours). The Uniflex membranes bound to the microposts were uniaxially and cyclically stretched (10 %, 0.5 Hz) for 19 hours. The total duration of the experiment, from seeding to fixation, was 33 hours. Strain fields on the elastomeric microposts were characterized within the central region of the Flexcell membrane on which the microposts

were bound by use of a Matlab-based (Mathworks Inc., Natick, MA) digital image correlation (DIC) code. A random pattern of fiducial markers was inked on the microposts bonded to the FlexCell membrane and images were recorded by mounted on a Zeiss stereomicroscope. By applying our uniaxial straining protocol (10%, 0.5 Hz, sine wave), results showed that in the area under consideration the strain field covers a range between 5% and 7%. Strains in the x direction (direction of applied strain) are 6.8% on average, and strains in y direction show a compression of 2%. Cells under static conditions grown for 33 hours on microposts bonded to glass coverslips were used as control.

Immunofluorescence labelling

After culturing, HVSC were washed with PBS and fixed with 4% formaldehyde in PBS (Sigma-Aldrich) for 10 minutes at room temperature. Next, they were permeabilized with 0.1% Triton-X-100 (Merck) in PBS for 10 minutes and incubated with 3% bovine serum albumin (BSA) in PBS in order to block non-specific binding. Subsequently, samples were incubated with FITC-conjugated phalloidin (1:500, Phalloidin-Atto 488, Sigma) and DAPI (100 ng/ml, Fluka) for 1 hour at room temperature for immunofluorescence of F-actin and nucleus. Finally, the samples were rinsed in PBS and mounted onto glass slides using Mowiol.

Microscopy and image analysis

For fluorescence visualization of actin stress fibers, cells were imaged using an inverted microscope (Zeiss Axiovert 200M, Zeiss, Gottingen, Germany), using 10 x/0.25 Ph1 e or 20 x/0.25 Ph1 objectives. Imaging of basal fibers, actin cap fibers and nucleus was performed with an inverted confocal microscope (Zeiss LSM 510 META), using a C-Apochromat water-immersion objective (63x, NA=1.2). The laser-scanning microscope was used according to the manufacturer's specification, using an argon laser at 488nm (30 mW) for FITC-conjugated phalloidin and Chameleon (Chameleon Ultra II, Coherent, Santa Clara, CA) for DAPI at 760 nm. Z-series were generated by collecting a stack consisting of optical sections using a step size of 0.45-1.00 μm in the z-direction.

Quantification of cell and nuclear orientation

Cell and nuclear orientation was measured with ImageJ. An ellipse was fitted to each cell outline and to the nucleus. The orientation angle θ , of the long axis of the ellipse with respect to the strain direction was measured.

Quantification of stress fibers orientation

Fluorescence images of HVSC stained for actin stress fibers and confocal images of the basal fibers and actin cap were analyzed with Fiji (<http://fiji.sc/Fiji>)⁴⁹. The orientation of actin stress fibers was calculated with respect to the straining direction for dynamic conditions or with respect to the x-axis of the image taken as a reference for static conditions. Fluorescence images of stress fibers were processed with Fiji before stress fiber tracking. Background subtraction and contrast enhancement were performed on the green channel images.

Finally, directionality analysis for stress fiber orientation was conducted with Fiji using the Directionality plug-in (<http://fiji.sc/wiki/index.php/Directionality>) based on the FFT of each image by means of fitting a Gaussian to the FFT signal, measuring its peak position. The directionality

algorithm takes into account only aligned elements in an entire image and is not sensitive to random elements. For each experiment, at least 40 cells were taken into consideration.

Analysis of the mean orientation of basal and actin cap fibers was calculated as follows. In the z-stacks, a rectangular region of interested was selected in order to fit the nucleus. The z-stack slices containing the basal and actin cap fibers were analyzed using the Directionality plug-in in Fiji.

Data analysis

For each individual experiment the average fiber fraction for each angle was calculated. Subsequently, these fractions were fitted with a bimodal function. The fiber distributions were approximated by a bi-modal periodic normal probability distribution function using nonlinear least-square approximation algorithm^{50, 51}:

$$\phi_f(\gamma) = A_1 \exp\left[\frac{\cos[2(\gamma - \alpha_1)] + 1}{\beta_1}\right] + A_2 \exp\left[\frac{\cos[2(\gamma - \alpha_2)] + 1}{\beta_2}\right] \quad (1)$$

Hereby, $\phi_f(\gamma)$ is the fiber fraction as a function of the fiber angle γ . Variables α_1 and α_2 are the two main fiber angles while β_1 and β_2 represent the dispersities of the two fiber distributions. For cyclic uniaxial straining, an angle of 90° is perpendicular to the strain direction. A_1 and A_2 are scaling factors for the total fiber fractions of the distributions. The quality of the bimodal approximation is represented by the R-squared value.

For the basal and actin cap fibers, analysis of the mean orientation was performed as follows. The main fiber directions (the one with least dispersity) for the basal and actin cap fibers were obtained from the bimodal fitting. The absolute values of these were averaged. Data for the basal and actin cap fibers mean orientation are expressed as mean \pm SEM. Statistical significance of differences between the mean orientations of basal and actin cap of fibers was determined using one-way ANOVA followed by post-hoc Bonferroni multiple comparison tests. A p value of 0.05 was considered significant.

Acknowledgments

This work was supported by NanoNextNL. Christine Obbink-Huizer and Anthal Smits of the department of Biomedical Engineering at the Eindhoven University of Technology (TU/e) are acknowledged for finite element modelling of the microposts and the graphic design of Figure 5, respectively.

References

1. Bettinger,C.J., Langer,R., & Borenstein,J.T. Engineering substrate topography at the micro- and nanoscale to control cell function. *Angew. Chem. Int. Ed Engl.* **48**, 5406-5415 (2009).
2. Kulangara,K., Yang,Y., Yang,J., & Leong,K.W. Nanotopography as modulator of human mesenchymal stem cell function. *Biomaterials* **33**, 4998-5003 (2012).
3. Oakley,C. & Brunette,D.M. The sequence of alignment of microtubules, focal contacts and actin filaments in fibroblasts spreading on smooth and grooved titanium substrata. *J. Cell Sci.* **106 (Pt 1)**, 343-354 (1993).
4. Subramony,S.D. *et al.* The guidance of stem cell differentiation by substrate alignment and mechanical stimulation. *Biomaterials* **34**, 1942-1953 (2013).
5. Dunn,G.A. & Heath,J.P. A new hypothesis of contact guidance in tissue cells. *Exp. Cell Res.* **101**, 1-14 (1976).
6. Flemming,R.G., Murphy,C.J., Abrams,G.A., Goodman,S.L., & Nealey,P.F. Effects of synthetic micro- and nano-structured surfaces on cell behavior. *Biomaterials* **20**, 573-588 (1999).
7. Petrie,R.J., Doyle,A.D., & Yamada,K.M. Random versus directionally persistent cell migration. *Nat. Rev. Mol. Cell Biol.* **10**, 538-549 (2009).
8. Teixeira,A.I., Abrams,G.A., Bertics,P.J., Murphy,C.J., & Nealey,P.F. Epithelial contact guidance on well-defined micro- and nanostructured substrates. *J. Cell Sci.* **116**, 1881-1892 (2003).
9. Fournier,M.F., Sauser,R., Ambrosi,D., Meister,J.J., & Verkhovsky,A.B. Force transmission in migrating cells. *J. Cell Biol.* **188**, 287-297 (2010).
10. Davis,M.J. & Hill,M.A. Signaling mechanisms underlying the vascular myogenic response. *Physiol Rev.* **79**, 387-423 (1999).
11. Deanfield,J.E., Halcox,J.P., & Rabelink,T.J. Endothelial function and dysfunction: testing and clinical relevance. *Circulation* **115**, 1285-1295 (2007).
12. Ateshian,G.A. & Humphrey,J.D. Continuum mixture models of biological growth and remodeling: past successes and future opportunities. *Annu. Rev. Biomed. Eng.* **14**, 97-111 (2012).
13. De,R. & Safran,S.A. Dynamical theory of active cellular response to external stress. *Phys. Rev. E. Stat. Nonlin. Soft. Matter Phys.* **78**, 031923 (2008).
14. Faust,U. *et al.* Cyclic stress at mHz frequencies aligns fibroblasts in direction of zero strain. *PLoS. One.* **6**, e28963 (2011).
15. Kaunas,R., Nguyen,P., Usami,S., & Chien,S. Cooperative effects of Rho and mechanical stretch on stress fiber organization. *Proc. Natl. Acad. Sci. U. S. A* **102**, 15895-15900 (2005).
16. Wang,J.H., Goldschmidt-Clermont,P., Wille,J., & Yin,F.C. Specificity of endothelial cell reorientation in response to cyclic mechanical stretching. *J. Biomech.* **34**, 1563-1572 (2001).
17. Geiger,B., Spatz,J.P., & Bershadsky,A.D. Environmental sensing through focal adhesions. *Nat. Rev. Mol. Cell Biol.* **10**, 21-33 (2009).
18. Fletcher,D.A. & Mullins,R.D. Cell mechanics and the cytoskeleton. *Nature* **463**, 485-492 (2010).
19. Chambliss,A.B. *et al.* The LINC-anchored actin cap connects the extracellular milieu to the nucleus for ultrafast mechanotransduction. *Sci. Rep.* **3**, 1087 (2013).
20. Kim,D.H. *et al.* Actin cap associated focal adhesions and their distinct role in cellular mechanosensing. *Sci. Rep.* **2**, 555 (2012).

21. Kim,D.H., Chambliss,A.B., & Wirtz,D. The multi-faceted role of the actin cap in cellular mechanosensation and mechanotransduction. *Soft. Matter* **9**, 5516-5523 (2013).
22. Nagayama,K., Yamazaki,S., Yahiro,Y., & Matsumoto,T. Estimation of the mechanical connection between apical stress fibers and the nucleus in vascular smooth muscle cells cultured on a substrate. *J. Biomech.* **47**, 1422-1429 (2014).
23. Khatau,S.B., Kim,D.H., Hale,C.M., Bloom,R.J., & Wirtz,D. The perinuclear actin cap in health and disease. *Nucleus.* **1**, 337-342 (2010).
24. Mann,J.M., Lam,R.H.W., Weng,S.N., Sun,Y.B., & Fu,J.P. A silicone-based stretchable micropost array membrane for monitoring live-cell subcellular cytoskeletal response. *Lab on A Chip* **12**, 731-740 (2012).
25. Seo,C.H., Jeong,H., Furukawa,K.S., Suzuki,Y., & Ushida,T. The switching of focal adhesion maturation sites and actin filament activation for MSCs by topography of well-defined micropatterned surfaces. *Biomaterials* **34**, 1764-1771 (2013).
26. Wen,J.H. *et al.* Interplay of matrix stiffness and protein tethering in stem cell differentiation. *Nature Materials* **13**, 979-987 (2014).
27. Trappmann,B. *et al.* Extracellular-matrix tethering regulates stem-cell fate. *Nature Materials* **11**, 642-649 (2012).
28. Chaudhuri,O. *et al.* Extracellular matrix stiffness and composition jointly regulate the induction of malignant phenotypes in mammary epithelium. *Nature Materials* **13**, 970-978 (2014).
29. Chaudhuri,O. & Mooney,D.J. Stem-Cell Differentiation Anchoring Cell-Fate Cues. *Nature Materials* **11**, 568-569 (2012).
30. Kumar,S. Cellular Mechanotransduction Stiffness Does Matter. *Nature Materials* **13**, 918-920 (2014).
31. Evans,N.D. & Gentleman,E. The role of material structure and mechanical properties in cell-matrix interactions. *Journal of Materials Chemistry B* **2**, 2345-2356 (2014).
32. Neidlinger-Wilke,C., Grood,E.S., Wang,J.H.C., Brand,R.A., & Claes,L. Cell alignment is induced by cyclic changes in cell length: studies of cells grown in cyclically stretched substrates. *J. Orthop. Res.* **19**, 286-293 (2001).
33. Wang,J.H. & Grood,E.S. The strain magnitude and contact guidance determine orientation response of fibroblasts to cyclic substrate strains. *Connect. Tissue Res.* **41**, 29-36 (2000).
34. Houtchens,G.R., Foster,M.D., Desai,T.A., Morgan,E.F., & Wong,J.Y. Combined effects of microtopography and cyclic strain on vascular smooth muscle cell orientation. *J. Biomech.* **41**, 762-769 (2008).
35. Wang,J.H., Grood,E.S., Florer,J., & Wenstrup,R. Alignment and proliferation of MC3T3-E1 osteoblasts in microgrooved silicone substrata subjected to cyclic stretching. *J Biomech.* **33**, 729-735 (2000).
36. Gopalan,S.M. *et al.* Anisotropic stretch-induced hypertrophy in neonatal ventricular myocytes micropatterned on deformable elastomers. *Biotechnol. Bioeng.* **81**, 578-587 (2003).
37. Ahmed,W.W. *et al.* Myoblast morphology and organization on biochemically micro-patterned hydrogel coatings under cyclic mechanical strain. *Biomaterials* **31**, 250-258 (2010).
38. Wang,J.H. & Grood,E.S. The strain magnitude and contact guidance determine orientation response of fibroblasts to cyclic substrate strains. *Connect. Tissue Res.* **41**, 29-36 (2000).
39. Shao,Y., Mann,J.M., Chen,W., & Fu,J. Global architecture of the F-actin cytoskeleton regulates cell shape-dependent endothelial mechanotransduction. *Integr. Biol. (Camb.)* **6**, 300-311 (2014).
40. Razafsky,D. & Hodzic,D. Bringing KASH under the SUN: the many faces of nucleo-cytoskeletal connections. *J. Cell Biol.* **186**, 461-472 (2009).

41. Kim,D.H., Cho,S., & Wirtz,D. Tight coupling between nucleus and cell migration through the perinuclear actin cap. *J. Cell Sci.* **127**, 2528-2541 (2014).
42. Schnell,A.M. *et al.* Optimal cell source for cardiovascular tissue engineering: venous vs. aortic human myofibroblasts. *Thorac. Cardiovasc. Surg.* **49**, 221-225 (2001).
43. Mol,A. *et al.* Autologous human tissue-engineered heart valves: prospects for systemic application. *Circulation* **114**, I152-I158 (2006).
44. Hinz,B. The myofibroblast: paradigm for a mechanically active cell. *J. Biomech.* **43**, 146-155 (2010).
45. Tomasek,J.J., Gabbiani,G., Hinz,B., Chaponnier,C., & Brown,R.A. Myofibroblasts and mechano-regulation of connective tissue remodelling. *Nat. Rev. Mol. Cell Biol.* **3**, 349-363 (2002).
46. Yang,M.T., Fu,J., Wang,Y.K., Desai,R.A., & Chen,C.S. Assaying stem cell mechanobiology on microfabricated elastomeric substrates with geometrically modulated rigidity. *Nat. Protoc.* **6**, 187-213 (2011).
47. Park,J. *et al.* Real-time measurement of the contractile forces of self-organized cardiomyocytes on hybrid biopolymer microcantilevers. *Anal. Chem.* **77**, 6571-6580 (2005).
48. Wang,N., Ostuni,E., Whitesides,G.M., & Ingber,D.E. Micropatterning tractional forces in living cells. *Cell Motil. Cytoskeleton* **52**, 97-106 (2002).
49. Schindelin,J. *et al.* Fiji: an open-source platform for biological-image analysis. *Nat. Methods* **9**, 676-682 (2012).
50. Driessen,N.J., Cox,M.A., Bouten,C.V., & Baaijens,F.P. Remodelling of the angular collagen fiber distribution in cardiovascular tissues. *Biomech. Model. Mechanobiol.* **7**, 93-103 (2008).
51. Gasser,T.C. & Holzapfel,G.A. Modeling plaque fissuring and dissection during balloon angioplasty intervention. *Ann. Biomed. Eng* **35**, 711-723 (2007).

Chapter 3

Cellular strain avoidance is regulated by a functional actin cap

In adhesive cells, the relevance of a structural mechanotransduction pathway provided by the perinuclear actin cap stress fibers has recently emerged. Here we investigate the impact of a functional actin cap on regulating cellular adaptive behaviours to topographical cues and uniaxial strain. We used *Imna*-lacking fibroblasts as our tool because they do not develop an intact actin cap but show only a basal layer of actin underneath the nucleus. We found that topographical cues induced alignment in normal and *Imna*-lacking cells, suggesting that topographical signal transmission occurred independently of the integrity of the actin cap. In response to cyclic uniaxial strain instead, *Imna*-lacking cells showed a compromised strain avoidance response, which was completely abolished when topographical cues and uniaxial strain were applied along the same direction. These findings point to the importance of an intact and functional structural mechanotransduction pathway for mediating the cellular response to cyclic strain.

The contents of this chapter are based on:

Tamiello,C., Kamps,M., Baaijens,F.P., Broers,J.L., & Bouten,C.V. Cellular strain avoidance is regulated by a functional actin cap. *Submitted*.

Introduction

Adhesive cells of tissues forming the human body are interconnected with the surrounding extracellular matrix. In physiological conditions, tissues and, consequently, cells are continuously exposed to a broad range of physical stimuli resulting from everyday use. These stimuli must be sensed and translated in appropriate cellular responses in order to maintain tissue homeostasis and functionality¹. This adaptive mechanism, named mechanotransduction, involves structural components, such as focal adhesions (FAs), cytoskeletal elements and nuclear shell, as well as biochemical events which transduce the stimuli from the cellular boundaries to the nucleus. In the nuclear interior, the activation of specific genes allows the orchestration of cellular responses²⁻⁴.

While the biochemical pathways of mechanotransduction have been target of many investigations in the last decades^{2,5,6}, there is growing evidence that a structural mechanotransduction pathway, linking the extracellular matrix to the nucleus, plays an equally important role in regulating cellular adaptive behaviour⁷. The possibility of a fast message passing system was first suggested by observing that the timescale of force propagation to the nucleus outmatches the speed of diffusion based biochemical signals by orders of magnitude⁸⁻¹¹. In addition, Wirtz and co-workers have demonstrated that, in a two-dimensional (2D) environment, the subset of actin stress fibers running on top of the nucleus (actin cap), together with the associated focal adhesions, forms a bridge for the direct transduction of extracellular stimuli all the way to the nuclear genome. This is the result of the direct anchoring of actin cap fibers to the nuclear envelope and the underlying lamina meshwork via LINC (Linker of Nucleoskeleton to the Cytoskeleton) complex proteins¹².

The nuclear lamina, a meshwork made of type V intermediate filaments called lamins, is essential for maintaining cellular structure and functionality. Firstly, it contributes in preserving nuclear shape and stiffness¹³. Next, it is involved in numerous nuclear functions such as chromatin organization, gene expression modulation, transcriptional activities, and epigenetic chromatin modifications¹⁴. Recently, the role of the nuclear lamina has been extended even further. Discher and co-workers found that the nuclear lamina acts as a “mechanostat” and is able to respond to changes in the mechanical properties of the surrounding cellular environment. In particular, it was observed that the nuclear lamina shifts its composition to a stiffer meshwork of protein with increasing stiffness of the surrounding environment. This suggests a major role for the nuclear lamina in mediating mechanosensing and cellular adaptation to the changing physical stimuli^{15, 16}.

The impact of nuclear lamins on cellular mechanics has become evident ever since mutations in the LMNA gene, encoding a family of nuclear lamins (A-type lamins), have been found to be implicated in the onset of a wide array of disease phenotypes. These are collectively called laminopathies, and include diseases such as progeria (HGPS), muscular dystrophies and cardiomyopathies^{17, 18}. However, although progress is being made, the mechanisms underlying this family of diseases remain to be elucidated. Strikingly, the same mutation in the LMNA gene can lead to different phenotypes¹⁹ making mutation analysis insufficient for precise diagnosis and prognosis. Indications that, in laminopathy cells, cellular defects occur (e.g. disruptions of nucleus-cytoskeleton connection by absence of actin cap fibers) in concurrence with dysfunctional mechanotransduction signalling, altered cellular mechanoresponse and cellular mechanical properties²⁰⁻²⁶, point to the relevance of structural mechanotransduction pathway defects as the cause of defective mechanoresponse.

Here, considering the aforementioned abnormalities in mechanotransduction and the additional lack of the actin cap in laminopathy cells^{27, 28}, we have used *Imna*-lacking cells as a tool for studying the relevance of the actin cap in mechanoresponse. We focused in particular on the response to strain and topographical cues (applied separately and simultaneously), since these two cues are relevant in the context of muscular dystrophies and cardiomyopathy, the most common laminopathies²⁹. Much is known about the individual responses of healthy cells to topographical cues and mechanical strain. Normally, tissue cells are able to recognize and respond to topographical cues at the cellular and sub-cellular level, by aligning the cell body and the actin cytoskeleton along the anisotropy of the substrate (contact guidance)^{30,31}. Despite many observational studies, only recently it has been proposed that the molecular mechanisms underlying this phenomenon involve the synergistic effect of cellular tension and adhesion maturation³². When cells are exposed to cyclic uniaxial strain of the underlying substrate, they reorient cell body and cytoskeleton to an angle away from the strain direction, the so called strain avoidance response^{33,34}. Thus, when contact guidance and strain are applied together, the two cues appear to be competing stimuli for actin cytoskeleton orientation response. In a recent study we have investigated the combined effects of strain and contact guidance applied along the same direction on the actin cytoskeleton of myofibroblasts. We demonstrated that the distinct orientation responses of the actin cap and actin basal fibers - found underneath the nucleus and not directly connected to the nuclear envelope - explain the competition between the extracellular stimuli. The actin cap stress fibers are prone to respond to strain, even in presence of contact guidance along the strain direction. Contrarily, the basal actin stress fibers are more sensitive to the topographical features and neglect the strain stimulation³⁵.

To apply contact guidance and cyclic uniaxial strain, we have used custom-developed stretchable microposts arrays³⁵ on top of which we seeded wild-type and *Imna*-lacking mouse embryonic fibroblasts (MEFs), a model for laminopathies. Here, we first report on the alignment of the actin cytoskeleton of the *Imna*-lacking cells compared to wild-type control cells in response to topographical cues. The response of both types of cells was unaltered as well as the maturation of their focal adhesions. Secondly, we show that the combination of topographical cues with cyclic uniaxial strain invoked distinct responses of the two cell types. In contrast to wild-type MEFs, the strain avoidance response of *Imna*-lacking MEFs was impaired. We link this observation to the distinct actin cytoskeleton architecture of the latter cell type. The presence of the actin cap, interconnected with the nucleus, triggers, in normal cells, a fast and uniform response to cyclic strain, even in presence of topographical cues along the direction of strain. Instead, the lack of an actin cap and the presence of a basal actin layer in *Imna*-lacking cells hinder the strain avoidance response. These results highlight the importance of an intact nucleo-cytoskeletal connection for correct mechanoresponse to strain and help understanding the relationship between laminopathy disease mechanisms and mechanotransduction.

Results

Topographical cues induce similar actin stress fiber alignment and focal adhesion maturation in normal and *Imna*-lacking fibroblasts

In accordance with previous studies^{36,37} the actin cytoskeletal architecture of wild type mouse embryonic fibroblasts (*Imna*^{+/+} MEFs) and that of MEFs lacking the *Imna* gene (*Imna*^{-/-} MEFs) appeared to be distinct. *Imna*^{+/+} MEFs were characterized by a prominent actin cap and showed to a less extent the presence of basal actin fibers. On the other hand, *Imna*^{-/-} MEFs showed an actin cytoskeleton mainly made up of basal actin fibers^{7,27,38,39} (Figure 3.1). When scored manually for the presence of actin cap in a previous study, around 60% of *Imna*^{-/-} MEFs had no cap, 25% a disrupted cap and 15% a cap²⁷. Our data confirmed these observations. Also, the characteristic actin architecture of the two kinds of cells allowed dissecting the response of cap and basal layer of actin stress fibers.

To study the response of *Imna*^{+/+} MEFs and *Imna*^{-/-} MEFs to topographical cues we have seeded the cells on elastomeric microposts characterized by an elliptical cross section (major axis 1.5 μm , minor axis 0.87 μm , length 3 μm). The substrates were functionalized with fibronectin on their tops prior to seeding. Cells were allowed to adhere to the microposts for 2, 6 and 24 hours. After sample fixation we examined the actin fiber orientation at the cap and basal layer (Figure 3.2a, Figure 3.3 a-f) in confocal images of stained actin stress fibers. In *Imna*^{+/+} MEFs, actin cap fibers aligned parallel to the micropost major axis already at 2 hours but lost the alignment within 24 hours from seeding, while basal actin fibers appeared to be increasingly oriented along the microposts. For *Imna*^{-/-} MEFs, we observed an increasing trend in alignment of actin cap fibers between 2 and 6 hours, which stabilized afterwards, while the basal layer of actin fibers remained aligned with the micropost major axis throughout the course of the experiment.

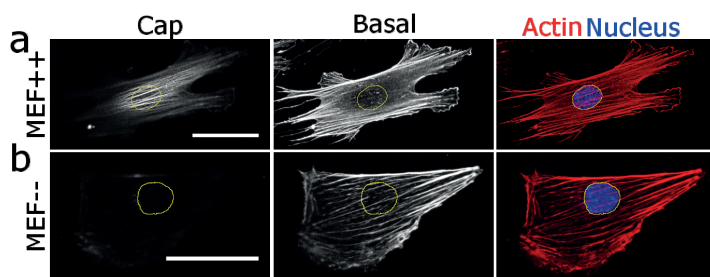


Figure 3.1. Distinct actin cytoskeleton architecture of *Imna*^{+/+} MEFs and *Imna*^{-/-} MEFs. Confocal fluorescence images of cap and basal layer of actin stress fibers in *Imna*^{+/+} MEFs (MEF++) and *Imna*^{-/-} MEFs (MEF--). The nucleus is outlined in yellow. Maximum intensity projections of the z-stacks of actins (red) and nuclear morphology (blue) are reported for comparison. Scale bar: 20 μm .

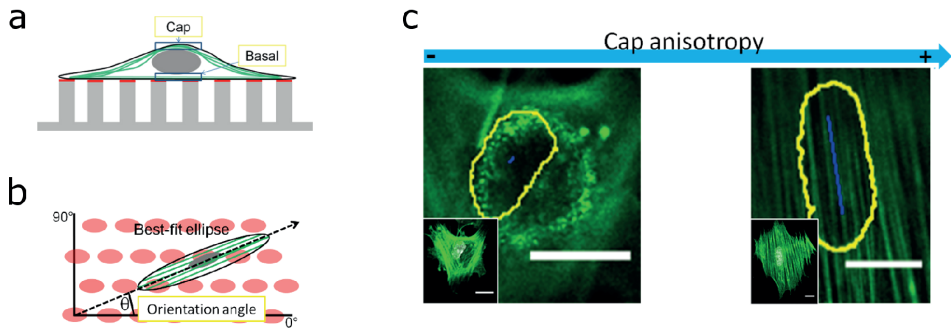


Figure 3.2. Schematic of the methods used to analyse cellular characteristics. (a) Cap and basal layer stress fiber orientation response was analysed from the z-projection of z-stack subsets of actin stress fibers confocal images located on top and below the nucleus respectively. (b) Cell overall orientation was measured by determining the angle between the best-fit ellipse and the micropost major axis in static conditions, or the strain direction in dynamic conditions. (c) Cap anisotropy measure was measured by the FibrilTool plug-in. The outline of the nucleus (yellow) is used as region of interest for measuring the characteristic anisotropy of the actin cap. The plug-in output is a value between 0 and 1, 0 represents a completely disrupted/absent cap while 1 represents parallel actin cap fibers. The blue line is a visual representation of the degree of cap anisotropy. Insets show the whole imaged cells (actin in green and nucleus in white). Scale bar: 20 μm .

In order to understand whether cap or basal actin fibers determine cellular orientation, cell overall alignment was determined by measuring the angle between the micropost major axis and the cell best-fitted ellipses (**Figure 3.2b** and **Figure 3.3 a-f**). These measurements revealed that cell orientation was parallel to the micropost major axis for both cell types. The degree of alignment showed a decreasing trend in time for *Imna*^{+/+} MEFs, while it increased for *Imna*^{-/-} MEFs between 2 and 6 hours. It was observed that *Imna*^{+/+} MEFs orientation corresponded to the actin cap fiber orientation at 2 and 6 hours, while it followed basal actin fiber orientation at 24 hours. For *Imna*^{-/-} MEFs, the orientation corresponded at the one of the basal layer for all timepoints of the experiment.

We also evaluated the formation of the actin cap in time, by quantifying the anisotropy of the actin cap fibers using the Fibril Tool⁴⁰ (**Figure 3.2c**). A high anisotropy factor indicated the presence of highly organized actin cap fibers while a low anisotropy factor represented disrupted or absent cap. For *Imna*^{+/+} MEFs, the anisotropy significantly increased between time points 2 and 6 hours ($p < 0.05$), while for *Imna*^{-/-} MEFs cap anisotropy remained stable. *Imna*^{-/-} MEFs showed significantly lower anisotropy values than *Imna*^{+/+} MEFs for all the course of the experiment ($p < 0.01$, **Figure 3.3g**). These data indicated that *Imna*^{-/-} MEFs did have a disrupted or absent cap, while for *Imna*^{+/+} MEFs complete cap formation occurred already within 2 hours from seeding.

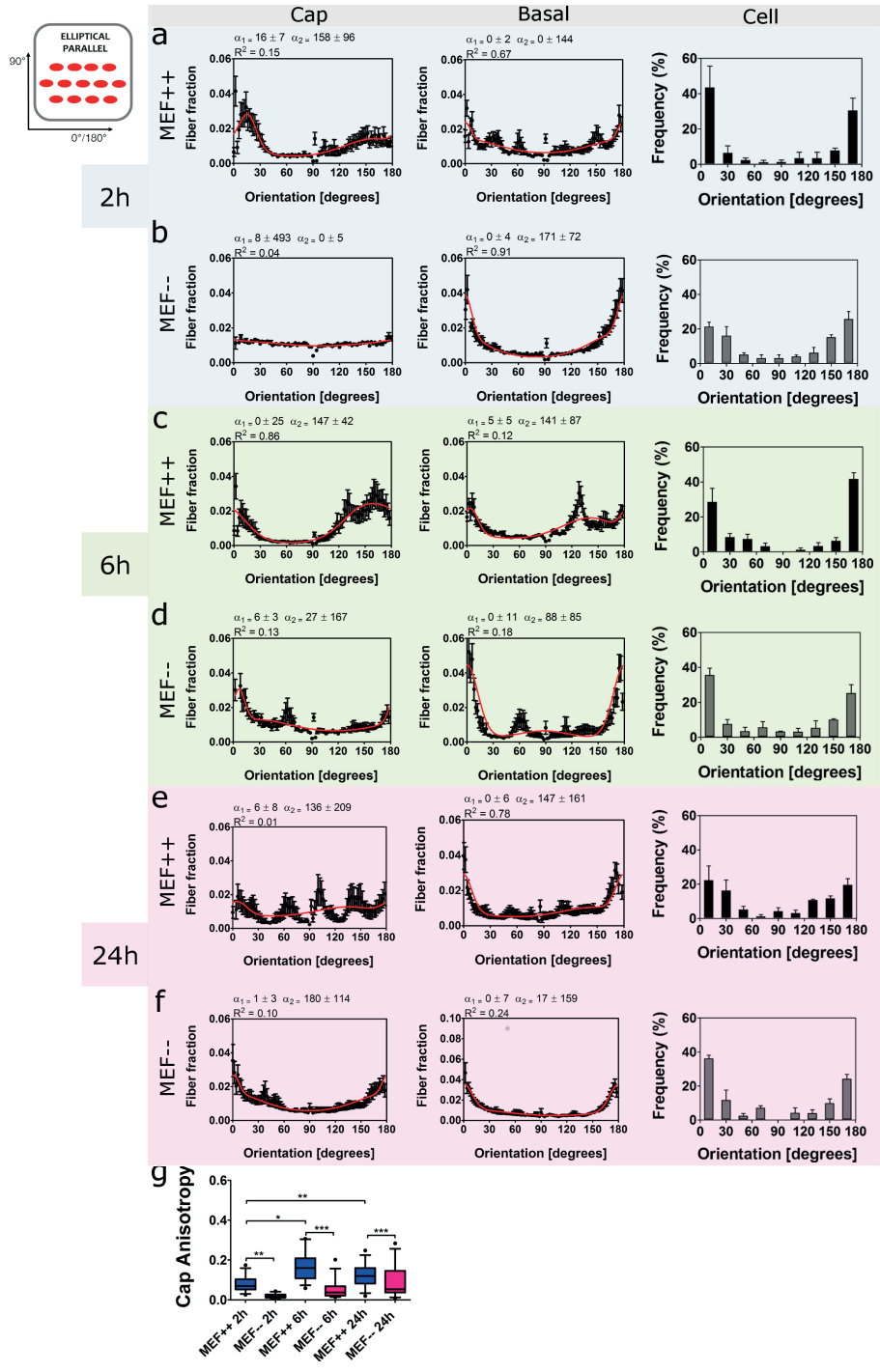


Figure 3.3. Temporal evaluation of topography sensing shows no impairment in *Imna*^{-/-} MEFs. (a-f) Outcomes of stress fiber orientation for cap, basal layer and cell orientation of *Imna*^{+/+} MEFs (MEF++) and *Imna*^{-/-} MEFs (MEF--) in static

conditions at 2, 6 and 24 hours from seeding on elliptical horizontal microposts. Bimodal fits of the stress fiber orientation at cap and basal layers (including the first and second dominant angle with standard deviations and R-squared value) at the different time points are reported as solid red lines. The major axis of the microposts corresponds to 0°/180° angle. Bin size for cell orientation=20°. Means \pm S.E.M. are reported. $n \geq 30$ per each condition. (g) Cap anisotropy values measured at each time point, represented as box-and-whisker plots (5-95 percentiles). *, ** and *** indicate respectively $p < 0.05$, $p < 0.01$ and $p < 0.001$. $n \geq 16$ for each condition.

To achieve contact guidance, it has been shown that FA maturation and sub cellular tension are required³². Therefore, we wondered whether FA maturation would occur similarly in *Imna*^{+/+} MEFs and *Imna*^{-/-} MEFs. For this reason, we checked the development and maturation of FAs by examination of staining patterns of alpha-actinin 4 and vinculin. Alpha-actinin 4 is recognized to play a major role in stabilizing the FAs⁴¹⁻⁴³, as it bridges vinculin⁴⁴, on one side, with actin stress fibers at the other side⁴⁵. Representative images of *Imna*^{+/+} MEFs and *Imna*^{-/-} MEFs on elliptical microposts stained for vinculin and alpha-actinin 4 are shown in **Figure 3.4**. These immunofluorescence images showed no overt differences between the two cell types. Alpha-actinin 4 was present on the microposts at the cell periphery. In *Imna*^{+/+} MEFs alpha-actinin 4 was also present along the fibers of the actin cap, while in *Imna*^{-/-} MEFs no alpha-actinin 4 was visible at the cap level and hardly along the basal layer stress fibers. Vinculin, as well, was present at the cell periphery and co-localized well with the alpha-actinin 4 staining. As expected, in contrast to alpha-actinin 4, vinculin was not found along the fibers of the actin cap of *Imna*^{+/+} MEFs.

Overall, these data suggest that both *Imna*^{+/+} MEFs and *Imna*^{-/-} MEFs sense the topographical cues of the elliptical microposts and respond to them by orienting along the major axis. Contrarily to *Imna*^{+/+} MEFs cells, *Imna*^{-/-} MEFs actin stress fiber and cell overall alignment remained stable over a time period of 24 hours, revealing a sustained sensitivity to topographical cues.

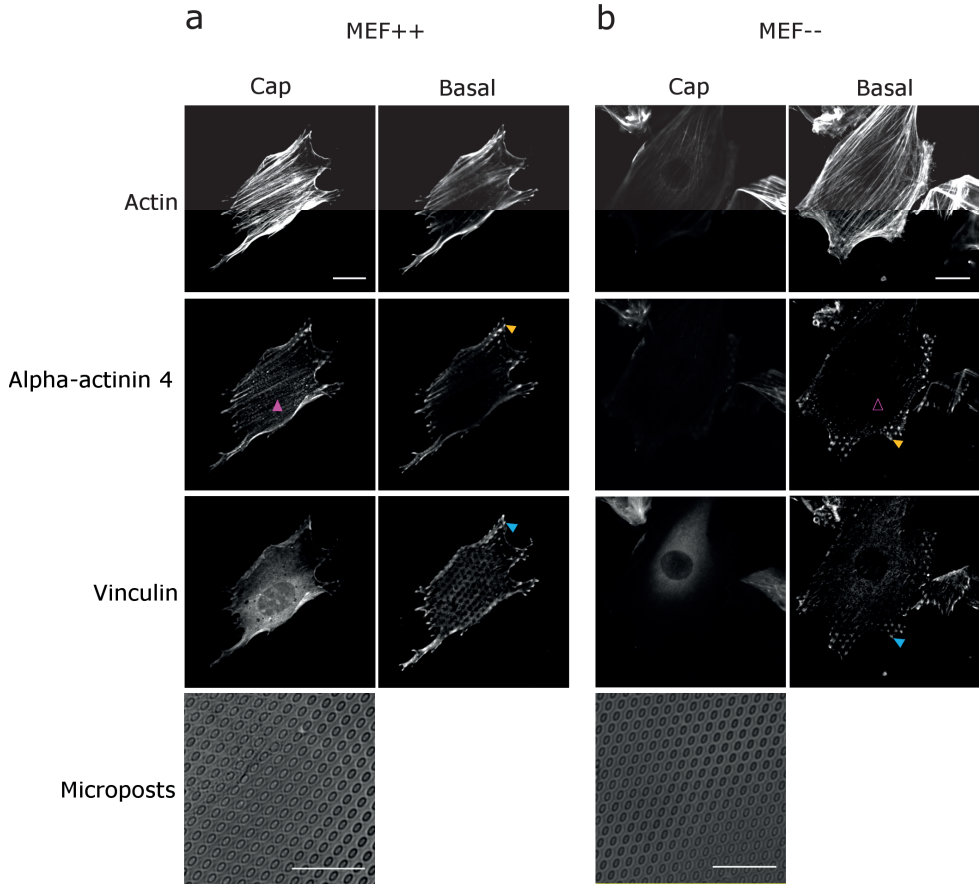


Figure 3.4. Focal adhesion maturation occurs similarly in *Imna*^{+/+} MEFs and *Imna*^{-/-} MEFs. Confocal images of *Imna*^{+/+} MEFs (MEF++) (a) and *Imna*^{-/-} MEFs (MEF--) (b) stained for actin stress fibers, alpha-actinin 4 and vinculin. Cells were cultured on top of elliptical microposts for 6 hours before staining. Z-projections of subsets of confocal images at the cap and basal layer of actin stress fibers, alpha-actinin 4 and vinculin show the co-localization of alpha-actinin 4 (orange arrowhead) and vinculin (cyan arrowhead) in both *Imna*^{+/+} MEFs and *Imna*^{-/-} MEFs, at the basal layer. In *Imna*^{+/+} MEFs, alpha-actinin 4 is present also along the actin cap stress fibers (magenta arrow head) while in *Imna*^{-/-} MEFs alpha-actinin 4 is not expressed along the basal stress fibers (magenta open arrowhead). Phase-contrast images show the elastomeric microposts with elliptical cross section used as substrate for cell culture. Scale bar: 20 μ m.

Impaired strain avoidance response of *Imna*-lacking fibroblasts

Here we hypothesized that, by using cells characterized by the presence and absence of cap, the response of these subgroups of stress fibers to combined contact guidance and cyclic strain applied along the same direction could be dissected. To study this, we seeded *Imna*^{+/+} MEFs and *Imna*^{-/-} MEFs on elliptical cross-section fibronectin coated elastomeric microposts for 4.5 hours (for ensuring complete cap formation in *Imna*^{+/+} MEFs) and subsequently applied cyclic uniaxial stretch (~7%, 0.5 Hz, sine wave) for 3.5 hours (in order to allow cell and actin stress fiber reorientation upon strain) along the major axis of the microposts. As a control, we performed the same experiment using circular cross section microposts (radius 1 μ m), as these substrates do not present directional topographical cues to the cells.

Within the experimental timeframe, on the circular microposts, we observed strain avoidance of the *Imna*^{+/+} MEFs actin cap fibers, as well as the cell overall reorientation to the (near) perpendicular direction (**Figure 3.5a**). *Imna*^{-/-} MEFs showed a less pronounced strain avoidance response at the basal layer only. *Imna*^{-/-} MEFs overall orientation did not show strain avoidance (**Figure 3.5b**). In general, the cell overall reorientation angles corresponded to the ones of the cap layer in *Imna*^{+/+} MEFs and basal layer in *Imna*^{-/-} MEFs.

When cells were presented to contact guidance and cyclic uniaxial strain along the same direction (i.e. on the elliptical horizontal microposts strained along their major axis), *Imna*^{+/+} MEFs responded by strain avoidance at the cap level, i.e. cap fibers reoriented to two mirror-image angles, while the basal actin layer fibers remained aligned along the micropost major axis (**Figure 3.5c**). In *Imna*^{-/-} MEFs the basal actin layer as well as the cap layer remained aligned with the microposts major axis. Cell overall alignment well reflected the main orientation of the actin cap fibers of *Imna*^{+/+} MEFs, and the basal fiber direction of *Imna*^{-/-} MEFs (**Figure 3.5 c and d**). Taken together, these data suggest that actin cap fibers sense the cyclic uniaxial strain and are able to govern the strain avoidance response of *Imna*^{+/+} MEFs, even in the presence of competing topographical cues along the direction of strain. The absence of the actin cap in *Imna*^{-/-} MEFs resulted in compromised strain avoidance response on circular microposts (in absence of contact guidance). Next to that, the combination of topographical cues with cyclic uniaxial strain resulted in completely abolished strain avoidance response. In this case, topographical cues apparently dictate the alignment of the actin stress fibers and consequently of the whole cells.

We investigated also the degree of cap formation upon stimulation by cyclic uniaxial strain. We observed that, *Imna*^{-/-} MEFs scored cap anisotropy values significantly lower than *Imna*^{+/+} MEFs on both circular and elliptical parallel microposts (**Figure 3.5e**). However, compared to static conditions, cap anisotropy upon cyclic uniaxial strain increased significantly for both cell types ($p < 0.001$), indicating that strain stimulation enhances cap formation.

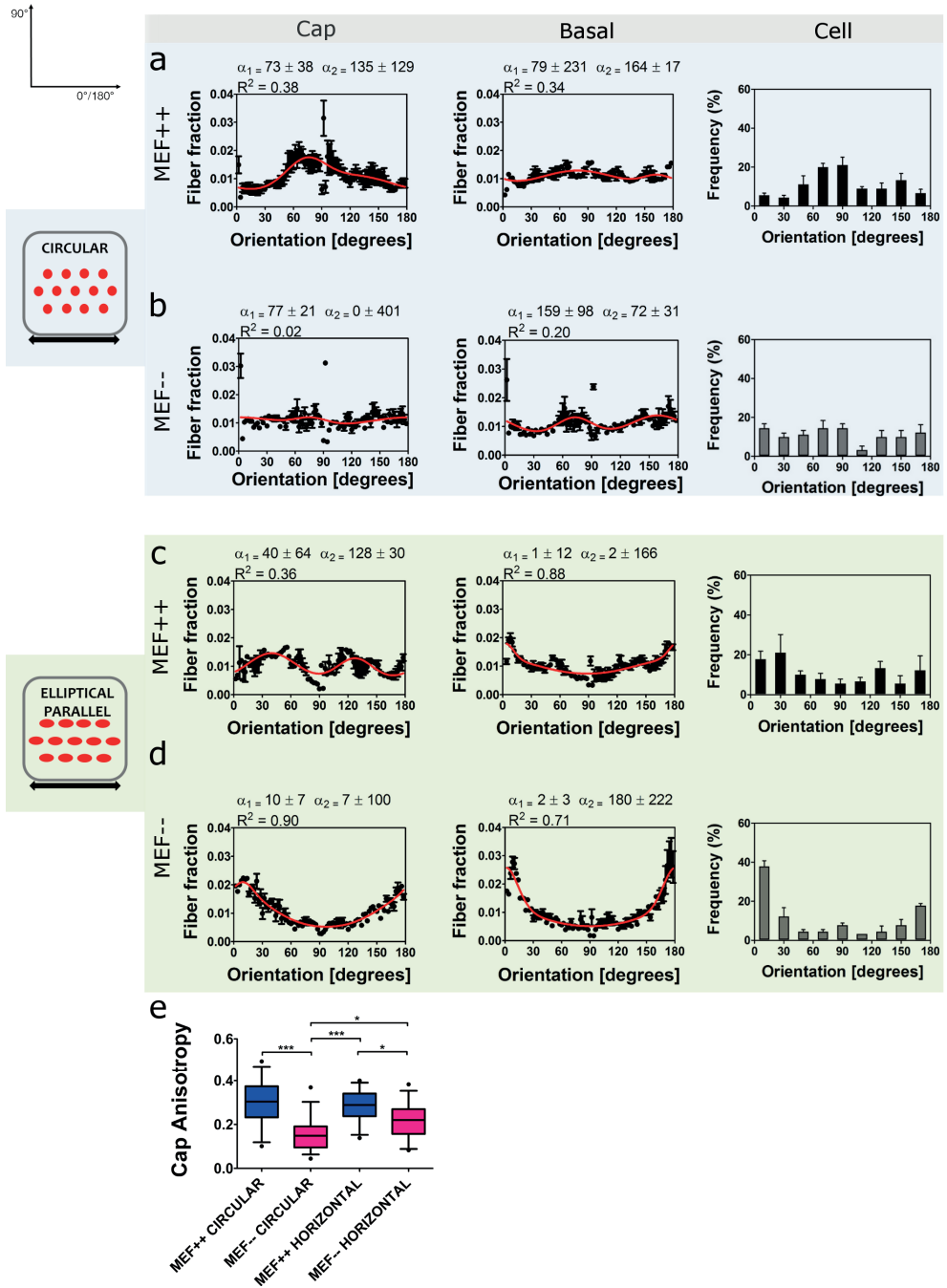


Figure 3.5. Basal and cap actin fiber orientation response to combined topographical cues and cyclic uniaxial strain reveal impaired strain avoidance response of *Imna*^{-/-} MEFs. (a-d) Outcomes of stress fiber orientation at basal and actin cap levels and cell overall orientation of *Imna*^{+/+} MEFs and *Imna*^{-/-} MEFs cultured on circular and elliptical horizontal microposts exposed, after 4.5 hours from seeding, to cyclic uniaxial strain along the 0°/180° angle corresponding to the major axis of the elliptical microposts (double-headed black arrow). Bimodal fits (red solid lines) of the stress fiber orientation of cap and basal layers (including the first and second dominant angle with standard deviations and R-squared

value) are reported. For circular microposts, actin cap fibers of *Imna*^{+/+} MEFs align almost perpendicular to the strain direction (strain avoidance). For *Imna*^{-/-} MEFs, the strain avoidance response is less pronounced. On the elliptical horizontal microposts, the strain avoidance response of actin cap of *Imna*^{+/+} MEFs is visible, while no reorientation occurs in *Imna*^{-/-} MEFs. $n \geq 77$ per each condition. Bin size of cell orientation = 20°. Means \pm S.E.M. are reported. (e) Cap anisotropy values measured after mechanical strain, represented as box-and-whisker plots (5-95 percentiles).*, ** and *** indicate respectively $p < 0.05$, $p < 0.01$ and $p < 0.001$. $n \geq 28$ per each condition.

Alpha-actinin 4 does not re-localize along stress fibers in *Imna*-lacking fibroblasts but accumulates at focal adhesions upon topographical cues and cyclic uniaxial strain

We wondered whether the lack of strain avoidance response on elliptical horizontal microposts could occur as a result of impaired stress fiber remodeling in *Imna*^{-/-} MEFs. Since alpha-actinin 4 together with other protein such as zyxin and VASP moves along stress fibers upon mechanical stimulation and enables the repair of strain sites⁴⁶, we investigated the localization of alpha-actinin 4 in *Imna*^{+/+} MEFs and *Imna*^{-/-} MEFs after mechanical strain. **Figure 3.6** shows the localization of alpha-actinin 4 in *Imna*^{+/+} MEFs and *Imna*^{-/-} MEFs. We observed that alpha-actinin 4 elongated at the sites of focal adhesions and formed a periodic pattern along the actin cap fibers of *Imna*^{+/+} MEFs. Instead, in *Imna*^{-/-} MEFs alpha-actinin 4 remained at the sites of focal adhesions. Strikingly, *Imna*^{-/-} MEFs having a cap were observed to have an alpha-actinin 4 pattern very similar to the one of *Imna*^{+/+} MEFs.

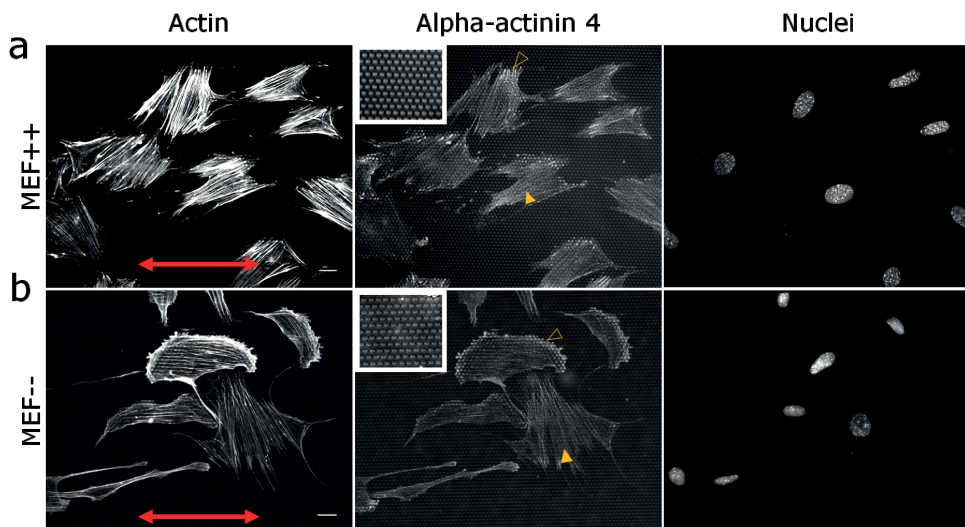


Figure 3.6. Alpha-actinin 4 does not re-localize along stress fibers in *Imna*^{-/-} MEFs. Fluorescent images of *Imna*^{+/+} MEFs (MEF++) (a) and *Imna*^{-/-} MEFs (MEF--) (b) stained for actin stress fibers, alpha-actinin 4 and nuclei. Actin stress fiber images give indication of the overall orientation of the cells after cyclic uniaxial strain. In *Imna*^{+/+} MEFs, alpha-actinin 4 is elongated at the focal adhesion sites (open orange arrowhead) and form a periodic pattern along the stress fibers indicating reinforcement of the actin cytoskeleton (orange arrowhead). Instead in *Imna*^{-/-} MEFs, alpha-actinin 4 accumulates at focal adhesion sites, similarly to the static condition (open orange arrowhead). Only in the reoriented *Imna*^{-/-} MEFs showing a prominent actin cap, alpha-actinin 4 gets a periodic pattern (orange arrowhead), similar to *Imna*^{+/+} MEFs. Insets show elliptical parallel microposts used as substrate. Double-headed red arrows show the strain direction. Scale bar: 20 μ m.

Cell reorientation is facilitated by actin cap presence and rounder cell morphology

Since the presence of cap seemed to be relevant for cellular reorientation, we checked whether, within the *Imna*^{-/-} MEFs population on elliptical parallel microposts, only cells with cap would reorient their stress fibers and the cell body. To do this, firstly, we categorized cells as “reoriented” when their angle relative to the micropost major axis/strain direction (θ) was more than 20° and less than 160° and “remaining” the cells which orientation angle was within 20° from the 0°/180° angle (**Figure 3.2b**). Secondly, we scored cells as 1) “no cap” if their cap anisotropy score was <1.5, 2) with “disrupted cap” if their cap anisotropy score was between 1.5 and 2.5 and 3) with “cap” if their cap anisotropy score was >2.5. We could not demonstrate that only cells with cap had reoriented since within the reoriented *Imna*^{-/-} MEFs (~40%), ~12% had a cap, ~12% had a disrupted cap and ~16% had no cap (**Figure 3.7a**). These data suggest that also cells with disrupted or absent cap can eventually reorient their cell body in presence of contact guidance and strain avoidance. Thus, the actin cap presence is not a prerequisite for reorientation upon strain and contact guidance but does facilitate cell reorientation.

To get further insight in the dynamics of cell and stress fiber reorientation, we focussed on the cellular aspect ratio. We measured the cell aspect ratio as the ratio between the long axis and short axis of its best-fitted ellipse, implying that a rounder cell has an aspect ratio close to 1 and a more elongated cell has a higher aspect ratio. For *Imna*^{+/+} MEFs, the aspect ratio was lower than the one of *Imna*^{-/-} MEFs in static condition and remained unchanged upon cyclic mechanical strain (**Figure 3.7b**). Further analysis in the *Imna*^{-/-} MEFs population showed that, the aspect ratio of reoriented cells decreased. Although the change did not attained significance, this represents loss of polarization of the cells. *Imna*^{-/-} MEFs that remained aligned with the elliptical parallel microposts, increased significantly their aspect ratio with respect to *Imna*^{-/-} MEFs in static condition ($p < 0.05$). Together, our results show that *Imna*^{+/+} MEFs are rounder by nature, while *Imna*^{-/-} MEFs elongate in presence of topographical cues. In response to mechanical strain, *Imna*^{-/-} MEFs have the tendency to get a rounder morphology in order to reorient but they tend to further elongate when they do not respond to the strain stimulation and remain aligned with the topographical cues.

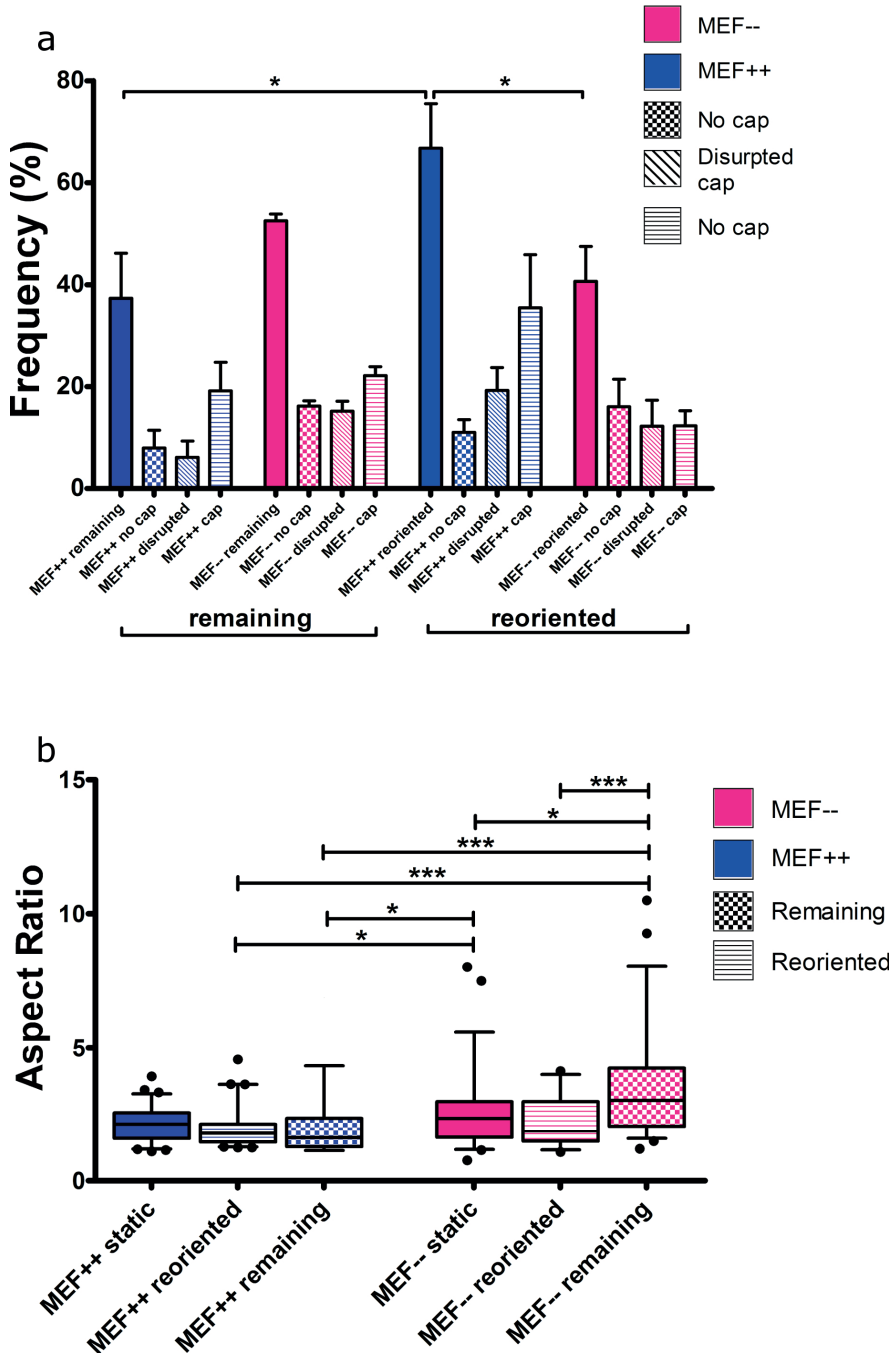


Figure 3.7. Presence of actin cap in *Imna*^{-/-} MEFs is not directly indicative of cell reorientation, while measure of aspect ratio is. (a) Frequency of cells (*Imna*^{+/+} MEFs (MEF++) and *Imna*^{-/-} MEFs (MEF--)) reoriented and remaining, further categorized according to absence of cap (no cap), presence of disrupted cap (disrupted cap) and well aligned actin cap (cap). Means ± S.E.M. are reported. (b) Box-whisker plots of cell aspect ratio for *Imna*^{+/+} MEFs (MEF++) and *Imna*^{-/-} MEFs (MEF--)) in static conditions and after cyclic uniaxial strain (categorized as reoriented and remaining). and indicate respectively p<0.05 and p<0.001. n≥21 in static conditions, n≥26 in dynamic conditions.

Discussion

The purpose of the current study was to understand whether the defective actin architecture of *Imna*-lacking cells leads to impaired mechanoresponse to topographical cues and cyclic uniaxial strain, applied separately or in combination. For this reason, we have studied the actin cytoskeleton orientation response of wild-type and *Imna*-lacking mouse embryonic fibroblasts. Since wild-type MEFs (*Imna*^{+/+} MEFs) show predominantly the actin cap structure on top of the nucleus while *Imna*-lacking MEFs (*Imna*^{-/-} MEFs) develop only the basal layer of stress fibers, we used these cells as a tool to dissect the response of the two actin layers to the different cues. Our findings demonstrate that, in *Imna*^{-/-} MEFs, the lack of the actin cap do not compromise the mechanosensing of topographical cues but does impair the response to strain. These observations reveal that the transmission of the topographical signals occurs independently of the actin architecture while actin cap presence is crucial for mechanoresponse to strain.

Using elliptical cross-section elastomeric microposts we found that both cell types can recognize and orient along the major axis of the microposts. Cellular mechanosensing and response to topographical cues in static conditions seem to be independent of the lack of *Imna* gene in *Imna*^{-/-} MEFs. This was confirmed by the alpha-actinin 4 patterns, which well co-localized with the vinculin ones, indicating maturation of focal adhesions⁴¹. On the 2D environment provided by the elastomeric microposts, *Imna*^{+/+} MEFs and *Imna*^{-/-} MEFs showed contact guidance response within 2 hours from seeding, by aligning the actin cap and the basal actin layer, respectively. For *Imna*^{+/+} MEFs the response became less prominent with increasing time, while, for *Imna*^{-/-} MEFs, we reported stable alignment of actin cytoskeleton and increasing cell overall alignment. These results suggest that A-type lamins are not needed for the orientation response of the actin cytoskeleton to topographical cues. Possibly, the lamina formed by remaining B-type lamins is sufficient for this response. In case of normal cell, we speculate that the topographic signals are quickly transmitted to the nucleus⁷ through the actin cap fibers. Instead, in cells characterized by the absence of an actin cap, focal adhesion proteins might act as compensatory mechanosensors and trigger signal transmission to the nucleus via slower biochemical pathways⁴⁷, consistently with the longer timescale required to align *Imna*^{-/-} MEFs cell bodies. However, the molecular machinery that mediates topography sensing remains largely elusive and merits future investigations. The alternative possibility that other cytoskeletal filaments play a role in the transduction of topography signals cannot be excluded at this point, however. Both intermediate filaments and microtubules have been shown to bind to the nuclear membrane. While the absence of A-type lamins also seems to mediate changes in the organization of these structures²⁵, these changes are not as dramatic as seen in the actin cap formation

Our analyses of actin stress fiber and cell reorientation on circular microposts subjected to cyclic uniaxial strain, revealed that, while *Imna*^{+/+} MEFs had a normal strain avoidance response^{33, 34}, *Imna*^{-/-} MEFs showed an attenuated response. Furthermore, the combination of uniaxial strain with contact guidance in the same direction totally abolished the strain avoidance response of *Imna*^{-/-} MEFs but not of *Imna*^{+/+} MEFs. While it has been observed that interfering with the nucleo-skeletal connection (knockdown of LINC protein nesprin-1) hinders the strain orientation response of endothelial cells⁴⁸, we demonstrated that the impaired strain avoidance response of *Imna*^{-/-} MEFs is correlated with a distinct actin cytoskeleton architecture comprehending only a basal layer of actin fibers. In a

previous study we have demonstrated that the combination of topographical cues and strain along the same direction results in overall competing effects on the actin cytoskeleton orientation response, as the basal layer tend to remained aligned with the underlying topographical cues, but the actin cap responded by strain avoidance³⁵. As a step forward, here we use a *Imna*-deficient cell type as a tool to underpin the relevance of the actin cap in cellular reorientation and we clearly dissect the behaviours of the two actin layers. Whereas it is known that the actin cap plays a critical role in mechanosensing of microenvironment stiffness³⁹ and mediates fast mechanotransduction in response to fluid shear stress⁷, its contribution to strain mechanosensing and mechanotransduction has been elucidated by this study. The high contractility and dynamicity of actin cap fibers make them a candidate for strain mechanosensing. In contrast, it is certainly conceivable that the numerous interconnections of the basal layer with the underlying topographical features, the exertion of high traction forces⁴⁸ and the low dynamicity of basal stress fibers⁷ result in the inability of this subset of stress fibers to adjust to the developing microenvironment. Whether the response of *Imna*-lacking cells is totally impaired or delayed needs still to be demonstrated, as, for our study, we have taken into consideration only a limited interval of time points and fixed settings for the straining protocol. Consistent with the hypothesis of impaired mechanoresponse, Ho *et al.*⁴⁹ have recently shown that altered actin dynamics are an intrinsic property of *LMNA*-deficient and mutant fibroblasts. Interestingly, our results indicate that it is not likely that biochemical signal transduction take charge of strain mechanotransduction to the nucleus when actin cap fibers are absent.

Although cell reorientation has been investigated for long, a consensus about the mechanisms basis of this cellular behaviour has not been reached. Previous work has shown that cell reorientation might include a phase in which cells gets a rounder morphology and subsequently enter a new phase of elongation at an angle to the strain direction⁵⁰. In our study we report no significant decrease in cellular aspect ratio for *Imna*^{+/+} MEFs but we observe a decrease in aspect ratio of *Imna*^{-/-} MEFs that actively reoriented, even in presence of topographical cues along the strain direction. This suggests that *Imna*^{-/-} MEFs indeed might need to acquire a rounder morphology in order to reorient away from the strain direction. In addition to this, our results let us speculate that, in healthy cells with an intact actin cap, reorientation is initiated and guided by the cap itself. Subsequently, via the interconnection of the actin cap with the nucleus, the signal gets transduced to the nucleus, which regulates the reorientation of the whole cell. Still, the details on the dynamics of stress fiber remodeling during reorientation are not fully understood. It has been suggested that stress fiber turnover⁵¹ as well as focal adhesion sliding and stress fiber rotation^{52,53} might play a role in this phenomenon. Here, we hypothesize that actin cap reorientation will be the result of focal adhesion sliding. On the other hand, at the basal layer, given the numerous adhesion sites, stress fiber turnover is the candidate mechanism for actin reorientation: stress fibers need to disassemble and *de novo* form at a more favourable angle for their maintenance. In order to further confirm this hypothesis, additional experiments should be carried out, such as real-time imaging of stress fiber remodeling during mechanical strain to visualize the dynamics of cap, basal actin stress fibers and focal adhesion reorientation. Furthermore, our results point out that cap anisotropy increases upon mechanical straining. This means that both cell types, either with or lacking the *Imna* gene, tend to produce and align more actin stress fibers on top of the nucleus, upon mechanical stimulation. This can be regarded as an adaptive cellular mechanism for promoting cellular reorientation. However, although cyclic strain induce *Imna*-lacking fibroblasts to develop thin actin fibers on top of their

nucleus, the defective actin dynamics and the low contractility associated with these actin structures seem to lessen the efficiency of such an actin cap in guiding cell reorientation.

Defective mechanosensing and/or mechanoresponse may be key mechanisms in developing a variety of diseases associated with evading harmful mechanical forces on cells and tissues. While many studies do not differentiate between mechanosensing and mechanoresponse, our studies indicate that mechanosensing in *Imna*-deficient cells seems to be largely intact while the response is not. These data are in line with a previous study showing a defective mechanoresponse due to LMNA mutations or ablation of the LINC complex both in three-dimensional (3D) and 2D culturing systems^{54,55}.

Insight into mechanoresponse of cells can aid in assessment of disease severity, both as diagnostic and prognostic tools. In laminopathies genetic mutation analyses are insufficient to diagnose the disease or to predict the disease development: some people with identical LMNA mutations develop a disease phenotype leading to heart failure, while others with the same mutations remain disease-free throughout their life. New tools to measure mechanosensing and, perhaps even more importantly, mechanoresponse, could aid in making important decisions in patient treatment and advice on behaviour: people with defective mechanoresponse are prone to generate excessive tissue damage upon heavy exercise.

In conclusion, we have demonstrated that topography sensing is not impaired in *Imna*-lacking fibroblasts, while strain sensing and response are compromised. The presence of the actin cap in tissue cells is thus suggested to be crucial for structural mechanotransduction in response to mechanical strain. The relevance of this study lies in the fact that for the first time we have looked at the role of the structural connectivity between extracellular environment, actin cytoskeleton and nucleus in the response to well defined topographical cues and mechanical strain applied separately and in combination. These cues are presented to tissue cells in a myriad of situations and the ability of the cells to respond to them is crucial for maintaining tissue functionality. The findings of this study broaden our understanding of cellular mechanotransduction and could be of high interest for shedding light on the mechanisms underlying the onset of human diseases of mechanotransduction such as laminopathies.

Materials and Methods

Cell culture

Wild type embryonic fibroblasts (*Imna*^{+/+} MEFs) as well as *Imna* knockout mouse embryonic fibroblast (*Imna*^{-/-} MEFs) were obtained as described previously⁵⁶. Cells were cultured in Dulbecco Modified Eagle's Medium (DMEM, Invitrogen) containing 10% of Fetal Bovine Serum (FBS, Greiner Bio-one), 1% of L-glutamine (Lonza) and penicillin streptomycin (PenStrep, Lonza) or gentamycin as antibiotics. Cell cultures were maintained at 37°C in a humidified atmosphere containing 5% CO₂. Cells were passaged by splitting at 1:3 to 1:5 ratio using trypsin-EDTA. Cell seeding density on substrates for experiments was between 2000 and 2500 cells/cm².

Micropost design and fabrication

The elastomeric microposts arrays were fabricated via standard photolithography processes, according to previous protocols^{35,57}. The fabrication was carried out with poly-dimethylsiloxane (PDMS, Sylgard 184, Dow Corning), spincoated on the master for 30 seconds at 1000 rpm and cured at 110° C for 20 minutes to reach a Young's Modulus of 1.8 MPa. The microposts were characterized by a radius (r) of 1 μm in case of circular cross section (circular microposts) and semi-major axis a of 1.5 μm and semi-minor axis b of 0.87 μm in case of elliptic cross section (elliptical parallel microposts). The center to center distance was 4 μm . The micropost length was 3 μm . For static experiments micropost arrays were bonded to glass coverslips (Menzel), while for dynamic experiments microposts were bonded to the flexible bottom of six-well plates (Uniflex Series Culture Plates, Flexcell FX 5000, Flexcell International) using a corona discharger.

Fibronectin micro-contact printing on microposts

To allow cell adhesion, the top of PDMS microposts were functionalized by fibronectin. Micro-contact printing was performed with a clean, flat PDMS stamp incubated with 50 $\mu\text{g}/\text{ml}$ fibronectin from human plasma (Sigma-Aldrich) or rhodamine fibronectin (Cytoskeleton) in deionized water for 1 hour. When dried, the stamp was deposited gently on the micropost arrays, previously subjected to UV ozone treatment. The contact between the microposts and the stamp was ensured for at least 1 minute. Sterilization of the substrates was performed afterwards with 70% ethanol. To prevent non-specific protein absorption to the non-functionalized surface of the PDMS microposts, a treatment with 0.4% Pluronic F127 (Sigma-Aldrich) was performed for 1 hour. The substrates were finally rinsed using sterile MilliQ water⁵⁷.

Static experiments

Before seeding, the microposts were equilibrated in medium at 37°C for at least 15 minutes. Next, cells were seeded on top of the fibronectin coated elastomeric micropost arrays and allowed to adhere under optimal culture conditions. At 2, 6 and 24 hours after seeding, cells were fixed in 3.7% formaldehyde in PBS for 15 minutes (RT) and prepared for analysis.

Loading protocol for cyclic uniaxial strain in dynamic experiments

The elastomeric microposts arrays were subjected to cyclic uniaxial stretch using the FX-5000 Flexcell system (Flexcell Corp. (Mc-Keesport)), applying maximum strain level of 10% at a frequency of 0.5 Hz. Strain fields on the elastomeric microposts were validated within the central region of the Flexcell membrane on which the microposts were bound via digital image correlation Matlab-based code (Mathworks Inc.). For this, a random pattern of dots was inked on the microposts bonded to the Flexcell membrane and images were collected by digital camera mounted on a stereo microscope (SteREO Discovery V8, Zeiss). By applying our straining protocol, results showed that in the area under consideration the strain field varied from 5 % to 7 %. Strains in the x direction (direction of applied strain) are 6.8% on average, and strain in the y direction show a compression of 2% (data not shown).

Before applying the loading protocol, cells were seeded on top of the microposts for a time period of 4.5 hours to allow cell adhesion. Thereafter, the loading protocol was performed for 3.5 hours. After that, cells on substrates were fixed with 4% formaldehyde in PBS (15 minutes, RT, Sigma-Aldrich) and prepared for examinations.

Immunofluorescence studies

To prepare for immunofluorescence studies, cells were permeabilized with 0.1% Triton-X-100 (Merck) in PBS for 10 minutes and incubated with 3% bovine serum albumin (BSA) in PBS in order to block non-specific binding. For actin stress fiber staining, FITC-conjugated phalloidin (1:500, Phalloidin-Atto 488, Sigma) or Texas-Red conjugated phalloidin (1:100, Molecular Probes) were applied for 1 hour at room temperature. For alpha-actinin 4, the rabbit primary antibody was anti-alpha actinin 4 antibody [IgG, EPR2533 (2), Abcam). For vinculin, the monoclonal mouse antibody hVIN-1 (IgG1, 1:200 to 1:400, Sigma-Aldrich) were used. As secondary antibodies, either goat anti mouse-Alexa 555 (Molecular Probes, to vinculin) and goat anti rabbit-Alexa 488 (Molecular Probes, to alpha-actinin 4) were used. Alternatively, the combination of goat anti mouse-Cy5 (to vinculin) and goat anti rabbit-FITC (to alpha-actinin 4) with Phalloidin-Texas-Red allowed a triple labelling of the cell adhesion and actin structures. For nuclear staining, cells were incubated in DAPI (100 ng/ml, Fluka) for 10 minutes or DAPI was added to the mounting medium at 0.5 µg/ml. After final washings in PBS, cells on microposts were mounted on glass coverslides using Mowiol or a glycerol mounting solution²⁵.

Microscopy

Imaging of stained cells was performed with an inverted confocal microscope (Zeiss LSM 510 META), using a C-Apochromat water-immersion objective (63x, NA=1.2). The laser-scanning microscope was used according to the manufacturer's specification, using an Ar laser at 488nm (30 mW), a HeNe laser at 543 (1 mW) and Chameleon laser (Chameleon Ultra II, Coherent) for DAPI at 760 nm. Z-series were generated by collecting a stack consisting of optical sections using a step size of 0.45-1.00 µm in the z-direction, while a minimum pinhole opening (1 AU) was used. Alternatively, Z-series were generated using a Leica TCS SPE confocal laser scanning fluorescence microscope (Leica DMRBE) using LAS-AF software (version 2.3, Leica) and an oil immersion lens (63x, NA=1.3).

For fluorescence imaging, samples were examined under an inverted microscope (Zeiss Axiovert 200M, Zeiss).

Quantification orientation actin stress fibers

Prior to directionality analysis aimed at measuring stress fiber orientation, actin stress fiber confocal Z-stacks of each analyzed cell were divided in 2 subsets, one on top of the nucleus (cap) and one on the bottom of the nucleus (basal). For each subset the maximum intensity projection images were calculated. Subsequently, the nuclear outline was tracked by thresholding the maximum intensity projection of the DAPI Z-stack. This outline was used as mask for the cap and basal projections. Directionality analysis of the confocal images of cap and basal actin stress fibers was conducted using the Directionality plug-in of Fiji (<http://fiji.sc/Fiji>). This method exploits the image Fast Fourier Transform (FFT) algorithms. The 2-D FFT determines the spatial frequencies within an image in radial directions and the output of the plug-in is a normalized histogram that reports the amount of structures at angles between 0° and 180° with a bin size of 2°. The reference angle was chosen as the major axis of the elliptical microposts in static conditions, and along the strain direction in dynamic conditions. Finally the values the average fiber fraction for each angle was calculated.

Cap anisotropy quantification

To quantify the extent of cap formation, the alignment of actin stress fiber on top of the nucleus was measured. This was carried out by using the FibrilTool plug-in of ImageJ on the confocal slice of actin stress fibers located on top of the nucleus. The nuclear outline was used as region of interest, in order to measure the features of the cell actin cap only. The cap anisotropy score is given between 0 (for no order in actin cap fibers orientation meaning absent/disrupted cap) and 1 (perfectly ordered, parallel actin cap fibers).

Cell orientation and aspect ratio

Cell orientation and aspect ratio were determined from outlines of cells in the maximum intensity projections of actin stress fibers visualized. Cell orientation was measured relative to the major axis of the elliptical microposts in static conditions and the strain direction in dynamic conditions. The orientation of best-fit ellipse to the outline of each cell was measured using ImageJ software. Orientation angles were reported as a histogram for each experiment with bin size of 20°. Finally the average cell orientation at each bin was calculated from 3 experiments. Cell aspect ratio was measured from the best-fit ellipse of cell outline. It is defined as the ratio between the long axis and short axis of the best-fitted ellipse. The aspect ratio is close to 1 for rounded cells and higher for more elongated cells.

Data analysis and statistics

To plot data and perform statistical analysis, Prism software (GraphPad Software) was used.

For stress fiber orientation, three experiments were conducted to achieve a minimum of 30 cells per condition (e.g. timepoint, static, dynamic (circular or elliptical microposts)). Histograms of stress fiber orientation were averaged and fitted with a bi-modal periodic normal probability distribution function using nonlinear least-square approximation algorithm^{58 59}:

$$\phi_f(\gamma) = A_1 \exp\left[\frac{\cos[2(\gamma - \alpha_1)] + 1}{\beta_1}\right] + A_2 \exp\left[\frac{\cos[2(\gamma - \alpha_2)] + 1}{\beta_2}\right] \quad (1)$$

Hereby, $\phi_f(\gamma)$ is the fiber fraction as a function of the fiber angle γ . Variables α_1 and α_2 are the two main fiber angles while β_1 and β_2 represent the dispersities of the two fiber distributions. For cyclic uniaxial straining, an angle of 90° is perpendicular to the strain direction. A_1 and A_2 are scaling factors for the total fiber fractions of the distributions. The quality of the bimodal approximation is represented by the R-squared value.

For cap anisotropy and cell orientation, data were collected from three experiments. Significant differences were assessed by either a non-parametric Kruskal-Wallis, with Dunn's *post-hoc* test (aspect ratio and cap anisotropy) or unpaired t-test (reoriented vs remaining cells). A p value of 0.05 was considered significant.

Acknowledgments

This work was supported by NanoNextNL. Wild-type and *Imna*-lacking MEFs were a gift from Dr. Brian Burke (Nuclear Dynamics and Architecture Group, Institute of Medical Biology, Immunos, Singapore, Singapore).and Dr. Colin Stewart (Development and Regenerative Biology Group, Institute of Medical Biology, Immunos, Singapore, Singapore).

We thank Lynn Poolen (Maastricht University) for her help in performing part of the experiments.

References

1. Humphrey, J.D., Dufresne, E.R., & Schwartz, M.A. Mechanotransduction and extracellular matrix homeostasis. *Nat. Rev. Mol. Cell Biol.* **15**, 802-812 (2014).
2. Vogel, V. Mechanotransduction involving multimodular proteins: converting force into biochemical signals. *Annu. Rev. Biophys. Biomol. Struct.* **35**, 459-488 (2006).
3. Ingber, D.E. Mechanobiology and diseases of mechanotransduction. *Ann. Med.* **35**, 564-577 (2003).
4. Jaalouk, D.E. & Lammerding, J. Mechanotransduction gone awry. *Nat. Rev. Mol. Cell Biol.* **10**, 63-73 (2009).
5. Hoffman, B.D., Grashoff, C., & Schwartz, M.A. Dynamic molecular processes mediate cellular mechanotransduction. *Nature* **475**, 316-323 (2011).
6. Chiquet, M., Gelman, L., Lutz, R., & Maier, S. From mechanotransduction to extracellular matrix gene expression in fibroblasts. *Biochim. Biophys. Acta* **1793**, 911-920 (2009).
7. Chambliss, A.B. *et al.* The LINC-anchored actin cap connects the extracellular milieu to the nucleus for ultrafast mechanotransduction. *Sci. Rep.* **3**, 1087 (2013).
8. Poh, Y.C. *et al.* Rapid activation of Rac GTPase in living cells by force is independent of Src. *PLoS. One.* **4**, e7886 (2009).
9. Na, S. *et al.* Rapid signal transduction in living cells is a unique feature of mechanotransduction. *Proc. Natl. Acad. Sci. U. S. A* **105**, 6626-6631 (2008).
10. Wang, Y. *et al.* Visualizing the mechanical activation of Src. *Nature* **434**, 1040-1045 (2005).
11. Wang, N., Tytell, J.D., & Ingber, D.E. Mechanotransduction at a distance: mechanically coupling the extracellular matrix with the nucleus. *Nat. Rev. Mol. Cell Biol.* **10**, 75-82 (2009).
12. Kim, D.H., Chambliss, A.B., & Wirtz, D. The multi-faceted role of the actin cap in cellular mechanosensation and mechanotransduction. *Soft. Matter* **9**, 5516-5523 (2013).
13. Dahl, K.N., Ribeiro, A.J., & Lammerding, J. Nuclear shape, mechanics, and mechanotransduction. *Circ. Res.* **102**, 1307-1318 (2008).
14. Garelick, M.G. *et al.* Chronic rapamycin treatment or lack of S6K1 does not reduce ribosome activity in vivo. *Cell Cycle* **12**, 2493-2504 (2013).
15. Swift, J. *et al.* Nuclear lamin-A scales with tissue stiffness and enhances matrix-directed differentiation. *Science* **341**, 1240104 (2013).
16. McNamara, L.E. *et al.* The role of microtopography in cellular mechanotransduction. *Biomaterials* **33**, 2835-2847 (2012).
17. Bertrand, A.T., Chikhaoui, K., Yaou, R.B., & Bonne, G. Clinical and genetic heterogeneity in laminopathies. *Biochem. Soc. Trans.* **39**, 1687-1692 (2011).
18. Worman, H.J. & Bonne, G. "Laminopathies": a wide spectrum of human diseases. *Exp. Cell Res.* **313**, 2121-2133 (2007).
19. Savage, D.B. *et al.* Familial partial lipodystrophy associated with compound heterozygosity for novel mutations in the LMNA gene. *Diabetologia* **47**, 753-756 (2004).
20. Emerson, L.J. *et al.* Defects in cell spreading and ERK1/2 activation in fibroblasts with lamin A/C mutations. *Biochim. Biophys. Acta* **1792**, 810-821 (2009).

21. Lammerding, J. *et al.* Lamin A/C deficiency causes defective nuclear mechanics and mechanotransduction. *J. Clin. Invest* **113**, 370-378 (2004).
22. Lammerding, J. *et al.* Abnormal nuclear shape and impaired mechanotransduction in emerin-deficient cells. *J. Cell Biol.* **170**, 781-791 (2005).
23. Schreiber, K.H. & Kennedy, B.K. When lamins go bad: nuclear structure and disease. *Cell* **152**, 1365-1375 (2013).
24. Hale, C.M. *et al.* Dysfunctional connections between the nucleus and the actin and microtubule networks in laminopathic models. *Biophys. J.* **95**, 5462-5475 (2008).
25. Broers, J.L. *et al.* Decreased mechanical stiffness in LMNA^{-/-} cells is caused by defective nucleo-cytoskeletal integrity: implications for the development of laminopathies. *Hum. Mol. Genet.* **13**, 2567-2580 (2004).
26. Tamiello, C. *et al.* Soft substrates normalize nuclear morphology and prevent nuclear rupture in fibroblasts from a laminopathy patient with compound heterozygous LMNA mutations. *Nucleus*. **4**, 61-73 (2013).
27. Khatau, S.B. *et al.* A perinuclear actin cap regulates nuclear shape. *Proc. Natl. Acad. Sci. U. S. A* **106**, 19017-19022 (2009).
28. Khatau, S.B., Kim, D.H., Hale, C.M., Bloom, R.J., & Wirtz, D. The perinuclear actin cap in health and disease. *Nucleus*. **1**, 337-342 (2010).
29. Burke, B. & Stewart, C.L. The laminopathies: the functional architecture of the nucleus and its contribution to disease. *Annu. Rev. Genomics Hum. Genet.* **7**, 369-405 (2006).
30. Dunn, G.A. & Heath, J.P. A new hypothesis of contact guidance in tissue cells. *Exp. Cell Res.* **101**, 1-14 (1976).
31. Teixeira, A.I., Abrams, G.A., Bertics, P.J., Murphy, C.J., & Nealey, P.F. Epithelial contact guidance on well-defined micro- and nanostructured substrates. *J. Cell Sci.* **116**, 1881-1892 (2003).
32. Saito, A.C., Matsui, T.S., Ohishi, T., Sato, M., & Deguchi, S. Contact guidance of smooth muscle cells is associated with tension-mediated adhesion maturation. *Exp. Cell Res.* **327**, 1-11 (2014).
33. Kaunas, R., Nguyen, P., Usami, S., & Chien, S. Cooperative effects of Rho and mechanical stretch on stress fiber organization. *Proc. Natl. Acad. Sci. U. S. A* **102**, 15895-15900 (2005).
34. Faust, U. *et al.* Cyclic stress at mHz frequencies aligns fibroblasts in direction of zero strain. *PLoS. One.* **6**, e28963 (2011).
35. Tamiello, C., Bouten, C.V., & Baaijens, F.P. Competition between cap and basal actin fiber orientation in cells subjected to contact guidance and cyclic strain. *Sci. Rep.* **5**, 8752 (2015).
36. Khatau, S.B. *et al.* A perinuclear actin cap regulates nuclear shape. *Proc. Natl. Acad. Sci. U. S. A* **106**, 19017-19022 (2009).
37. Broers, J.L.V. *et al.* Decreased mechanical stiffness in LMNA^{-/-} cells is caused by defective nucleo-cytoskeletal integrity: implications for the development of laminopathies. *Human Molecular Genetics* **13**, 2567-2580 (2004).
38. Khatau, S.B., Kim, D.H., Hale, C.M., Bloom, R.J., & Wirtz, D. The perinuclear actin cap in health and disease. *Nucleus*. **1**, 337-342 (2010).
39. Kim, D.H. *et al.* Actin cap associated focal adhesions and their distinct role in cellular mechanosensing. *Sci. Rep.* **2**, 555 (2012).
40. Boudaoud, A. *et al.* FibrilTool, an ImageJ plug-in to quantify fibrillar structures in raw microscopy images. *Nat. Protoc.* **9**, 457-463 (2014).
41. Feng, Y. *et al.* alpha-actinin1 and 4 tyrosine phosphorylation is critical for stress fiber establishment, maintenance and focal adhesion maturation. *Exp. Cell Res.* **319**, 1124-1135 (2013).

42. Ye,N. *et al.* Direct observation of alpha-actinin tension and recruitment at focal adhesions during contact growth. *Exp. Cell Res.* **327**, 57-67 (2014).
43. Choi,C.K. *et al.* Actin and alpha-actinin orchestrate the assembly and maturation of nascent adhesions in a myosin II motor-independent manner. *Nat. Cell Biol.* **10**, 1039-1050 (2008).
44. Wachsstock,D.H., Wilkins,J.A., & Lin,S. Specific interaction of vinculin with alpha-actinin. *Biochem. Biophys. Res. Commun.* **146**, 554-560 (1987).
45. Kanchanawong,P. *et al.* Nanoscale architecture of integrin-based cell adhesions. *Nature* **468**, 580-584 (2010).
46. Smith,M.A. *et al.* A zyxin-mediated mechanism for actin stress fiber maintenance and repair. *Dev. Cell* **19**, 365-376 (2010).
47. Isermann,P. & Lammerding,J. Nuclear mechanics and mechanotransduction in health and disease. *Curr. Biol.* **23**, R1113-R1121 (2013).
48. Chancellor,T.J., Lee,J., Thodeti,C.K., & Lele,T. Actomyosin tension exerted on the nucleus through nesprin-1 connections influences endothelial cell adhesion, migration, and cyclic strain-induced reorientation. *Biophys. J.* **99**, 115-123 (2010).
49. Ho,C.Y., Jaalouk,D.E., Vartiainen,M.K., & Lammerding,J. Lamin A/C and emerin regulate MKL1-SRF activity by modulating actin dynamics. *Nature* **497**, 507-511 (2013).
50. Jungbauer,S., Gao,H., Spatz,J.P., & Kemkemer,R. Two characteristic regimes in frequency-dependent dynamic reorientation of fibroblasts on cyclically stretched substrates. *Biophys. J.* **95**, 3470-3478 (2008).
51. Lee,C.F., Haase,C., Deguchi,S., & Kaunas,R. Cyclic stretch-induced stress fiber dynamics - dependence on strain rate, Rho-kinase and MLCK. *Biochem. Biophys. Res. Commun.* **401**, 344-349 (2010).
52. Goldyn,A.M., Rioja,B.A., Spatz,J.P., Ballestrem,C., & Kemkemer,R. Force-induced cell polarisation is linked to RhoA-driven microtubule-independent focal-adhesion sliding. *J. Cell Sci.* **122**, 3644-3651 (2009).
53. Chen,B., Kemkemer,R., Deibler,M., Spatz,J., & Gao,H. Cyclic stretch induces cell reorientation on substrates by destabilizing catch bonds in focal adhesions. *PLoS. One.* **7**, e48346 (2012).
54. Bertrand,A.T. *et al.* Cellular microenvironments reveal defective mechanosensing responses and elevated YAP signaling in LMNA-mutated muscle precursors. *J. Cell Sci.* **127**, 2873-2884 (2014).
55. Brosig,M., Ferralli,J., Gelman,L., Chiquet,M., & Chiquet-Ehrismann,R. Interfering with the connection between the nucleus and the cytoskeleton affects nuclear rotation, mechanotransduction and myogenesis. *Int. J. Biochem. Cell Biol.* **42**, 1717-1728 (2010).
56. Sullivan,T. *et al.* Loss of A-type lamin expression compromises nuclear envelope integrity leading to muscular dystrophy. *J. Cell Biol.* **147**, 913-920 (1999).
57. Yang,M.T., Fu,J., Wang,Y.K., Desai,R.A., & Chen,C.S. Assaying stem cell mechanobiology on microfabricated elastomeric substrates with geometrically modulated rigidity. *Nat. Protoc.* **6**, 187-213 (2011).
58. Gasser,T.C. & Holzapfel,G.A. Modeling plaque fissuring and dissection during balloon angioplasty intervention. *Ann. Biomed. Eng.* **35**, 711-723 (2007).
59. Driessen,N.J., Cox,M.A., Bouten,C.V., & Baaijens,F.P. Remodelling of the angular collagen fiber distribution in cardiovascular tissues. *Biomech. Model. Mechanobiol.* **7**, 93-103 (2008).

Chapter 4

Soft substrates normalize nuclear morphology and prevent nuclear rupture in fibroblasts from a laminopathy patient with compound heterozygous LMNA mutations

Laminopathies, mainly caused by mutations in the LMNA gene, are a group of inherited diseases with a highly variable penetrance; i.e. the disease spectrum in persons with identical LMNA mutations range from symptom-free conditions to severe cardiomyopathy and progeria, leading to early death. LMNA mutations cause nuclear abnormalities and cellular fragility in response to cellular mechanical stress, but the genotype/phenotype correlations in these diseases remain unclear. Consequently, tools such as mutation analysis are not adequate for predicting the course of the disease.

Here, we employ growth substrate stiffness to probe nuclear fragility in cultured dermal fibroblasts from a laminopathy patient with compound progeroid syndrome. We show that culturing of these cells on substrates with stiffness higher than 10 kPa results in malformations and even rupture of the nuclei, while culture on a soft substrate (3 kPa) protects the nuclei from morphological alterations and ruptures. No malformations were seen in healthy control cells at any substrate stiffness. In addition, analysis of the actin cytoskeleton organization in this laminopathy cells demonstrates that the onset of nuclear abnormalities correlates to an increase in cytoskeletal tension.

Together, these data indicate that culturing of these LMNA-mutated cells on substrates with a range of different stiffnesses can be used to probe the degree of nuclear fragility. This assay may be useful in predicting patient-specific phenotypic development and in investigations on the underlying mechanisms of nuclear and cellular fragility in laminopathies.

The contents of this chapter are based on:

Tamiello, C. *et al.* Soft substrates normalize nuclear morphology and prevent nuclear rupture in fibroblasts from a laminopathy patient with compound heterozygous LMNA mutations. *Nucleus*. **4**, 61-73 (2013).

Introduction

The structural continuity between the intracellular (nucleus and cytoskeleton) and the extracellular environment of adherent cells is crucial for cell fate^{1,2}. The coupling between nucleus and cytoskeleton via proteins embedded in the nuclear envelope and the connection between cytoskeletal filaments and the extracellular matrix (ECM) via focal adhesions, together are part of the mechanotransduction mechanism, i.e. the process of converting physical forces into biochemical signals and integrating these signals into cellular responses³⁻⁵.

Some of the structural connections between the nucleus and the cytoskeleton are altered by mutations in the LMNA gene, which encodes for lamina-type proteins, i.e. lamin A, lamin C and lamin AΔ10. Lamins are located just underneath the inner nuclear membrane of most differentiated somatic cells and form the nuclear lamina, a fibrillar network part of the nuclear envelope which plays a crucial role in the maintenance of nuclear shape and gives structural support to the nucleus^{6,7}. Consequent to disturbances in the structural connections with the cytoskeleton and in the nuclear lamina assembly, LMNA mutations lead to decreased cellular stiffness and increased mechanical weakness leading to increased sensitivity to mechanical stress^{8,9}. Abnormal nuclear morphology, compromised nuclear integrity and tendency to spontaneous nuclear disruption, even in the absence of external forces, are also reported for these cells⁸⁻¹⁶.

The family of genetic diseases associated with mutations in the LMNA gene is called laminopathies. Laminopathies are associated with a diverse array of tissue-specific degenerative disorders as well as syndromes with overlapping features. The most important pathologies included are: different types of striated muscle diseases, such as Limb-girdle muscular dystrophy, Emery-Dreifuss muscular dystrophy, and dilated cardiomyopathy; abnormalities in adipose tissue development, including Familial Partial Lipodystrophy, type II (Dunningan syndrome) and type II diabetes; peripheral nerve diseases such as Charcot Marie-Tooth disease; and systemic failure diseases such as Hutchinson Gilford Progeria Syndrome (premature ageing). Most of the symptoms develop in the postnatal phase and may lead to early death¹⁷. The molecular mechanisms giving rise to tissue-specific laminopathies are still largely unknown. The complexity of these diseases is further exemplified by the fact that identical genetic mutations can give rise either to a severe disease phenotype in one patient, or no clinical symptoms at all in another person. These observations indicate that mutation analysis alone is not conclusive for diagnosis or prognosis of laminopathy development and consequent functional losses.

Here we propose to use cell culture on substrates with different stiffness to probe laminopathy cells from a progeroid syndrome patient with compound heterozygous mutations in the LMNA gene, consisting of p.T528M in combination with p.M540T¹⁸. We hypothesize that soft substrates can protect nuclei of these laminopathy cells from morphological disturbances and structural weakness, as in this case lower forces are propagated to the weakened nucleus. We examined dermal fibroblasts from the laminopathy patient and healthy control dermal fibroblasts seeded on collagen-I coated polyacrylamide gels (PA gels) with stiffness varying over a physiologic range (3 - 80 kPa) and glass substrates as control. After 48 hours from seeding, we analyzed nuclear shape and rupture, as well as actin cytoskeleton organization, which is the main determinant of cell shape, structure and cellular stiffness¹⁹⁻²¹. Our results show that that only on soft substrates (3 kPa) the laminopathy cells

tested respond similar to healthy control cells. Interestingly, we were able to probe the intracellular response of these cells by varying the stiffness of the extracellular environment. This suggests that modulation of substrate stiffness is an attractive tool to investigate mechanical functioning and fragility of genetically affected cells of individual patients as a phenotypic marker of the disease stage.

Results

We investigated the intracellular effect of increasing substrate stiffness on diseased dermal fibroblasts, isolated from a patient suffering from a progeroid syndrome due to compound heterozygous missense mutations (p.T528M and p.M540T) in the LMNA gene (*LMNAMut*) and we compared these findings with control human fibroblast cell line (NHDF α). For this purpose both cell types were seeded on collagen I coated polyacrylamide (PA) gels with stiffnesses ranging from 3 kPa to 80 kPa, as well as on collagen I coated glass substrates. Both cell types adhered and elongated when plated on the surface of the collagen I coated PA gels and glass substrates, except for the 3 kPa where fewer cells adhered and reduced cell spreading after attachment was observed after 48 hours from seeding (**Figure 4.1A**). Fluorescent staining (phalloidin-TRITC) of the actin cytoskeleton at 48 hours after seeding suggested that both cell types could equally sense the stiffness of the substrates as their actin cytoskeleton became more stretched and organized in bundles for substrates stiffer than 3 kPa (**Figure 4.1B**). Quantitative measurement of cell area and aspect ratio confirmed that soft substrates (3 kPa) with $E = 3$ kPa elicit significant lower cell spreading and elongation in both cell types (**Figure 4.1 C-D**) However, no significant differences were observed on the 10, 20, 80 kPa PA gels and glass.

Nuclear shape of *LMNAMut* is abnormal on stiff substrates but preserved on soft substrates

Morphologically visible nuclear abnormalities are common in laminopathy cells²². These abnormalities, seen as nuclear blebs, herniation's, and so-called honeycomb structures after immunostaining, seem to indicate the presence of weak spots at the nuclear membrane and/or nuclear interior. Here, we tested whether the extracellular substrate stiffness affects the frequency of these nuclear abnormalities in the *LMNAMut* cells. From the images of DAPI and lamin B1 immunolabeled nuclei, it became obvious that few abnormally shaped nuclei were seen in cells seeded at low stiffness after 48 hours from seeding (between 3 and 4% of all nuclei) (**Figure 4.2**). Representative images of normal and abnormally shaped nuclei are shown in **Figure 4.3A**. Further quantitative analysis of 600 nuclei per cell genotype showed that on soft substrates (3 kPa) both *LMNAMut* and NHDF α nuclei overall have a normal appearance ($2.9 \pm 0.4\%$ NHDF α , $3.7 \pm 0.4\%$ *LMNAMut*, **Figure 4.3B**). However, while in the NHDF α control fibroblasts abnormally shaped nuclei were detected in about $3.0 \pm 0.7\%$ of the cells regardless of the substrate stiffness, a significant increase of abnormally shaped *LMNAMut* nuclei was observed on 10, 20, 80 kPa PA gels and glass substrates (respectively $8.2 \pm 0.7\%$, $26.9 \pm 5.0\%$, $44.7 \pm 1.7\%$, $22.5 \pm 2.4\%$) (**Figure 4.3 B-C**). The fraction of misshapen nuclei in *LMNAMut* cells increased significantly on the 80 kPa gel (up to $44.7 \pm 1.7\%$ compared to $26.9 \pm 5.0\%$ on 20 kPa). A reason for this significant increase could be the higher

cell density observed on the 80 kPa gels seeded with *LMNA*mut cells. As in a side experiment we observed increased nuclear aberrations with increased cell density, we therefore hypothesize that cell-cell contact played a role in the formation of nuclear abnormalities (**Figure 4.4**). On the glass substrate results were similar to those on the 20 kPa PA gels ($22.5 \pm 2.4\%$). The findings on glass are in agreement with earlier studies, showing that 36% of all cells from this *LMNA*mut patient cultured on glass substrates had irregularly shaped nuclei with blebs, honeycomb figures, large and poorly defined protrusions¹⁸.

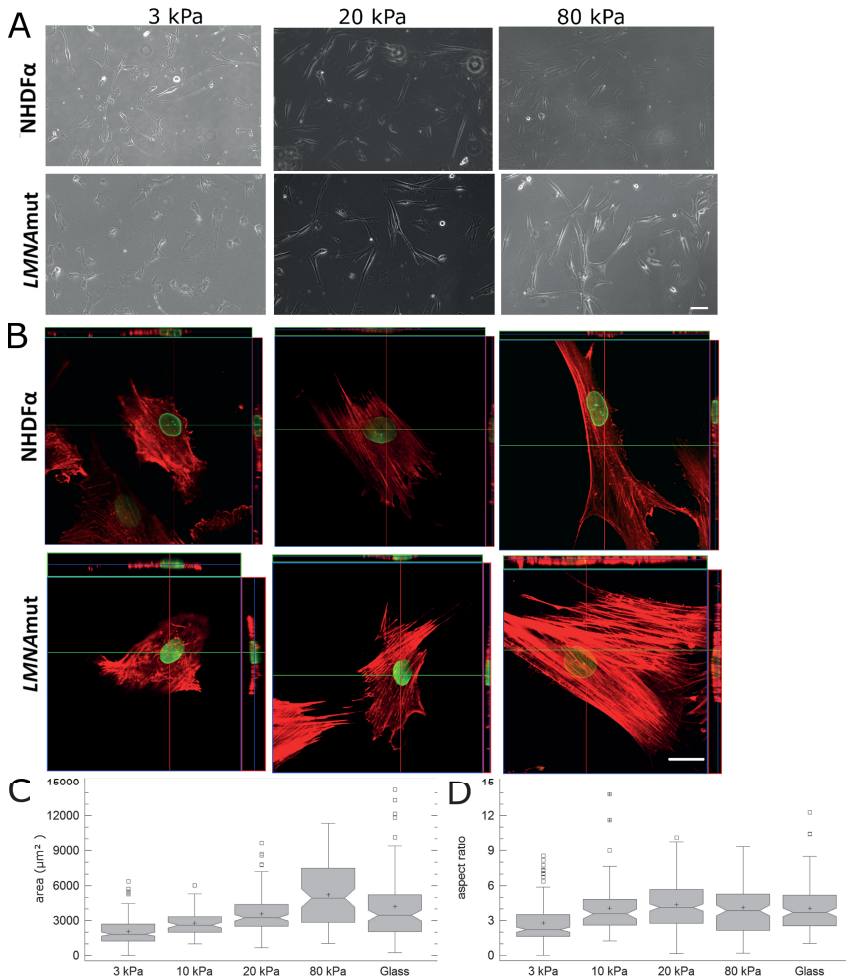


Figure 4.1. Effect of substrate stiffness on cell morphology and actin cytoskeleton organization. (A) Representative bright field images of NHDF α and *LMNA*mut cells seeded on polyacrylamide gels with stiffness ranging from 3 kPa to 80 kPa taken 48 hours after seeding. Fewer and less spread cells were present on 3 kPa polyacrylamide gels than on stiffer substrates for both cell types. Scale bar: 100 μm . (B) Actin organization in NHDF α and *LMNA*mut (phalloidin-TRITC, red) showed increased organization and tension on substrates stiffer than 3 kPa. Green colour is given by lamin B1 staining. Scale bar: 20 μm . (C-D) Cell area and aspect ratio presented as box-and-whisker plots. The measurements of NHDF α and *LMNA*mut did not show significant difference, thus the values were considered as a group.

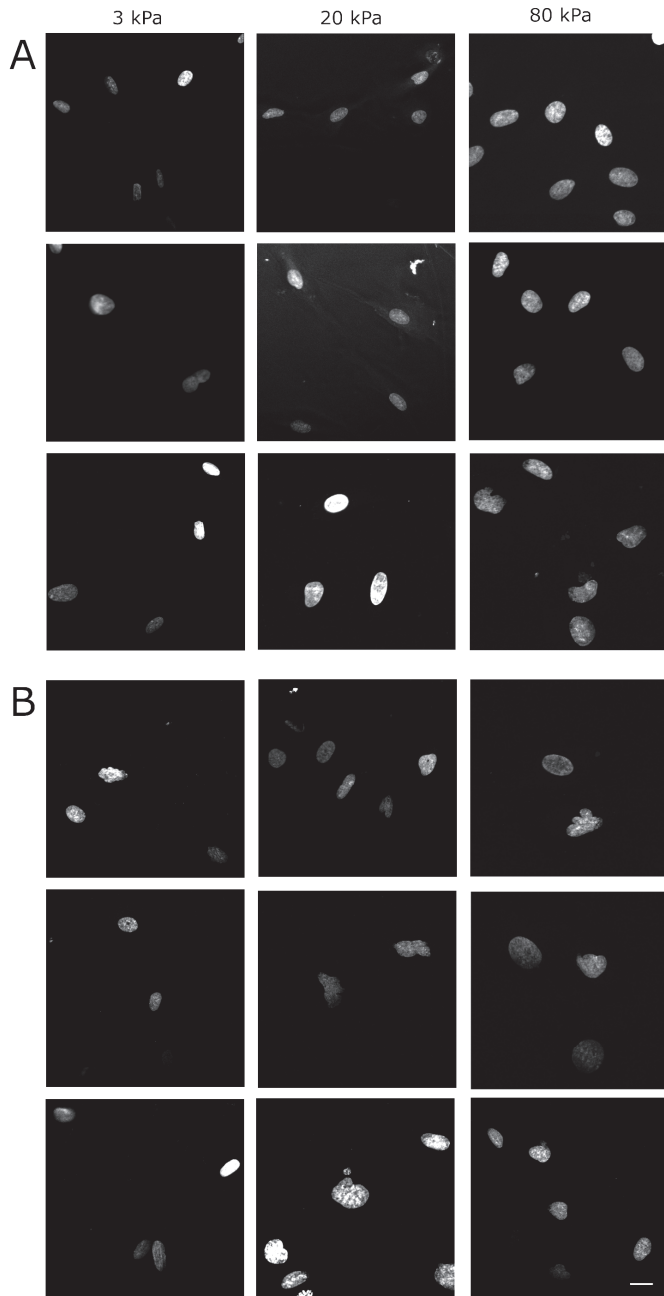


Figure 4.2. Nuclear abnormalities in *LMNA*mut cells. Nuclear morphology of NHDF α (A) and *LMNA*mut fibroblasts (B) cultured on 3, 20, 80 kPa polyacrylamide gels. Scale bar: 10 μ m.

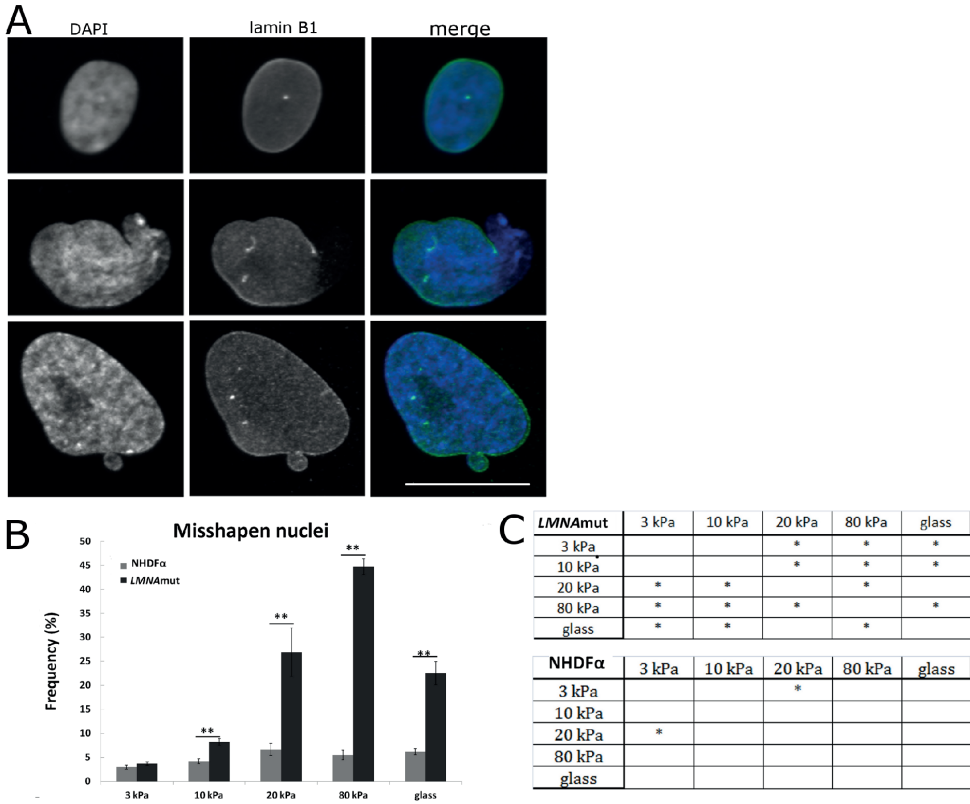


Figure 4.3. Nuclear morphological abnormality regulation by substrate stiffness. (A) Immunofluorescent labelling of cell nuclei with DAPI (blue), lamin B1 (green) and overlay of the two in the most right panels allowed to distinguish between normally (upper row) and abnormally shaped nuclei (second and third row). In particular, the nucleus in the second row shows a protrusion and in the third row a bleb can be observed. Scale bar: 10 μ m. (B) Frequency of abnormally shaped nuclei on increasing PA gel stiffness for *LMNA*mut and control NHDF α . Values represent means from at least 300 cells from 2 experiments. Bars represent SEM. * $p < 0.05$, ** $p < 0.01$ vs NHDF α on the same substrate stiffness (C) Statistical analyses of differences in frequency of misshapen nuclei for *LMNA*mut and NHDF α on the different substrate stiffness's. *, $p < 0.05$; no star, $p > 0.05$.

***LMNA*mut cells show a defective actin cytoskeleton on stiff substrates but not on soft substrates.**

In order to provide insight into the role of the actin cytoskeleton on the onset of nuclear abnormalities (protective mechanism of a soft environment on nuclear integrity), we investigated actin fiber organization using phalloidin-TRITC labelling. The actin cytoskeleton is known indeed to respond to substrate stiffness and affect cell shape and migration. Confocal microscopy of the phalloidin stained cells plated on 3 kPa PA gels showed a rounded morphology for both cell genotypes, with little polymerized actin formation that barely formed bundling of tensed fibers. In the perinuclear region there seemed to be no actin fibers, while we observed fibers running on top of the nucleus (actin cap) (Figure 4.5A).

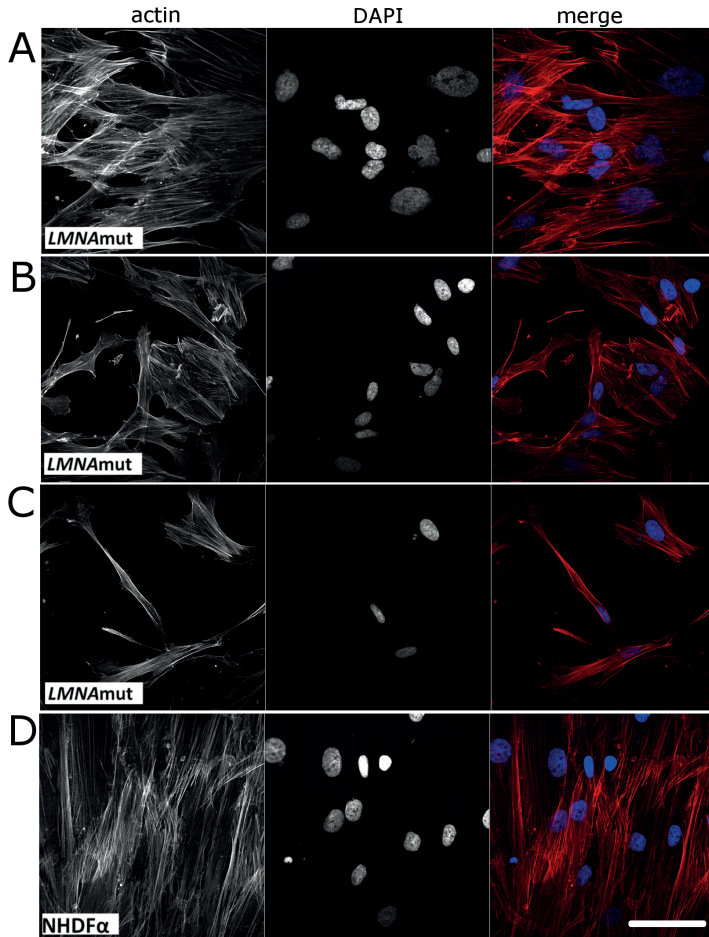


Figure 4.4. Effect of increased cell density on nuclear abnormalities. Representative confocal sections of *LMNAmut* seeded on glass substrates immunocytochemical stained for F-actin in red (phalloidin-TRITC) and DAPI in blue at 48 hours after seeding. (A-B) High density *LMNAmut* cells show misshapen nuclei. (C) Low density *LMNAmut* cells show intact nuclear morphology. (D) High density NHDF cells show normal nuclear morphology.

At 10 kPa and higher stiffnesses, cells demonstrated the typical well-spread and flattened morphology with development of bundles of tense stress fibers (**Figure 4.1A** and **Figure 4.5 B and E**). According to Khatau *et al.*²³, *LMNA* mutant cells can lack the characteristic actin cap running above the nucleus. After analysis of confocal z-stacks of both cell genotypes in our study, we could not confirm a difference in actin cap presence. However, we did detect aberrations in actin cytoskeleton organization in about 5% of the *LMNAmut* cells plated on 10, 20, 80 kPa and glass, at 48 hours after seeding but not on the 3 kPa. These aberrations included detachment of actin stress fibers in the perinuclear region with formation of a speckled pattern of actin which suggests actin depolymerisation in these areas (**Figure 4.5 C-D**). Similar observations were already reported for cells cultured on glass cover slips^{7,17,24,25}.

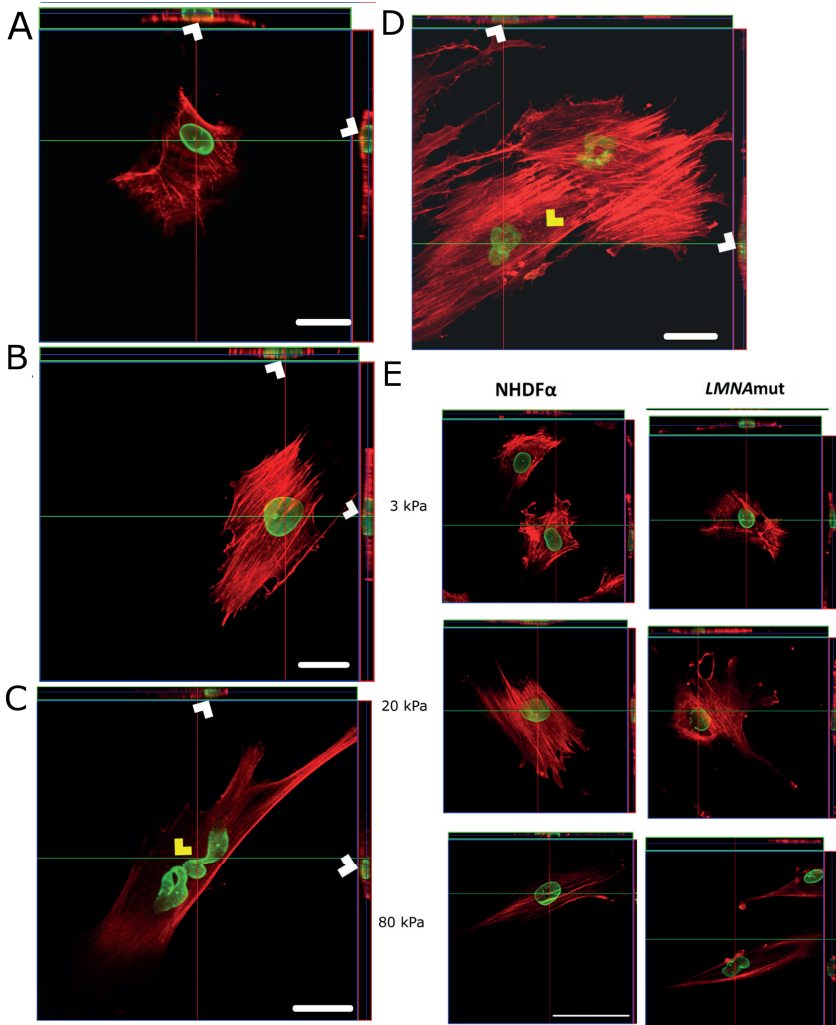


Figure 4.5. Influence of substrate stiffness on cytoskeletal actin organization and aberrations. Confocal z-series taken from half height of the whole cell and relative orthogonal cross sections of NHDF α and LMNAmut immunocytochemical stained for F-actin in red (phalloidin-TRITC) and Lamin B1 in green at 48 hours after seeding. (A) Representative fibroblast seeded on 3 kPa PA gels. It shows short and not tensed actin fibers, which are missing in the perinuclear region. An actin cap is running above the nucleus (white arrowhead). No differences could be noticed between LMNAmut and NHDF α . Thus no aberrations could be detected in the actin cytoskeleton of cells plated on soft substrates. (B) Control NHDF α on PA gel stiffer than 3 kPa, precisely on the 20 kPa PA gel. Actin stress fibers are tensed and well-structured also in the perinuclear region. The actin cap made of thick stress fibers run above the nucleus the (white arrowhead) nucleus. (C-D) Representative aberrations found in LMNAmut seeded on 20 (C) and 80 kPa (D) PA gels. Cells have a misshapen nucleus. Yellow arrowhead indicates the lack of actin fibers in the perinuclear region (C) and a speckled distribution of actin (D). The actin cap is running above the nucleus (white arrowhead). Scale bars: 20 μ m. (E) Representative images of cells on three substrate stiffnesses. NHDF α (left panel) and LMNAmut (right panel) on 3kPa, 20 kPa and 80 kPa PA gels. Scale bar: 50 μ m.

Disruptions of the actin-cytoskeleton and trypsinization partially normalize nuclear abnormalities in *LMNA*mut cells.

To further prove the correlation between actin cytoskeletal tension and the onset of nuclear abnormalities, *LMNA*mut cells grown on collagen I coated glass bottom culture dishes were incubated for different period of times with cytochalasin D (cytoD), which inhibits actin dynamics and, consequently, causes disruption of the actin-cytoskeleton (**Figure 4.6**). Next, the drug was removed and *LMNA*mut cells were allowed to recover in normal growth medium for 1 hour to overnight. Confocal microscopy on phalloidin-TRITC and DAPI stained *LMNA*mut cells showed that the short treatment (30 minutes) followed by 1 hour recovery (short treatment + short recovery) disrupted the actin-cytoskeleton only mildly compared to untreated control *LMNA*mut (**Figure 4.6 A-B**). Yet, there was no difference between the frequency of misshapen nuclei in this group and in the untreated control *LMNA*mut ($18.4 \pm 2.1\%$ vs $22.3 \pm 4.0\%$, Fig. 4E). There was presumably not enough time for the nucleus to respond to the decrease in cytoskeletal tension or the degree of disruption did not allow any response. In contrast, a three hour treatment followed by an hour recovery (long treatment + short recovery) leads to serious disruption of the actin cytoskeleton and significantly less misshapen nuclei ($11.8 \pm 0.8\%$, **Figure 4.6C**). Upon 3 hours cytoD treatment followed by overnight recovery (long treatment + long recovery), the actin cytoskeleton completely recovered from the treatment and tensed stress fibers were visible (**Figure 4.6D**). The frequency of misshapen nuclei ($19.1 \pm 1.6\%$) was found to be comparable to that of untreated *LMNA*mut cells (**Figure 4.6E**).

Moreover we analyzed the changes in nuclear morphology due to cellular detachment of *LMNA*mut cells by trypsin, followed by re-adhesion to a glass substrate (**Figure 4.7**). At 30 and 60 minutes after seeding, nuclear folding due to trypsin treatment did not yet allow a reliable analysis of nuclear shape. At this stage of attachment the actin cytoskeleton was largely disorganized, seen as absence of tense stress fibers in these cells. Starting from 2 till 8 hours after seeding the frequency of misshapen nuclei was significantly lower than that at 72 hours ($11.0 \pm 2.0\%$, $13.3 \pm 3.8\%$, $14.6 \pm 2.3\%$, $15.6 \pm 2.2\%$, $28.3 \pm 3.5\%$ respectively at 2, 4, 8, 24 and 72 hours). At these time points actin reorganization did take place in the lower regions of the cell, making contact with the glass substrate, but stress fibers were absent at close distance to the nucleus. While after 24 hours of attachment the actin organization was mainly restored, showing actin fibers in close contact with the nucleus, it took even longer (up to 72 hours) until cells were fully stretched, and showing the regular percentage of abnormal nuclei (**Figure 4.7 A-B**).

Strikingly, not only the number of cells with blebs, but also bleb size itself increased considerably with time, ranging from $1\text{-}25 \mu\text{m}^2$ after 2 hours (average $5.24 \mu\text{m}^2$, $n=12$) to $3\text{-}62 \mu\text{m}^2$ (average $24.4 \mu\text{m}^2$, $n=10$, **Figure 4.7C**). This shows that nuclear morphology becomes partially normalized after trypsinization, which hydrolyzes the protein-protein bonds that attach cells to the extracellular matrix and consequently induces cell rounding along with reduction of cytoskeletal tension. All together, these results suggest a direct correlation between the level of actin-cytoskeleton tension and the prominence of nuclear abnormalities.

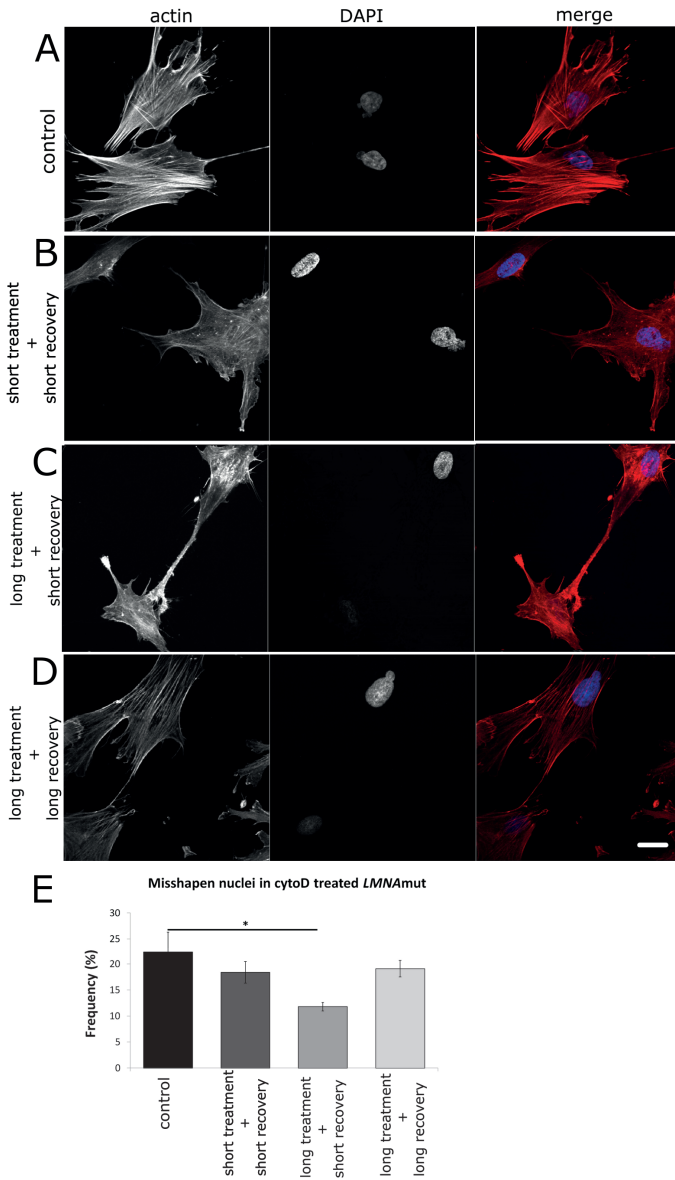


Figure 4.6. Effects of transient cytoD treatment on LMNAmut nuclei. Representative confocal sections of LMNAmut seeded on collagen I coated glass substrates incubated with cytoD 1 μ M and recovered in normal growth medium. After fixation, cells were stained with DAPI (blue) to check for nuclear abnormalities and phalloidin-TRITC (red) to check for actin organization. (A) Untreated control LMNAmut. (B) Short treatment + short recovery: LMNAmut treated for 30 minutes with cytoD and recovered for 1 hour. (C) Long treatment + short recovery: LMNAmut treated for 3 hours with cytoD and recovered for 1 hour. (D) Long treatment + long recovery LMNAmut treated for 3 hours with cytoD and recovered overnight. Scale bar: 20 μ m. (E) Frequency of misshapen nuclei in LMNAmut upon treatment with cytoD. At least 600 cells were assessed per each group. *, $p < 0.05$; no star, $p > 0.05$.

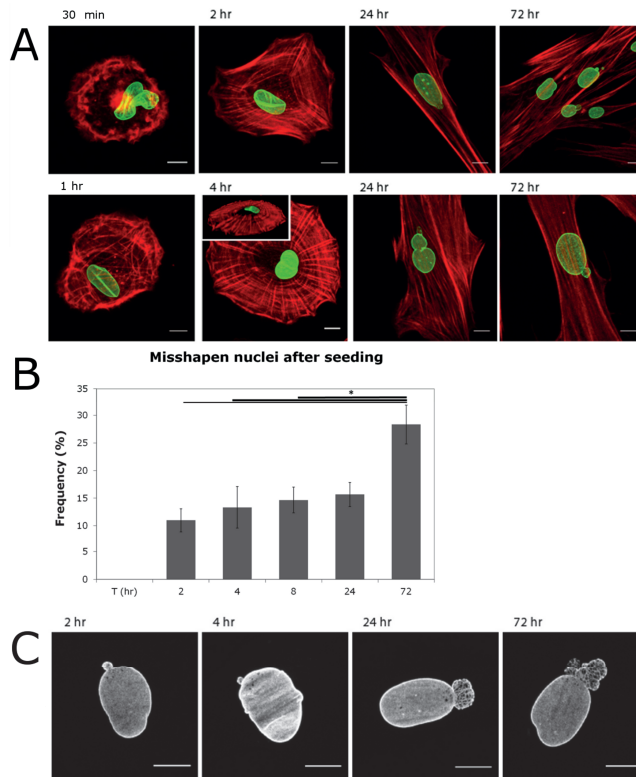


Figure 4.7. Alterations in nuclear shape and actin organisation upon attachment of cells after trypsin treatment. (A) Representative confocal sections of *LMNA*mut seeded on collagen I coated glass substrates at 30 minutes, 1, 2, 4, 24 and 72 hours after seeding. Cells were immunocytochemical stained for F-actin in red (phalloidin-TR) and lamin A/C in green. Inset at 4 hours: 3D view (generated by ImageJ 3D-viewer, showing the position of the nucleus (green) at the upper region of the cell, with very few tense actin stress fibers (red) surrounding the nucleus). Scale bar: 10 μ m. (B) Frequency of misshapen nuclei after seeding. *, $p < 0.05$; no star, $p > 0.05$. (C) Changes in nuclear bleb size upon attachment, visualized by immunofluorescence using the Jo12 lamin A/C antibody. Note the increase in size as well as the aberrant shape of the nuclear blebs. Note also that in most blebs a typical honeycomb structure of the lamina staining can be seen. Scale bar: 10 μ m.

Cellular compartmentalization in *LMNA*mut cells is not compromised on soft substrates.

Given the increased presence of abnormally shaped nuclei in *LMNA*mut cells cultured on substrates stiffer than 3 kPa, we tested whether this was correlated to a loss of cellular compartmentalization. We chose promyelocytic leukaemia nuclear bodies (PML-NBs) as marker, as these assemblies of PML proteins are normally confined to the nuclear interior of non-proliferating cells²⁶ (Figure 4.8A). Earlier studies by De Vos *et al.* and Houben *et al.* showed that frequent loss of PML-NBs from the nucleus to the cytoplasm can be found in laminopathy cells^{14,27,28}. In the current experiment, approximately 600 cells for each genotype, on each substrate, were screened manually for PML-NBs localization using fluorescent microscopy. We observed cytoplasmic PML-NBs (cytPML-NBs) in cases of abnormally shaped nuclei as well as for intact nuclei (Figure 4.8 B-C). Therefore it is not possible to directly correlate abnormalities in the nuclear shape to the loss of cellular compartmentalization.

Similarly to previous findings¹⁴, $4.4 \pm 1.1\%$ NHDF α control cells demonstrated cytPML-NBs, regardless of the substrate stiffness (**Figure 4.8D**). On the 3kPa substrate, *LMNAMut* and NHDF α control cells showed no significant differences in the frequency of cells with cytPML-NBs ($3.1 \pm 0.5\%$ *LMNAMut* and $2.0 \pm 0.2\%$ NHDF α). However, we did observe a gradual increase of *LMNAMut* cells with cytPML-NBs with increasing stiffness of the substrates between 3 and 20 kPa (from $3.1 \pm 0.5\%$ to $12.8 \pm 1.2\%$), indicating increased frequency of cytPML-NBs in *LMNAMut* cells (**Figure 4.8 D-E**).

Nuclear ruptures in *LMNAMut* cells increase with substrate stiffness, but are prevented on soft substrates.

A recent study by De Vos *et al.*¹⁶ showed the occurrence of spontaneous nuclear ruptures in cells from laminopathy patients cultured on glass substrates. These ruptures never occurred in wild type cells (NHDF α) under the same culturing conditions. Based on these results and triggered by the finding of variable cytPML-NBs on different substrate stiffness, we hypothesized that mechanical cues provided by the extracellular environment might affect the frequency of nuclear rupture events. For this purpose we monitored living cells (about 20) for 2 hours at 1 or 2 minute intervals under a fluorescent microscope on 3, 10, 20, 80 kPa PA gels and glass substrate after 24-36 hours from transfection with EYFP-nuclear localization signal (EYFP-NLS), which helped to check for nuclear integrity. Correct expression of EYFP-NLS was revealed by a constant intense intranuclear fluorescent signal. In NHDF α cells, as well as in *LMNAMut* cells on 3kPa substrates we could not detect a nuclear rupture event in any cell examined. In contrast, for the stiffer substrates an increased frequency of nuclear rupture was detected in the *LMNAMut* cells, increasing from 20% (4/20) of *LMNAMut* with nuclear rupture on the 10 kPa substrate to 34.5% (10/29) on 80 kPa. The ruptures were visible as a sudden transient efflux of EYFP-NLS from the nucleus to the cytoplasm (Figure 4.9 and Video www.tandfonline.com/doi/suppl/10.4161/nucl.23388/suppl_file/kncl_a_10923388_sm0001.zip). This phenomenon, which lasts about 20 minutes and can occur repetitively in the same cell, was followed by restoration of EYFP-NLS signal in the nucleus and was not lethal for the cells. All together, these results confirm that soft substrates do not compromise the nuclear integrity of *LMNAMut* cells, while stiff environments do.

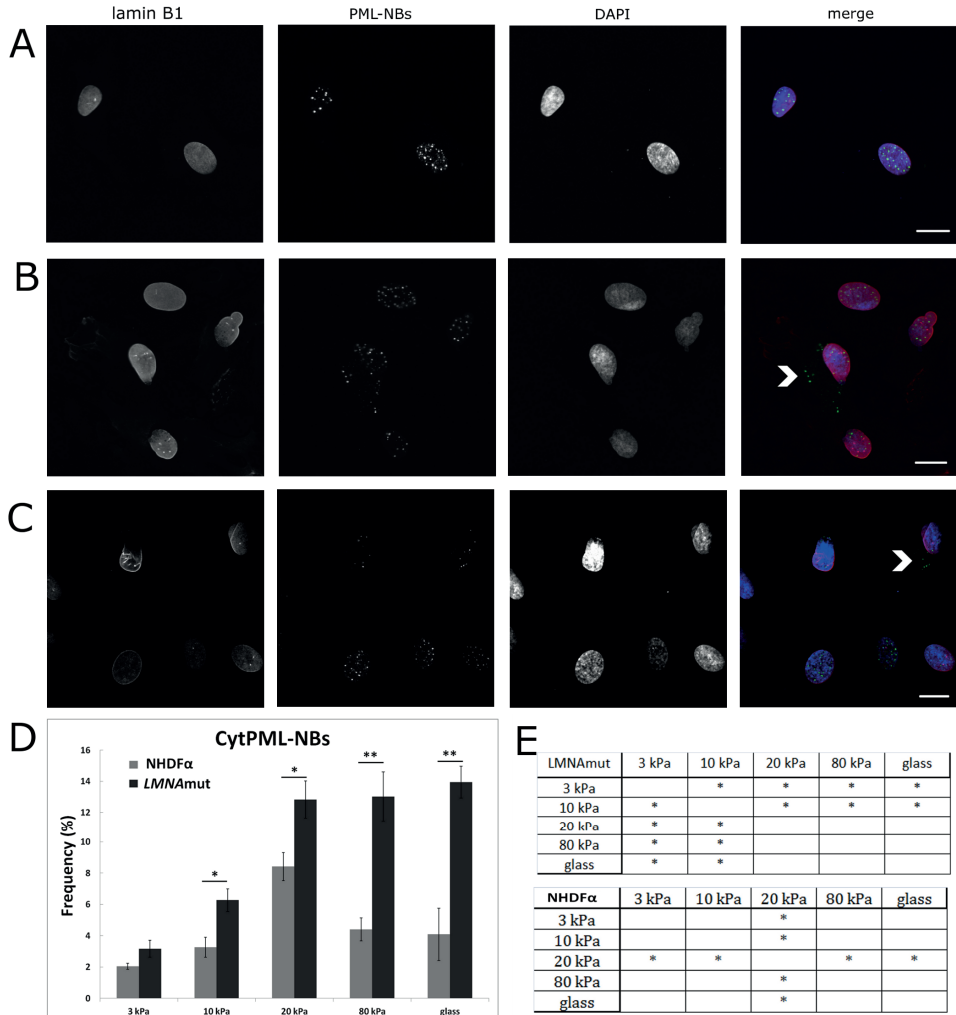


Figure 4.8. PML-NBs localization as a marker for cellular compartmentalization. (A-C) Confocal sections representative of cell nuclei were immunolabeled with Lamin B1 (red), DAPI (blue) and PML-NBs (green) to investigate the localization of PML-NBs. Nuclei were counterstained with DAPI (blue). The most right panel shows the triple overlay. Scale bars: 10 μ m. (A) Nuclei showing normal morphology and internal localization of PML-NBs. Cellular compartmentalization is intact. (B) Cytoplasmic localization of PML-NBs (cytPML-NBs) around a nucleus showing an abnormal morphology (white arrowhead). Loss of cellular compartmentalization is indicated by the exit of PML-NBs to the cytoplasm. (C) CytPML-NBs could be found also in normally shaped nuclei (white arrowhead) indicating that loss of cellular compartmentalization is not directly related to nuclear morphology abnormalities. (D) Relative frequency of NHDF α and LMNAmut showing cytPML-NBs. Values represent means from at least 600 cells from 2 experiments. Bars represent SEM. * $p < 0.05$, ** $p < 0.01$ vs NHDF α on the same substrate stiffness (E) Statistical analyses of differences in frequency of cytPML-NBs for LMNAmut and NHDF α on the different substrate stiffness's. *, $p < 0.05$; no star, $p > 0.05$.

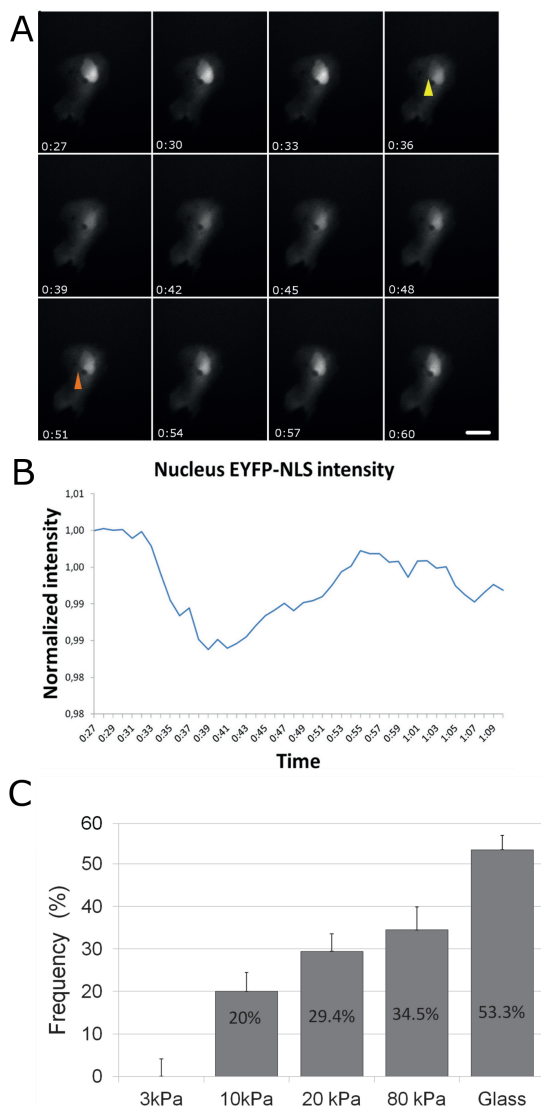


Figure 4.9. Spontaneous ruptures of the nuclear membrane do not occur on soft substrates. (A) Montage of selected images from a time-lapse recording of *LMNA*mut cell cultured on 10 kPa PA gel and transfected with EYFP-NLS, sampled at 1 min intervals for 2 h (Supplementary Video). Nuclear membrane rupture causes the decrease in intranuclear EYFP signal and increase in cytoplasmic EYFP signal (at 0:36, yellow arrowhead). Subsequently, the nuclear signal is gradually up taken by the nucleus and the rupture appears to be restored (at 0:51, orange arrowhead) (B) Evolution in time of EYFP-NLS (mean) intensity in the nucleus of the cell shown in (A). (C) Frequency of spontaneous nuclear membrane ruptures on the different substrates for *LMNA*mut. Error bars represent the square root of the number of recording.

Discussion

In this study we showed that, on soft substrates with stiffness of 3kPa, abnormal nuclear morphology and nuclear ruptures in dermal fibroblasts from a laminopathy patient with compound heterozygosity for mutations in LMNA can be normalized. Normalization of nuclear shape at low substrate stiffness, i.e. in presence of low cytoskeletal tension, indicates that nuclear abnormalities correlate to the mechanical properties of the ECM, such as the collagen I-coated PA gels used in here. For the purpose of this study and in view of a future clinical application, we chose to investigate dermal fibroblasts because it is and easily accessible cell source to probe and investigate²⁹.

A crucial finding is that the nuclei of LMNAmut cells used in this study do not develop an abnormal morphology when they are cultured on soft gels (3 kPa), while on stiffer substrates nuclei appear to have a misshapen shape (**Figure 4.3**) as reported also by Verstraeten *et al.*¹⁸. Abnormal nuclear phenotypes are normally found in cells with LMNA mutations^{10,11,18,30}, but the relevance of morphological abnormalities in the pathogenesis of laminopathies is not unravelled. Nuclear abnormalities are indeed not present in all diseased cells and there is no direct association between nuclear abnormalities and disease phenotype or severity³¹. However, previous studies have been performed only on glass or stiff silicon substrates and did not consider the mechanotransduction feedback-loop, which influences the cellular response based on the ECM mechanical cues. Still, in order to establish correlations between genotype and phenotype repeated measures using cells from different patients or families of patients are needed, as the phenotypic variability in this family of diseases may lead to different responses of the nucleus to developing intracellular tension.

One reason for increased nuclear abnormalities, nuclear ruptures and loss of cellular compartmentalization might be that, on soft substrates, the nuclear membrane is exposed to reduced cytoskeletal forces, transduced from the ECM. This can be inferred by our results on the actin cytoskeleton organization and from the partial normalization of the nuclear abnormalities upon disruption of the actin cytoskeleton by cytoD and after cell trypsinization. When actin is not assembled into tensed stress fibers, it is likely that the force exerted on the nucleus is not enough to tear apart the nuclear membrane or to compress the nucleus, causing nuclear rupture at weak spots. Furthermore, disorganization of the actin cytoskeleton in the perinuclear region of LMNAmut, was observed particularly on stiffer substrates and gave indication for an abnormal distribution of forces exerted to the nucleus, enhancing nuclear morphology disturbance. In contrast to Kathau *et al.*²³, we observed in the LMNAmut cells the presence of the nuclear shaping actin cap. Therefore, to explain these findings, we propose that a pulling mechanism in addition to a compressive pushing mechanism might play a role in altering nuclear morphology. We suspect that, on stiff substrates, the actin cap presses tightly against the nucleus and, in addition, organization of the stress fibers around the nucleus is abnormal, enhancing the probability of disturbance and rupture in the morphology of the genetically disorganized and weakened nucleus (**Figure 4.10**). This physical model can explain the observations on the different substrate stiffnesses. However the significant increase of misshapen nuclei on the 80 kPa PA gel is, in our opinion, due to an increase of cell-cell contact and increase in cell area and aspect ratio, which imply increase of cytoskeletal forces exerted on the nucleus. Reasons for the increase in cell area and cell aspect ratio might be found in changes in adhesive properties of the substrates. Hydrogels of increasing stiffnesses lead to increasing

anchoring densities and thereby increase in cell spreading³², while collagen absorption onto glass substrate could determine an anchoring density similar to that of the 20 kPa PA gel. While these *in vitro* studies cannot be directly interpolated to the *in vivo* situation, our assay to measure nuclear weakness could well predict the development of a laminopathy phenotype in patients. A common denominator in (nearly) all laminopathies is the loss of specific tissues, seen as muscular dystrophies and/or lipodystrophies. For each of these laminopathies, its value will have to be proven.

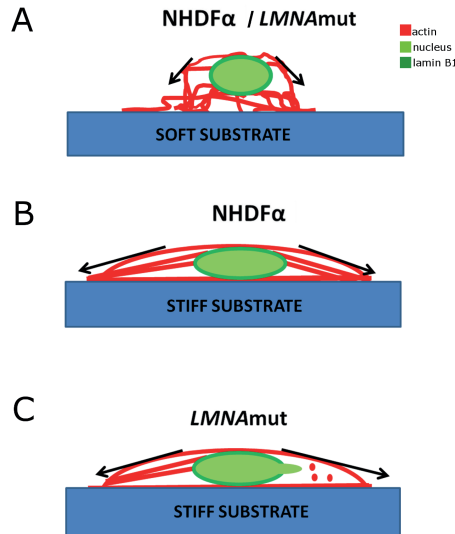


Figure 4.10. Proposed mechanism for actin cytoskeleton organization and effects on nuclear abnormalities on soft and stiff substrates. Schematic representation of the cross section of a cell seeded on substrates with different stiffness. Red represents the actin cytoskeleton while green the nucleus (dark green nuclear lamina). (A) When seeded on a soft substrate NHDFα and LMNAmut cells have the same response. They develop not tensed actin stress fibers which are not directly connected to the nucleus in the perinuclear region. Fibers run below and on top of the nucleus. Since low forces are exerted on the nucleus, the onset of nuclear abnormalities is prevented. (B) NHDFα cells seeded on a stiff substrate (stiffer than 3 kPa) develop tensed actin stress fibers which are well-organized in the whole cytoplasm. Stress fibers connect to the nucleus and form also the actin cap running on top of the nucleus. (C) LMNAmut cells on top of a stiff substrate develop tensed stress fibers. These stress fibers appear to be lacking in the perinuclear region and aggregates of actin are often visible. The pushing action of the actin cap (stress fibers running on top of the nucleus) together with the uneven distribution of pushing actin in the area around the nucleus lead to the development of nuclear abnormalities, further resulting in nuclear damage.

Taken together our data suggests that we were able to probe the response of the nucleus from the outside of the LMNAmut cells by using the mechanoresponsive pathways of the actin cytoskeleton. However, presently, we cannot rule out the involvement of microtubules, as they are known to be connected to actin via kinesin 1, and to the nuclear membrane via nesprin-4³. Studies on nucleus and cytoskeletal elements co-transfected laminopathy cells could give insights on the precise mechanisms of nuclear rupture.

Substrate stiffness appears to modulate also nuclear integrity. Indeed, we detected that repetitive disruptions of the nuclear membrane, previously reported by De Vos *et al.*¹⁶ in cells from different laminopathy patients under standard culturing conditions, are prevented on soft substrates (3 kPa)

but increasingly occurs on stiffer substrates. It is not clear how the cells can survive a repetitive disruption of the nuclear membrane, as mixing of cytoplasmic and nuclear components prevents appropriate nuclear localization of nuclear factors that can be crucial for several mechanisms (such as replication and transcription).

Also PML-NBs, often lost from the nucleus in laminopathy cells cultured on a glass substrate, were retained in the nucleus of *LMNA*mut seeded on soft substrate. However, since we observed cytoplasmic localization of PML-NBs without nuclear abnormalities (**Figure 4.8**), the presence of PML bodies in the cytoplasm is not indicative for dysfunctions of the nuclear lamina. Moreover, in a parallel study a direct correlation between occurrence of cytoplasmic PML-NBs and nuclear rupture as seen with EYFP-NLS could not be established: while in some cases of nuclear rupture PML-NBs moved out of the nuclei, in other cases this did not happen. Conversely, leakage of PML-NB proteins into the cytoplasm, or incomplete import of PML-NB proteins can cause cytoplasmic assembly of PML bodies without nuclear rupture¹⁶.

In conclusion, despite the fact that the data reported were from cells of only one laminopathy patient with rare compound mutation in the *LMNA* gene, our findings suggest that soft substrates could be used protect and possibly rescue cell from laminopathy patients with morphological disturbances and structural weakness. This study shows the value of using substrate stiffness based approach for improved diagnosis of genetically diseased cells in order to understand the interplay between genotype and phenotype. Elucidating the mechanotransduction pathways involved in the response of *LMNA*-mutated cells to changes in the extracellular environment will also help to provide new insight into the genotype phenotype correlations

Materials and methods

Cell cultures

Cells used in this study were primary skin fibroblasts. The laminopathies cells (*LMNA*mut) were obtained from a skin biopsy taken from a 2-year old male subject diagnosed with apparently typical Hutchinson Gilford Progeria Syndrome, which showed compound heterozygous mutations (*LMNA*^{T528M/M540T})¹⁸. Informed consent was obtained from the parents of the proband for this study. Normal human dermal fibroblasts (NHDF α) obtained from the European Collection of Cell Cultures (Salisbury, United Kingdom) were used as a control. NHDF α and *LMNA*mut were grown at 37°C in a humidified incubator containing 5% CO₂ and cultured in Advanced Dulbecco's modified Eagle's medium (DMEM, Invitrogen, Carlsbad, USA) supplemented with 10% fetal bovine serum (FBS; Greiner Bio-one, Frickenhausen, Germany), 1% L-glutamine and 1% penicillin/streptomycin (Lonza, Walkersville, USA). Cells were passaged by splitting at a 1:2 or 1:3 ratio every 3 days using trypsin. For seeding onto the substrates, cells were trypsinized at sub-confluency and plated at a density of 5000 cells/cm². NHDF α were used between passage 5 and passage 15. *LMNA*mut were used between passage 10 and passage 20. No differences were seen in the growth behaviour between passage numbers.

Transfection for live-cell imaging

*LMNA*mut were transiently transfected with an EYFP-NLS construct³³ (kind gift from Dr. J. Goedhart, University of Amsterdam, the Netherlands) using GeneJammer (Invitrogen, 204132) according to manufacturer's instructions at a GeneJammer/DNA ratio of 6:1 (μl per μg DNA). Transfection was performed 24 hours after seeding of the cells and culture medium was changed 4 hours after transfection to minimize cytotoxicity.

Coated polyacrylamide (PA) gels and glass substrates

Polyacrylamide (PA) gels coated with collagen I were used to create 2 dimensional substrates with controlled stiffness for NHDF α and *LMNA*mut. PA gel stiffness (expressed as elastic modulus, E) was controlled by modulating the bis-acrylamide crosslink concentration and was verified using an indentation test³⁴. The method used for the preparation was adapted from Pelham and Wang³⁵. In short, glass bottom culture dishes (singles or multi-well; 35 mm-diameter dish, 20mm-diameter glass, coverslip No. 1.5, MatTek Corporation, Ashland, USA) were cleaned with 1% NaOH, silanized with pure 3-(aminopropyl)trimetoxysilane (Sigma-Aldrich, St. Louis, USA) for 10 minutes and, finally, functionalized by means of 0.5% glutaraldehyde (25% solution, Sigma-Aldrich) in PBS for 30 minutes. Precursors mixtures of PA gels were made from acrylamide (40%, Sigma) and N, N', N'-methylene-bisacrylamide (bis-AA, \%, Sigma-Aldrich) mixed with MilliQ water and Hepes 50mM. Final acrylamide concentrations were 5% or 10%, while bis-AA varied between 0.03% to 3%. Cross-linking was induced by adding 10% ammonium-persulfate (APS) (1/200 vol/vol; Fisher, Pittsburgh, USA) and N,N,N',N'-tetramethyl-ethane-1,2-diamine (TEMED) (1/2000 vol/vol; Merck, Schipol-Rijk, The Netherlands). For each gel, 10 μl of the acryl-bisacrylamide solution was pipetted onto the functionalized glass bottom culture dish. A small coverslip (No. 0, 13-mm diameter; Menzel, Braunschweig, Germany), cleaned with 1% NaOH and instantaneously siliconized by immersion in Sigmacote (Sigma-Aldrich), was placed onto the droplet in order to flatten the gel and produce a surface without irregularities. After polymerization and soaking in Hepes 50mM, the siliconized coverslip was taken off and the inert surface of the PA gels was functionalized by a covalent coating with Collagen I. For this purpose, first the photoreactive heterobifunctional protein crosslinker N-succinimidyl-6-[4'-azido-2'-nitrophenylamino] hexanoate (sulfo-SANPAH; Pierce Biotechnology, Rockford, USA) was dissolved in DMSO (Merck) and Hepes 50mM (ph 7.4) obtaining a 1.0mM solution that was added on top of the gel. Subsequently PA gels were exposed to ultraviolet (UV) light to allow photo-activation of sulfo-SANAPH; this process was performed twice with fresh sulfo-SANPAH to ensure activation of the entire surface. After washing with 50mM Hepes, rat tail collagen I (BD biosciences, Bedford, MA) was diluted in PBS (Sigma-Aldrich) in order to obtain a 0.20 mg/ml solution and added to the gels (500 μl). Incubation with collagen solution occurred for 4 hours on a shaking table at room temperature. The PA gels and were subsequently sterilized under germicidal UV-C light for 10 minutes, washed with PBS and incubated with culture medium for at least 30 minutes before seeding to ensure equilibration of the space within the gel and the medium. PA gels were stored and used within 3 weeks from preparation

The elastic modulus (E-modulus) of the PA gels was determined on gels prepared on coverslips (Menzel) with 25 μl of solution. Indentation was applied to the centre of the gels with a spherical indenter (2mm-diameter) while measuring force and indentation depth. Afterwards a numerical model was iteratively fitted to these experimental data using a parameter estimation algorithm. The mechanical properties of the PA gels were quantified in 3 gels for each group in the same day when

the cells were seeded. The indentation test revealed that differences between the batches and in time were not significant (data not shown). The gels prepared with 5% acrylamide/0.01% bisacrylamide, 5% acrylamide/0.05% bisacrylamide 5% acrylamide/0.3% bisacrylamide, 10% acrylamide/0.26% bisacrylamide had elastic moduli of 3.8 ± 0.9 , 9.9 ± 3.7 , 19.8 ± 3.6 and 81.7 ± 2.4 kPa respectively (mean \pm SD), as shown in Table 1. This stiffness range (3-80 kPa) was created to mimic physiologically-relevant stiffness values similar to fat tissue (3 kPa), muscle (10-20 kPa) and collagenous bone (>20 kPa).

The glass substrates (coverslips No. 0, 13-mm diameter; Menzel), were sterilized in 70% ethanol and, subsequently, coated with adsorbed collagen I. The covalent binding of collagen I coating to the substrates was examined by immunolabeling. The antibody used were mouse monoclonal antibody to collagen I (IGg1, diluted 1:100, Sigma-Aldrich) and, as secondary antibodies, goat anti-mouse IGg1 Alexa 488 (diluted 1:500, Molecular Probes).

Table 4.1 Composition and elastic modulus of the polyacrylamide gels used as substrates.

	3 kPa	10 kPa	20 kPa	80 kPa
Acrylamide	5%	5%	5%	10%
Bis-Acrylamide	0.01%	0.03%	0.3%	0.26%
E (kPa)	3.8 ± 0.9	9.9 ± 3.7	19.8 ± 3.6	81.7 ± 2

Immunofluorescence labelling and imaging

At 48 hours after seeding, NHDF α and LMNAmut grown onto PA gels of 3, 10, 20, 80 kPa and glass bottom culture dishes coated with collagen I were washed with PBS and fixed with 4% formaldehyde in PBS (Sigma-Aldrich) for 10 minutes at room temperature. Next, they were permeabilized with 0.1% Triton-X-100 (Merck) in PBS for 10 minutes and incubated with 2% bovine serum albumin (BSA) in PBS in order to block non-specific binding. Afterwards, they were incubated for 2 hours with primary antibodies in NET-gel. The following primary antibodies were used: mouse MoAb to PML proteins (IgG1, diluted 1:200, sc-966, Santa Cruz) and rabbit polyclonal to LaminB1 (IgG1 1:500, diluted, ab16048, AbCam). After washing with PBS (3 times, 10 minutes), secondary antibodies in NET-gel were applied for 1 hour. Goat anti-mouse IgG1 Alexa 488 (diluted 1:500, Molecular Probes) was used against PML-NBs antibody while goat anti- rabbit IgG Alexa 555 or Alexa 488 (diluted 1:500, Molecular Probes) were used against Lamin B1 antibody. For F-actin staining phalloidin-TRITC (1:200, Molecular Probes) was used. After 2 washing steps with PBS, cells were incubated for 5 minutes with DAPI (1:500, Molecular Probes) for nuclear counterstaining. Imaging for the immunofluorescence studies was performed by means of an inverted confocal microscope connected to an inverted Axiovert 200M (Zeiss LSM 510 META, Zeiss). A C-Apochromat water-immersion objective (63x, NA=1.2) was used to minimize the effects of spherical aberration when focusing deep into PA gels, while for cells plated on glass a Plan-Apochromat oil immersion objective was used (63x, NA=1.4). The laser scanning microscope was used in the dual parameter setup, according to the manufacturer's specification, using dual wavelength excitation: the Ar laser at 488nm (30 mW) and the HeNe laser at 543 nm (1 mW). Z-series were generated by collecting a stack consisting of optical sections using a step size of 0.3-0.45 μ m in the z-direction while a minimum pinhole opening was used (1AU). Alternatively, a Leica SPE confocal microscope was used, mounted

on a DMI 4000 inverted microscope. Excitation lines were 405 nm (DAPI), 488 nm (FITC) and 532 nm (Phalloidin).

Cytochalasin D treatment

At 24 hours after seeding, *LMNAMut* grown onto collagen I coated glass bottom culture dishes were transiently treated with cytochalasin D (cytoD, Sigma-Aldrich) 1 μ M to inhibit actin filament dynamics. Successively the growth medium was refreshed with normal growth medium. Three different treatments were carried out:

- Short treatment + short recovery = 30 minutes cytoD treatment and 1 hour recovery in normal growth medium.
- Long treatment + short recovery = 3 hours cytoD treatment and 1 hour recovery in normal growth medium.
- Long treatment + long recovery = 3 hours cytoD treatment and overnight recovery in normal growth medium.

Finally, *LMNAMut* cells were fixed and stained for actin organization and nuclear abnormalities.

Cell spreading assay

Cells were detached using a trypsin solution containing 0.125% trypsin (Invitrogen Life Technologies, Breda, the Netherlands), 0.02 M EDTA and 0.02% glucose in PBS. Duration of trypsin treatment was kept to a minimum (approximately 3 min at 37°C), Trypsin was inactivated by adding an excess of culture medium with serum, and cells were seeded onto glass coverslips. Cells were allowed to attach for a variable period of time (0.5 hr, 1 hr, 2hr, 4 hr, 8 hr, 24 hr or 72 hr.) under standard culture conditions, and were fixed and processed for immunofluorescence as described above. As primary antibody the mouse monoclonal lamin A/C antibody Jol2 (IgG1, diluted 1:20; a kind gift from Dr. C.J. Hutchison (Durham University, United Kingdom)) was used. The percentage of cells with abnormal nuclei (blebs) was estimated by counting 3x100 cells per time point.

Image analysis

Brightfield images of cell cultures were obtained with an Axio Observer Z1 (Zeiss). For cell area and aspect ratio measurements, NHDF α and *LMNAMut* were manually outlined in relative brightfield images. Using ImageJ (1.45) freeware software, cell area and cell aspect ratio were measured. Cell aspect ratio was calculated as the length of the long axis of the cell divided by the length of the short axis. At least 60 cells were analyzed on the substrate of each type

Abnormal nuclei or cytoplasmic PML bodies were scored manually on about 100 cells in 3 random locations on 2 samples per each stiffness (600 cells in total) for each cell genotype. Nuclei were scored as abnormally shaped when their appearance, after laminB1 staining and DAPI counterstaining, showed abnormalities such as blebs, large and poorly defined protrusions and invaginations. In scoring of PML bodies, a second non-specific channel was acquired (550LP) to avoid counting of autofluorescent foci. Mitotic cells, identified by the shape of the DAPI staining, were rejected from the analysis, as they also show cytoplasmic PML bodies.

Live-cell imaging

In order to perform live-cell imaging, *LMNAMut* were seeded on PA gels of 3, 10, 20, 80 kPa and on glass bottom dishes and, after 24 hours, were transfected with EYFP-NLS. After 24 to 36 hours from

transfection, *LMNAMut* were supplemented with pre-warmed phenol-free serum-containing culture medium (DMEM 31053, Invitrogen) complemented with 15mM Hepes. Evaporation of the medium was prevented by covering it with an approximate 2mm layer of mineral oil (Sigma) previously washed with culture medium. Time-lapse recording with an interval of 1 or 2 minutes were taken using an inverted automated microscope (Leica DMRBE, Manheim, Germany) equipped with a black and white CCD-camera (CA4742-95, Hamamatsu, Bridgewater, NJ, USA). Image acquisition was achieved using Openlab software (Improvision, Lexington, MA, USA). The microscope was equipped with a heated stage which temperature was set at 37°C. This allowed imaging the sample while keeping it in optimal cell culture conditions. A 20x (N.A.-0.45) objective was used. For image processing and analysis of time-lapse videos, ImageJ (1.45) freeware was used. Briefly, for each time-lapse recording the analysis of the fluctuations of the fluorescence intensity in representative nuclear regions was performed. Values were normalized and then plotted as function of the time.

Statistical Analysis

Data are expressed as mean±SEM and mean±SD for PA gels elastic modulus. Statistical analysis was performed using StatGraphics (Manugistics, Inc., Rockville, MD). The data were analyzed by unpaired t-test (allowing different SD), one-way ANOVA (followed by Tukey's multiple comparison test) or, in case of non-Gaussian distribution, the Mann-Whitney or Kruskal Wallis tests (the latter when comparing more than two groups, followed by Tukey's multiple comparison test). A p-value of 0.05 was considered statistically significant.

Acknowledgments

The authors are grateful to Cor Semeins, Emanuela Fioretta and Marloes Janssen-van den Broek for helping with protocol development, gel preparation and the many helpful discussions.

References

1. Gilbert, P.M. *et al.* Substrate Elasticity Regulates Skeletal Muscle Stem Cell Self-Renewal in Culture. *Science* **329**, 1078-1081 (2010).
2. Discher, D.E., Janmey, P., & Wang, Y.L. Tissue cells feel and respond to the stiffness of their substrate. *Science* **310**, 1139-1143 (2005).
3. Wilson, K.L. & Foisner, R. Lamin-binding Proteins. *Cold Spring Harbor Perspectives in Biology* **2**, (2010).
4. Crisp, M. *et al.* Coupling of the nucleus and cytoplasm: role of the LINC complex. *Journal of Cell Biology* **172**, 41-53 (2006).
5. Huang, H.D., Kamm, R.D., & Lee, R.T. Cell mechanics and mechanotransduction: pathways, probes, and physiology. *American Journal of Physiology-Cell Physiology* **287**, C1-C11 (2004).
6. Broers, J.L. *et al.* A- and B-type lamins are differentially expressed in normal human tissues. *Histochem. Cell Biol.* **107**, 505-517 (1997).
7. Dahl, K.N., Ribeiro, A.J.S., & Lammerding, J. Nuclear shape, mechanics, and mechanotransduction. *Circulation Research* **102**, 1307-1318 (2008).
8. Broers, J.L.V. *et al.* Decreased mechanical stiffness in LMNA^{-/-} cells is caused by defective nucleo-cytoskeletal integrity: implications for the development of laminopathies. *Human Molecular Genetics* **13**, 2567-2580 (2004).
9. Lammerding, J. *et al.* Lamin A/C deficiency causes defective nuclear mechanics and mechanotransduction. *Journal of Clinical Investigation* **113**, 370-378 (2004).
10. Vigouroux, C. *et al.* Nuclear envelope disorganization in fibroblasts from lipodystrophic patients with heterozygous R482Q/W mutations in the lamin A/C gene. *Journal of Cell Science* **114**, 4459-4468 (2001).
11. Muchir, A. *et al.* Nuclear envelope alterations in fibroblasts from patients with muscular dystrophy, cardiomyopathy, and partial lipodystrophy carrying lamin A/C gene mutations. *Muscle & Nerve* **30**, 444-450 (2004).
12. Sullivan, T. *et al.* Loss of A-type lamin expression compromises nuclear integrity leading to muscular dystrophy. *Molecular Biology of the Cell* **10**, 237A (1999).
13. Nikolova, V. *et al.* Defects in nuclear structure and function promote dilated cardiomyopathy in lamin A/C-deficient mice. *Journal of Clinical Investigation* **113**, 357-369 (2004).
14. De Vos, W.H. *et al.* Increased plasticity of the nuclear envelope and hypermobility of telomeres due to the loss of A-type lamins. *Biochimica et Biophysica Acta-General Subjects* **1800**, 448-458 (2010).
15. Lee, J.S.H. *et al.* Nuclear lamin A/C deficiency induces defects in cell mechanics, polarization, and migration. *Biophysical Journal* **93**, 2542-2552 (2007).
16. De Vos, W.H. *et al.* Repetitive disruptions of the nuclear envelope invoke temporary loss of cellular compartmentalization in laminopathies. *Human Molecular Genetics* **20**, 4175-4186 (2011).
17. Broers, J.L.V., Ramaekers, F.C.S., Bonne, G., Ben Yaou, R., & Hutchison, C.J. Nuclear lamins: Laminopathies and their role in premature ageing. *Physiological Reviews* **86**, 967-1008 (2006).
18. Verstraeten, V. *et al.* Compound heterozygosity for mutations in LMNA causes a Progeria Syndrome without prelamin A accumulation. *Journal of Investigative Dermatology* **126**, 42 (2006).

19. Janmey,P.A., Euteneuer,U., Traub,P., & Schliwa,M. Viscoelastic Properties of Vimentin Compared with Other Filamentous Biopolymer Networks. *Journal of Cell Biology* **113**, 155-160 (1991).
20. Malek,A.M. & Izumo,S. Mechanism of endothelial cell shape change and cytoskeletal remodeling in response to fluid shear stress. *Journal of Cell Science* **109**, 713-726 (1996).
21. Mizutani,T., Haga,H., & Kawabata,K. Cellular stiffness response to external deformation: Tensional homeostasis in a single fibroblast. *Cell Motility and the Cytoskeleton* **59**, 242-248 (2004).
22. Favreau,C., Higuete,D., Courvalin,J.C., & Buendia,B. Expression of a mutant lamin A that causes Emery-Dreifuss muscular dystrophy inhibits in vitro differentiation of C2C12 myoblasts. *Molecular and Cellular Biology* **24**, 1481-1492 (2004).
23. Khatau,S.B. *et al.* A perinuclear actin cap regulates nuclear shape. *Proceedings of the National Academy of Sciences of the United States of America* **106**, 19017-19022 (2009).
24. Houben,F., Ramaekers,F.C.S., Snoeckx,L.H.E.H., & Broers,J.L.V. Role of nuclear lamina-cytoskeleton interactions in the maintenance of cellular strength. *Biochimica et Biophysica Acta-Molecular Cell Research* **1773**, 675-686 (2007).
25. Houben,F. *et al.* Disturbed nuclear orientation and cellular migration in A-type lamin deficient cells. *Biochimica et Biophysica Acta-Molecular Cell Research* **1793**, 312-324 (2009).
26. Borden,K.L.B. Pondering the promyelocytic leukemia protein (PML) puzzle: Possible functions for PML nuclear bodies. *Molecular and Cellular Biology* **22**, 5259-5269 (2002).
27. Houben,F. *et al.* Cytoplasmic localization of PML particles in laminopathies. *Histochemistry and Cell Biology* **139**, 119-134 (2013).
28. Jul-Larsen,A., Grudic,A., Bjerkvig,R., & Boe,S.O. Cell-cycle regulation and dynamics of cytoplasmic compartments containing the promyelocytic leukemia protein and nucleoporins. *Journal of Cell Science* **122**, 1201-1210 (2009).
29. Jensen,B.C. Skin deep: What can the study of dermal fibroblasts teach us about dilated cardiomyopathy? *Journal of Molecular and Cellular Cardiology* **48**, 576-578 (2010).
30. Capanni,C. *et al.* Failure of lamin A/C to functionally assemble in R482L mutated familial partial lipodystrophy fibroblasts: altered intermolecular interaction with emerin and implications for gene transcription. *Experimental Cell Research* **291**, 122-134 (2003).
31. Worman,H.J., Fong,L.G., Muchir,A., & Young,S.G. Laminopathies and the long strange trip from basic cell biology to therapy. *Journal of Clinical Investigation* **119**, 1825-1836 (2009).
32. Trappmann,B. *et al.* Extracellular-matrix tethering regulates stem-cell fate. *Nature Materials* **11**, 642-649 (2012).
33. Kremers,G.J., Goedhart,J., van Munster,E.B., & Gadella,T.W.J. Cyan and yellow super fluorescent proteins with improved brightness, protein folding, and FRET Forster radius. *Biochemistry* **45**, 6570-6580 (2006).
34. Cox,M.A.J., Driessen,N.J.B., Bouten,C.V.C., & Baaljens,F.P.T. Mechanical characterization of anisotropic planar biological soft tissues using large indentation: A computational feasibility study. *Journal of Biomechanical Engineering-Transactions of the Asme* **128**, 428-436 (2006).
35. Pelham,R.J. & Wang,Y.L. Cell locomotion and focal adhesions are regulated by substrate flexibility. *Proceedings of the National Academy of Sciences of the United States of America* **94**, 13661-13665 (1997).

Chapter 5

General discussion

Main findings of this thesis and implications for understanding interplay between cell cytoskeleton response and complex biophysical environments

This thesis addresses important aspects of the interplay between actin cytoskeleton remodeling of adherent cells and the biophysical environment. Cells are active entities in the physiological environment. The structural continuity between the extracellular environment and the cellular interior grants the cells the ability to continuously sense and adapt to the developing microenvironment. The mechanical feedback of cells to the extracellular environment is mediated by an interconnected network of intracellular structures, among which the actin cytoskeleton plays a pivotal role. The actin cytoskeleton is a dynamic and well-organized network of fibers that drives, among others, the fundamental processes of cell motility, contractility and differentiation¹. To serve these functions, the actin cytoskeleton arranges and remodels itself to adapt its geometrical, mechanical and dynamic properties.

In this thesis, we aimed at getting a quantitative understanding of actin cytoskeleton remodeling in response to changes in the physiological cellular microenvironment. The obtained fundamental knowledge is of particular relevance for application in (re)building and regenerating diseased or damaged tissues in regenerative medicine strategies. In view of this, we focussed first on cellular organization. Achieving *in vivo*-like tissue organization is a major goal of regenerative strategies because cellular organization determines the biological and mechanical properties, and hence the functionality, of the whole tissue. Cellular organization, as seen in the intracellular actin cytoskeleton, is the result of the complex interaction between the biophysical cues of the surrounding extracellular environment and the cellular interior. Among many biophysical cues, topographical cues and cyclic strain are considered the most relevant stimuli capable of inducing cellular alignment by invoking an actin cytoskeleton response (reviewed in chapter 1). However, in the physiological environment these cues are presented to the cells simultaneously. To understand the mechanisms of actin orientation response to the combination of both cues, we have developed and employed a dedicated experimental model system. By using this system, we studied the actin orientation response in normal (healthy) adherent cells and in cells with disturbances of the actin cytoskeleton. The latter also serve a model cells for so-called 'diseases of the mechanotransduction'. To evaluate our understanding of structural defects, we used substrate stiffness as a tool to rescue these cells, by inducing less tension in the actin cytoskeleton thanks to soft substrates. The main findings of this work are reported below (**Figure 5.1**).

A model system capable of dissecting the effects of separate and combined topographical cues and cyclic strain

The influence of topographical cues and cyclic uniaxial strain on the actin cytoskeleton of adherent cells was studied by using a newly developed model system consisting of elastomeric microposts capable of imposing both cues to the cells growing on top of the microposts. The topographical cues employed for guiding actin cytoskeleton alignment (contact guidance) were created by using microposts with elliptical cross section. Bounding of the microposts to a flexible membrane of commercially available stretching device (FlexCell) allowed us to apply cyclic uniaxial strain directly to the microposts. Micropost arrays characterized by different cross sections (circular and elliptical)

were included on the same membrane, as well as different arrangements of the elliptical microposts to the strain direction (**Figure 2.1**). Such system enabled testing and evaluating of the actin cytoskeleton remodeling in different conditions during the same experiment, without the need to prepare different samples per each experimental condition. Adherent cells could be grown on top of the microposts coated with fibronectin and exposed to the different stimuli applied separately or in combination (chapter 2). Therefore, this model system is suitable for dissecting the effects of topographical cues and cyclic uniaxial strain on the actin cytoskeleton.

Cap and basal actin fibers have distinct response to combined cyclic strain and topographical cues

To understand to what extent and how topographical cues and cyclic strain influence the actin cytoskeleton orientation of adherent cells, we first used the developed model system with healthy human vena Saphena cells, previously characterized as myofibroblasts. We analyzed the orientation response of their actin cytoskeleton upon dual stimulation, by topographical cues and cyclic uniaxial strain applied separately and in combination. The main finding of this study is that the subcellular organization of the actin cytoskeleton is of fundamental relevance to explain the whole actin cytoskeleton reorientation response. In particular, we have demonstrated that, due to the competition between the responses of two particular subsets of stress fibers, a clear actin fiber orientation response is lacking upon exposure to topographical cues and cyclic uniaxial strain along the same direction. On the one hand, the subset of actin stress fibers running on top of the nucleus (actin cap) responds to the cyclic uniaxial strain despite the presence of competing topographical cues presented along the same direction of the mechanical strain. On the other hand, the stress fibers lying underneath the nucleus (basal actin fibers) are more prone to follow the topographical cues. Actin cap fibers and basal layer respond in the same way when competing stimuli are not present.

The existence and the role of these two different subsets of actin stress fibers in adherent cells grown on two-dimensional (2D) substrates have only recently started to be characterized. Regarding actin cap stress fibers, their role in cell mechanotransduction and mechanosensing on 2D substrates was pointed out first by Kathau *et al.*² Actin stress fibers are directly interconnected with the nucleus via the LINC complex and nuclear lamins. This strategic location of the actin cap stress fibers results in their direct involvement in shaping of the nucleus of somatic (differentiated) cells. Further investigations revealed that the actin cap is also responsible for the intra-cellular positioning of the nucleus³⁻⁶. The particular interconnection with the nuclear interior via the LINC complexes makes the actin cap also a more suitable route for transducing forces directly from the extracellular environment to the genome contained by the nucleus. Chambliss *et al.*⁷ have indeed demonstrated that the stress fibers of the actin cap and their associated focal adhesions build up ultra-fast machinery for cellular mechanotransduction and can respond very rapidly to shear stress stimulation. Our results add to this knowledge that the actin cap stress fibers are able to respond to cyclic uniaxial strain by strain avoidance even in presence of topographical cues directed along the same direction of the strain. Moreover, in this study, we also observed that the nuclear and cellular orientation after application of combined topographical cues and cyclic strain correlated with the orientation of the actin cap. This suggests that the actin cap might be the key player in cellular reorientation in response to cyclic strain. Overall, this study contributed to the knowledge of the mechanisms inducing cellular orientation via actin cytoskeleton by elucidating that coordinated

response of both actin cap and basal layer of fibers is necessary to obtain an anisotropic organization of cells when stimulation by topographical cues and cyclic strain are presented to the cells simultaneously.

The actin cap is crucial for response to cyclic strain

To further investigate the relevance of the actin cap for cellular mechanoreponse to topographical cues and strain stimulation, applied separately and in combination, we adopted the developed model system on diseased cells (chapter 3). As our control, we used wild-type mouse embryonic fibroblasts normally expressing the actin cap, while, as our tool, we employed diseased cells with an abnormal conformation of the actin cytoskeleton, more precisely fibroblasts without actin cap formation (*Imna*-lacking fibroblasts). The loss of actin cap in these cells was invoked by genetically eliminating the lamins, the meshwork of proteins in the nuclear interior interconnected with the LINC complexes.

Our findings showed that the absence of a cap does not impair topography sensing since cells without the actin cap succeeded in aligning along the topographical cues. This was also observed in cells plated on fibronectin lines³. On uniform substrates, basal actin fibers orient randomly underneath the nucleus and they do not follow the polarization axis of the cells as the actin cap^{8,9}, while on micro- and nanotopographical features, they appear to be the first to respond by contact guidance and further direct the alignment of actin cap stress fibers⁹. Thus, it seems that basal actin fibers are relevant for topographical sensing and response. Considering that these stress fibers are not connected to the nucleus and do not apply any tension on it^{7,8}, it is suggested that regulatory pathways of topography sensing and response might be an interplay of structural mechanotransduction and biochemical signaling. Alternatively, this basal actin fiber behaviour could arise as a compensatory mechanism adopted by the cell to adhere.

Absence of the actin cap, instead, affects strain avoidance-induced reorientation. Cells lacking the actin cap were observed to have an impaired strain avoidance response even in absence of topographical cues, and a completely abrogated response in case of topographical cues and when cyclic uniaxial strain was applied in the same direction. Thus, we concluded that an intact actin cap is of fundamental importance for strain avoidance response induced by cyclic uniaxial strain. The actin cap is presumably passing the signals coming from the strain stimulation to the nuclear interior, where the overall cell response is regulated. The interplay between nuclear-cellular movements through the actin cap has been demonstrated to be crucial for cell migration³. Our study confirms that the fibers of the actin cap play an essential role in cellular mechanoreponse. While the role of the actin cap stress fibers has been and continues to be elucidated, we still lack a comprehensive understanding of the function and response to the biophysical cues of the basal stress fibers.

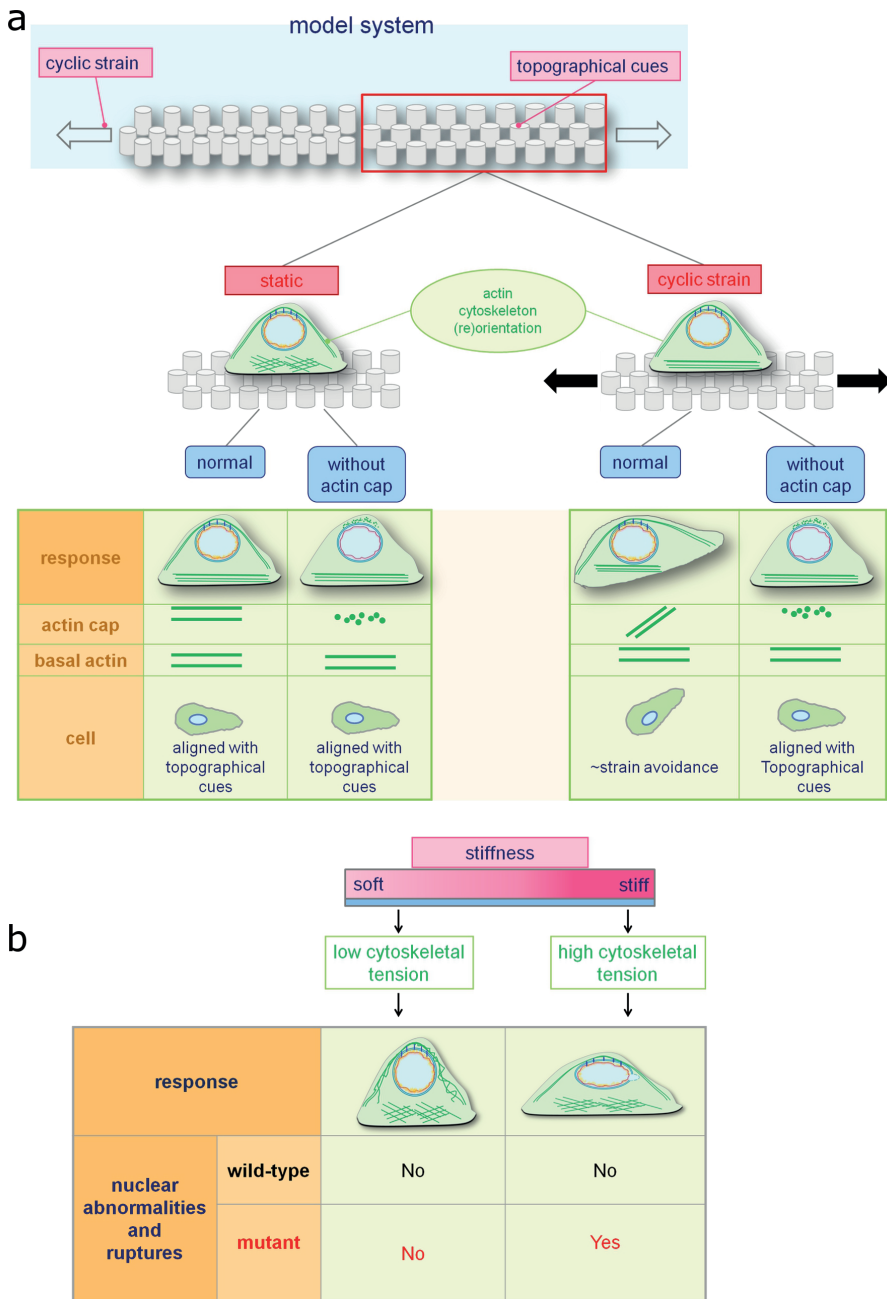


Figure 5.1. Schematic overview of the main findings of this thesis. a) A model system made of stretchable microposts characterized by circular and elliptical cross sections was developed to stimulate adherent cells with topographical cues and cyclic uniaxial strain. In static conditions both normal cells and cells without the actin cap align along the topographical cue, i.e. the major axis of the elliptical microposts. When cyclic uniaxial strain was applied, investigations on normal cells revealed that the competition between topographical cues and cyclic strain applied in the same direction is due to the distinct response of actin cap and basal actin fibers to the combined cues. (See next page)

To explain the impaired reorientation response observed even in the absence of topographical cues, it might be relevant to consider that cells suffering from lack of, or mutated, *Imna* have altered actin dynamics¹⁰. Alternatively, the impaired response can be related to the fact that cells were grown on substrates where adhesion was restricted to the top of regularly spaced fibronectin-coated circular microposts. There is indication that topographic features increase the stability of focal adhesions compared to flat uniform substrates¹¹. This would result in a competition between the stimuli arising from the topographical cues and the stimuli inducing cell reorientation by strain avoidance. The cell might then opt for the most energetically favourable condition, thus to maintain its original orientation. Most likely, these two scenarios are synergistically affecting the response of *Imna*-lacking cells¹². Importantly, since the cap-lacking cell are *Imna*-lacking cells, they represent a model for the family of diseases arising from mutation in LMNA gene and resulting not only in a weakened and abnormally structured lamin network, but also in a myriad of tissue specific phenotypes. Thus these cells represent a useful model for studying the development of laminopathies as mechanotransduction diseases. The impaired mechanoreponse of the laminopathy cells observed in this and previous investigations, and the altered nucleo-cytoskeleton shuttling of mechanosensitive transcription factors such as ERK and MLK with important roles in the cardiovascular system, contribute to shedding new light on the development of the cardiac phenotype in many laminopathies¹⁰.

Structural weakness of laminopathy cells can be rescued by soft culture substrates

We further investigated the structurally weakened laminopathy cells and we attempted to rescue them by modulating the extracellular environment. Loss of nuclear structural integrity is a particular feature of LMNA mutant cells *in vivo*¹³⁻¹⁵. We hypothesized that the onset of such structural abnormalities is caused by the tension of the actin cytoskeleton exerted directly on the (structurally weak) nucleus. We investigated this hypothesis by modulating the intracellular actin cytoskeleton tension by varying the stiffness of the cell culture substrates, as it is well known that stiffer extracellular environments induce the formation of tensed actin stress fibers. Our results demonstrated that nuclear abnormalities of LMNA mutant (laminopathy) cells correlate with the stiffness of the surrounding environment. Cells cultured on soft substrates (3 kPa) did not develop nuclear malformations, while aberrant nuclear morphologies were observed on substrate stiffer than 10 kPa, leading to spontaneous ruptures of the nuclear membrane in LMNA-mutated cells.

The actin cap reorients almost perpendicular to the strain direction by strain avoidance while the basal actin fibers follow the topographical cues. Cellular reorientation is governed by actin cap behaviour. Investigations on cells without the actin cap pointed out that presence of an intact actin cap is crucial for cellular response to cyclic strain. Cells expressing only the basal layer do not respond to strain but keep following the topographical cues prescribed by the elliptical microposts even if strain is applied along the same direction of the micropost major axis. b) While normal fibroblasts never show nuclear ruptures, cells with structural defects such as cells with abnormal conformation of the lamina (mutant) can be protected from nuclear abnormalities and ruptures when cultured on soft substrates. A soft extracellular environment causes low actin tension in the cell, while a stiff substrate invokes high tension in the actin cytoskeleton which is ultimately transferred to the weak nucleus causing disruptions of the nuclear integrity.

The cells used in this study originate from a patient with heterozygous LMNA mutations. These mutations do not result in complete lack of lamin A. In this and similar situations, mutant lamins appear as stable as wild-type lamin and are expressed at similar level¹⁶. Therefore the stability of the nucleo-cytoskeletal connection, including the LINC complexes, does not get affected and the actin cap fibers can normally develop. Indeed, we did not observe a clear loss of actin cap in the patient cells. Recently, also Scharner *et al.* observed actin cap formation in laminopathies cells¹⁷. The unvaried capability of the actin cytoskeleton to form the actin cap fibers and respond to the cues of the extracellular environment in these patient cells allowed us to modulate the tension developed in the actin cytoskeleton by varying the stiffness of the culture substrate modulate the cell response. The actin cap structure has been demonstrated indeed to be crucial for cellular mechanoreponse to substrate stiffness¹⁸. Although the formation of the actin cap was not impaired, the laminopathy cells used in this study developed abnormalities in the actin cytoskeleton organization in the surrounding of the nucleus. These disturbances are suspected to be related to the nuclear abnormalities observed on the stiffer substrates. The blebs and the invaginations characteristic of the mutated cells are hypothesized to perturb the local balance of forces around the nucleus, causing a heterogeneous distribution of actin filaments^{19,20}. This suspected redistribution of forces in laminopathies cells can eventually result in changes in DNA organization and, consequently, in abnormal cellular mechanoreponse.

Overall, this thesis demonstrates that it is relevant to analyse stress fiber response at different subcellular levels in order to get a deeper understanding of actin cytoskeletal remodeling in response to biophysical cues of the cellular environment. Actin cap and basal stress fibers seem to play a different role on the mechanical environment of the nucleus; actin cap fibers appear to be relevant for the mechanoreponse to cyclic strain and stiffness sensing while basal actin fibers seem to play a major role in sensing and responding to topographical cues. The obtained knowledge is of particular relevance for the development of regenerative and therapeutic approaches as knowledge is obtained about how modulate cytoskeletal alignment and cytoskeletal tension by biophysical cues of the cellular environment.

Methodological challenges

The multidisciplinary work presented in this thesis represents advances in the area of cell mechanobiology for the understanding of the interplay between cell responses and complex biophysical environments. The developed model system of elastomeric microposts has led to the discovery of distinct behaviors of the actin cytoskeleton in healthy and diseased cells exposed to topographical cues and cyclic strain. Substrate stiffness was also used as a tool to modulate the response of the actin cytoskeleton in order to study structural abnormalities in weakened cells. In this section we report on the considerations and limitations on the engineering and biological aspects of the investigations performed in chapter 2, 3 and 4.

Technological Challenges

On the technical side, in chapter 2, we have designed, fabricated and used a novel model system made of microfabricated elastomeric microposts coated with fibronectin. The micropost system

allows to impose strain as well as contact guidance to the adhering cells, as it is bound to a stretchable membrane and designed with posts with an elliptical cross section, thus presenting a favoured direction for cell attachment. We have shown that such a model system, when used in static condition, is able to induce cell alignment in the direction of the major axis of the elliptical microposts and trigger strain avoidance reorientation when cyclic uniaxial strain is applied, demonstrating that it is a viable tool to study the influence of contact guidance and strain on adherent cells such as fibroblasts. Moreover, by combining arrays of different microposts with different cross sections (circular and elliptical) on the same membrane we were able to greatly ease the experimental procedure by testing several topographical cues using identical experimental conditions.

The advantage of microposts is that they can be created using readily available soft-lithography processes. This makes it possible to accurately control the biophysical stimuli within the cellular microenvironment. While elastomeric microposts have been largely designed and used as circular cylinders, in our model system we have introduced microposts with elliptical cross section in order to impose cell directionality. To our knowledge, only Saez *et al.*²¹ have done this previously. Their design has inspired the development of our elliptical micropost. When comparing our study to the one by Saez *et al.*, some contrasting considerations emerge. To explain cell alignment on elliptical microposts, Saez *et al.* support the idea that cell contact guidance is guided by the cellular ability to sense differential stiffness between the major and minor axis of the micropost (anisotropic rigidity sensing). This was concluded after they observed that the cells they used (epithelial cells) did not align along any favoured direction on very stiff microposts, suggesting that they could not discriminate between the two stiffnesses. In our study instead, myofibroblasts did align along the micropost major axis also when they were plated on extremely stiff microposts. It is plausible that the different cell kinds used in the two studies sense and align along the topographical cues employing different mechanisms. We suspect that the myofibroblasts are more sensitive to the edges provided by the microposts, as also suggested previously by Teixeira *et al.*^{22,23}. To understand whether this is the case, it would be necessary to check the actin cytoskeleton alignment of myofibroblasts adhered on elliptical island of fibronectin patterned on a uniform substrate. In this way, the effect of the geometrical features provided by the sharp edges of the microposts would be excluded. Unfortunately, accurate micro-contact printing of such small islands remains a practical challenge. Development of improved techniques for obtaining these patterns is currently under investigation in our research group. Our hypothesis that contact guidance is induced by the geometrical features of the elliptical microposts finds support in recent observations of accumulation of focal adhesion proteins along the edges of topographical patterns since early time point from cell adhesion. The existence of fast and very sensitive mechanism of local topography sensing at the cellular membrane could explain the alignment of focal adhesions and the cytoskeleton along the anisotropy of the topography²⁴. Considering also the results of our investigation of chapter 3, illustrating that the basal actin fibers that are not connected to the nucleus, seem to be the dominant factor for cellular alignment, we speculate also that contact guidance might be induced by a combination of mechanical and biochemical signalling. Nevertheless, cellular mechanotransduction systems are not generalizable between cell types since cell-specific differences are well known to exist, perhaps due to the specific role of each cell type in the native conditions. Based on the current understanding it, it is conceivable to hypothesize that

several signaling pathways - biochemical and mechanical - act synergistically during cellular response to topographical cues.

The main reason for the introduction of elastomeric microposts in the field of mechanobiology, is that they can be used as force sensors for (sub)-cellular measurements²⁵. Forces are calculated by imaging the micropost deflections, which are related to the force knowing the bending stiffness of a single micropost (given by the microposts geometry and Young's modulus of the polymer used for the fabrication). In the current experimental model system we did not use the elastomeric microposts as force sensors, therefore no information can be extrapolated about the traction forces developed at the level of single focal adhesions in aligned or randomly oriented cells. This could be of relevant importance to unravel the structural and functional coordination and integration of actin cytoskeleton, cellular contractile forces and focal adhesion dynamics. Preliminary investigations of this kind have been performed by Shao *et al.*²⁶ in the Fu laboratories. Interesting results revealed that the relative position of the cells to the strain direction has relevant effects on the subcellular distributions of contractile force and focal adhesion distribution. Thus, traction force measurement would be a major integration to the used model system for future investigations. This can be achieved by using more flexible microposts or higher resolution scanning microscopy (e.g. STORM)²⁷. More flexible, thus longer microposts are needed to be able to capture micropost displacements with standard imaging systems currently used in our laboratory. However, producing longer microposts has practical drawbacks, as softer rods tend to easily collapse.

The data reported in this thesis are acquired from fixed cells after performing experiments. More information on the actin cytoskeleton remodeling could be obtained by capturing real time changes in the actin structure upon stimulation via biophysical cues. To this end, a custom made device incorporating the stretchable micropost model system should fit under a confocal microscope. Next to this, image acquisition timing should allow to capture phenomena whose timescales vary from fractions of seconds to minutes^{28,29}. Moreover, probes for live-cell imaging that do not interfere with the cell physiological behaviour should be employed. Finally, to mimic the multi-axial deformation fields to which cells are exposed in physiological environment such as the cardiovascular tissues, cyclic biaxial mechanical loading should be applied on the model system that we have developed.

Finally, in the present work, *in vitro* studies were performed on 2D substrates to study the effects of topographical cues and cyclic uniaxial strain in a controlled manner. However, in the *in vivo* environment, cells are embedded in a three-dimensional (3D) matrix. The unnatural conditions to which cells are exposed when studied on 2D environments are likely to artificially influence the cell response. Therefore, further work should concentrate on investigating actin cytoskeleton remodeling in 3D. Preliminary studies performed in our laboratory have attempted to investigate cell orientation in more physiologically relevant environments. Foolen *et al.*³⁰ have shown that it is possible to study actin cytoskeleton remodeling in 3D collagenous microtissues upon stimulation by cyclic strain. Their results have demonstrated that cells at the core of the 3D microtissue become insensitive to the straining stimulation since contact guidance provided by the scaffolding collagen dominates the orientation response of the actin cytoskeleton. Yet, the influence of the matrix integrity and the cell density in these constructs might play a pivotal role in determining the sensitivity of the cells to the biophysical cues of the environment. Thus, more studies need to be implemented after having overcome relevant technical challenges in order to move our understanding of the cytoskeleton remodeling in 3D.

Mimicking substrate stiffness

The micropost model system used to perform the investigations reported in chapter 2 and 3 of this thesis can also be used to mimic substrate stiffnesses relevant to cells. The major advantage is that substrate stiffness can be changed without altering surface chemistry, since the micropost length is proportional to the bending stiffness and the fibronectin, which is microcontact printed on the top of the microposts, creates a homogenous distribution of adhesive proteins. Previous work making use of micropost substrates has been published by different groups and has shown that these substrates are suitable to study the influence of substrate stiffness on cell behaviour. Ladoux and colleagues showed that using microposts of different bending stiffnesses, clear effects could be observed on traction forces exerted by 3T3 fibroblastic cells, cell adhesion and migration³¹. Moreover Fu *et al.*³² have reported on the design of a library of microfabricated elastomeric posts that can be used to investigate the effects of substrate stiffness on cell morphology, focal adhesions, cytoskeletal contractility and stem cell differentiation. Also Sochol *et al.*³³ have shown that migration of bovine aortic endothelial cells is influenced by the bending stiffness of the microposts.

Our study (chapter 2) seems, to some extent, to contradict these findings. Although we have performed our experiments on three micropost arrays with different stiffnesses (bending stiffness from 16 to 774 nN/ μm), i.e. three different micropost lengths, we could not detect differences in the actin cytoskeleton behaviour of myofibroblasts (chapter 3). One would expect that on softer substrates the alignment as well as the reorientation response upon cyclic strain are less pronounced on soft substrates since the mechanosensing apparatus is not well established³⁴. One possible explanation for our results is that the local mechanism of stiffness sensing at the cell boundary dominates the response of the myofibroblasts. Alternatively, the stiffness range used in our study does not represent a relevant spectrum to observe difference in this cell kind. To clarify these aspects, further investigations are needed to accurately elucidate the forces sensed by the cells when exposed to the micropost arrays both in static and dynamic conditions.

In chapter 4, we have employed polyacrylamide gels of different stiffness to probe the intracellular response of wild type and mutant cells. We have prepared collagen I-coated gels with stiffness ranging from 3 and 80 kPa and we have shown that we can correlate the degree of nuclear weakness in the mutant cells with the stiffness of the polyacrylamide gels. The results of this study and similar ones employing hydrogels whose changes in stiffness are achieved by modifying its crosslinking density were put under discussion when conflicting evidences emerged from the study of Trappmann *et al.*³⁵. They showed that spreading and differentiation of stem cells depends on the tethering of molecules of the extracellular matrix to the substrate. For hydrogels like the polyacrylamide gel, changing the bulk material stiffness by varying the crosslinker concentration can produce secondary effects such as altering the density of cell-adhesive ligands and thereby modify the mechanical feedback of the extracellular matrix protein used as coating. The risk is then that, as a consequence, the overall cell behaviour gets affected. However, as commented by Ovijt Chaudhuri and David J. Mooney³⁶, the relationship between stiffness and anchoring density is likely to be quite complex and deserves further investigations. Recently, David Mooney and colleagues³⁷ and Adam Engler and colleagues³⁸ tried to further explore this topic of debate. They did this by studying the effects on cell behaviour of the independent modulation of the extracellular matrix stiffness and ligand density. The common result of these two studies is that stiffness, rather than ligand tethering, regulates cell behaviours such as cell adhesion and differentiation³⁹. However, it remains unknown how cells integrate bulk stiffness with local mechanics and stiffness. This mechanism could well be

cell type, integrin type and extracellular matrix material dependent. To elucidate the whole physiological interplay between cells and their surrounding matrix, many technical challenges need to be overcome in the search for tissue-mimetic material retaining the modularity of the synthetic material and the biological instructiveness of native matrices⁴⁰. However, next to the technological challenges, an important question related to cell biology still needs to be addressed: on which scale stiffness is sensed by the adherent cell?

Biological Challenges

In chapter 2, we have used primary human vena saphena cells (HVSC), harvested from the vena saphena magna of one patient. These cells have been previously characterized as myofibroblasts. Our choice was based on the knowledge that these cells have been shown to develop prominent stress fibers in 2D and, in general, to be sensitive and respond to mechanical cues^{41,42}. Moreover they have been used in our laboratory for engineering in vitro heart valve substitutes^{43,44}. Primary cells are chosen because their biological response may be closer to an *in vivo* situation; however myofibroblasts need to be harvested from patients in an invasive manner. The main striking observation when using HVSC under competitive stimuli (contact guidance and cyclic strain along the same direction) is that their response is not completely homogenous as 50% of the cells reorient at an angle to the strain direction and 50% do not. We can relate these results to the fact that populations of genetically identical cells are not homogeneous, but contain subpopulations with phenotypic heterogeneity in their response to external stimuli. Indeed the HVSC used here have earlier been partially shown to express α -SMA (around 70% of the cells^{45,46}). In our study we did not perform a thorough cell phenotype characterization. Thus, it might well be that the cell phenotype changed towards the normal fibroblasts with passage number or by the thawing-freezing procedure. Since reorientation occurs through cell-wide remodeling, and it is plausible that the whole process requires contractile fibers capable to synergistically regulate the response of the actin cap and the basal layer of fibers, loss of contractility (loss of α -SMA) might result in impaired ability of the cell to orchestrate the whole reorientation. Also we cannot exclude that, within the same population, cells have heterogeneous sensibility to the biophysical cues or unsynchronized response. As our investigation makes use of only one straining regime and one observation timepoint, it is not possible to decipher whether these hypothesis are reasonable.

In chapter 3 we further studied and dissected the relevance of the actin cap and basal actin in mechanoresponse. Two different kinds of cells have been challenged by topographical cues and cyclic strain with the same model system developed in chapter 2. The first kind of cells showed (almost) only actin cap fibers (the normal wild type mouse embryonic fibroblasts) while the other cell type expressed only the basal actin fibers. The latter were mouse embryonic fibroblasts from a mouse where A-type lamins had been eliminated by gene targeting. The complete loss of A-type lamins caused the disruption of the actin caps in the majority of the cells. The choice of using *Imna*-lacking fibroblasts as a tool for studying the role of the actin cap in the response to biophysical cues has revealed to be crucial for this mechanobiology study. In this way we could prove that the lack of the messaging system from the cell membrane to the nucleus given by the actin cap is of fundamental importance for the correct response to strain. Moreover, the knockout mice from which the *Imna*-lacking cells were harvested exhibit overtly normal embryonic development but their postnatal growth is marked by the rapid onset of muscular dystrophy and cardiomyopathy.

Therefore the *Imna*-lacking cells used in our study can also be seen as model for the family of diseases comprehending muscular dystrophy and cardiomyopathy, the so called laminopathies.

In chapter 4 we proceeded with studying laminopathy cells in the attempt to understand their onset and develop new tools for their detection. More precisely, we studied laminopathy cells from a progeroid syndrome patient (Hutchinson-Gilford progeria syndrome, HGPS) with rare compound heterozygous mutations in the LMNA gene, consisting of p.T528M in combination with p.M540T⁴⁷ (chapter4). Our experiments have demonstrated that nuclear abnormalities develop in these patient cells when the culture substrate is as stiff as muscular tissue (10 kPa).

Since in our investigation cells from only one patient were used, the results obtained allow only conclusions with respect to this particular cell culture. Certainly, future work is needed to generalize the results to other laminopathies. Additional work should include additional patient cell lines or in case of limited availability in cells with reduced levels of lamins A/C (e.g. by RNA interference) and/or *Imna*^{-/-} mouse embryonic fibroblasts used in the study of chapter 3. An interesting extension of the research would be determining whether also disruption of LINC complexes using either RNAi or dominant negative SUN/KASH (LINC proteins) mutants can emulate the effects of a compliant substrate.

Yet, generalization of the findings of our study to the family of diseases arising from mutations in genes encoding for proteins of the nucleo-cytoskeletal interconnection are not straightforward. In different cell types, the biophysical route of signal transduction can be different. For instance in cardiomyocytes the interconnection between the extracellular and the sarcomere, is formed by the costameres that could represent an alternative route for mechanotransduction via the actin-myosin network.

Road towards the translation to tissue regeneration and therapeutic strategies

This thesis has helped gaining fundamental insights in the relation between biophysical cues, actin cytoskeleton remodeling and cell function. A direct translation of the results obtained in this work into new clinical applications or in the clinical setting is difficult. Nevertheless, the knowledge gained raises the attention to several interesting research directions, for instance towards tissue regeneration strategies and potential therapeutic approaches for diseased cellular states.

A micropost model system for comprehensive mechanobiological studies

A potential spin-off from our research is the model system that we have developed. Our micropost model system is suitable for systematic studies of cell mechanoresponse to combined topographical cues, substrate stiffness and cyclic strain. The microposts cross-section can be designed to impose different topographical cues to the cells. The stiffness of the substrate can be varied by changing the microposts length and the strain protocol can be tuned via the FlexCell controller. Eventually, the system can be miniaturized and incorporated into micro devices at the cellular level towards the development of high-throughput platforms for the investigations of cellular mechanoresponse. The

use of a systematic approach for cellular studies is beneficial for moving toward a comprehensive understanding of the complex interplay between the biophysical cues and cellular mechanoresponse. Studies employing our model system can be performed with different kind of cells. In our vision the use of cells with impaired mechanotransduction represents a valuable tool for understanding the onset of diseased phenotypes, which can eventually lead to pathology.

Actin cytoskeleton remodeling by biophysical cues for regenerative and therapeutic strategies

Results obtained in this thesis (chapter 2 and 3) show that cellular alignment is intimately linked to the interplay between cyclic strain and contact guidance. This knowledge will certainly have implications for the rational development of new and more efficient regenerative strategies for tissues that are constantly exposed to a combination of biophysical cues, such as the cardiovascular tissues. When developing synthetic tissue analogues, firstly the proper substrate for cell survival and differentiation needs to be chosen. Further the appropriate environmental conditions for tissue maintenance should be provided. Our results represent an advance in the understanding how combined biophysical cues in the cell environment, such as topography and cyclic strain, can steer cellular behaviours. *In situ* tissue engineering can exploit the response of cells to well-known biophysical cues to produce organized cellular structure that recapitulate the native, healthy anisotropic tissue organization to ensure tissue functionality. In spite of the myriad of accomplishments in the field, the current platforms for tissue engineering and regeneration still fail to use both structural anisotropy and proper cell-matrix contacts to promote functional cellular phenotypes. Therefore, our findings can be useful in the development of scaffolds for *in situ* tissue engineering.

From previous studies performed in our group, it has emerged that for the realization of a functional tissue engineered heart valve the degree of anisotropy of the construct is of fundamental importance to achieve the anisotropic biomechanical function of native heart valves⁴⁸. These results suggest new scaffold design guidelines that could possibly help to overcome the leaflet retraction problem and valve regurgitation observed *in vivo* after implantation of the currently available tissue engineered heart valves⁴⁹. However, in our view, these results need to be integrated with the ones obtained in our study as it is necessary to understand to what extent topographical cues provided by the scaffold and cyclic strain resulting from the *in vivo* hemodynamic loading influence the final cellular organization in the engineered construct.

The knowledge of actin cytoskeleton remodeling knowledge obtained in this thesis come from *in vitro* studies performed on 2D substrates. Although this represents a valuable first step, the road to reach knowledge which is directly applicable for the design of *in vivo* 3D scaffolds is complex and long. Firstly, it is needed to move to studies performed in 3D settings, using scaffolds that can eventually be used for human implantation. Then, it is also fundamental to look at the maintenance of the anisotropy over time, as well upon scaffold degradation and by considering the influence of cell collective behaviours. Moreover, further research should focus on human cell types interesting for cellular regeneration, such as the cardiomyocytes for cardiac regeneration or cells from the circulation, especially stem cells.

Even though, the road to clinical research will not end there. For instance, after the initial design of an optimal scaffold for *in situ* engineering, in order to translate the use of the end product into

clinical practice, several steps need to be accomplished, i.e. scaling-up, pre-clinical studies, validation, and improved production processes until clinical research and commercialization.

The indication that relative orientation of cells to the strain direction has direct influence on the cellular mechanoresponse can also open the way to the understanding of pathological processes. Misaligned cells, lacking a preferred orientation could represent dysregulated cellular phenotypes, while cells aligned perpendicular to the strain direction may represent cells in a healthy state, able to maintain cellular homeostasis²⁶. Further studies, concentrating for instance on cellular secretome and inflammasome could help complete the picture. From there, the obtained knowledge could support the design of more detailed strategies for guiding cellular orientation in view of restoring anisotropic tissue organization reducing also the host response to scaffold implantation.

Furthermore our studies contribute to an in-depth understanding of the cellular diseased state by demonstrating that the lack of the actin cap results in impaired strain avoidance response. The impairments of the structural mechanotransduction pathway and the loss of the connections between the extracellular environment and the nuclear interior caused by the lack of the actin cap or disturbances in binding partners from the LINC complex and/or lamin abnormalities can result in abnormal cellular responses. This can eventually lead to the perturbation of the delicate homeostasis of native tissues. Therefore, this knowledge can help understanding the development of diseases such as laminopathies, and in general diseases arising from mutations of protein building up the interconnection between cellular exterior and the nuclear interior. Thus, our study suggests that an attractive solution for treating diseases such as laminopathies could be to restore structural defects of the mechanotransduction pathway, to achieve the transduction of biophysical stimuli to the genome. Surely, these aspects need to be further investigated as until now, most of the research has focussed on developing treatments for the impaired signalling in laminopathy cells⁵⁰.

As a conclusive note, it is clear that the incorporation of the cellular mechanotransduction and mechanoregulation concepts of this thesis into clinical research are promising, but far from realization. Nevertheless, the results reported in this thesis have provided the foundation for new PhD projects within our research group, aiming at developing an in-depth understanding of the role of focal adhesions and actin cytoskeleton dynamics in cellular organization in physiological and pathological conditions, as well as in fibrous scaffold environments.

Towards an assay for laminopathy detection

The observation that nuclear abnormalities in laminopathy cells correlates with the stiffness of the culture substrate opens up new avenues for the interpretation of the pathogenesis of laminopathies, their diagnosis and potential therapeutic strategies.

Our findings support the idea that A-type lamin mutations result in increased susceptibility to mechanical stress⁵¹. Strikingly the most diffuse laminopathies affect mechanically challenged tissues such as the striated and cardiac muscles. The complex nature of laminopathies for which the causative links between genotype and phenotype remain unknown and for which tissue-specific as well as overlapping phenotypes are observed, let us speculate that an interdisciplinary research can yield better diagnosis, better follow-up and therapeutic chances.

In our studies we used polyacrylamide gels to probe the laminopathy cells. The *in vitro* assay using a series of polyacrylamide gels of varying stiffness has demonstrated to be a useful tool to assess the degree of nuclear weakness. This type of assay can have predictive value for the behavior of laminopathy cells *in vivo*. For the diagnosis of laminopathies, mutation analysis alone is not a useful tool as systematic correlation of phenotype with genotype cannot be established. Thus, the potential of the polyacrylamide gel method makes it an attractive tool for investigating the mechanical functioning and fragility of genetically affected cells of individual patients as a phenotypic marker of the disease stage. This represents a first step for bringing cell mechanics research into clinical applications. However, before proceeding towards the clinical application, the validation of the method by testing other patient cells under a wide range of condition is crucial.

Outlook and future perspectives: where do we go from here?

The achievement of a comprehensive understanding of the actin remodeling by biophysical cues in physiological and pathological conditions is a long road. The work performed in this thesis represents another small but potentially important step towards it. Still several key challenges need to be overcome in the field of mechanobiology for an in-depth understanding of the mechanism underlying the response of the actin cytoskeleton to complex biophysical environments. These aspects include studies in 3D environment performed by means of live-cell imaging and elucidation of the influence of structural and biochemical mechanotransduction pathways. Moreover, actin cytoskeleton remodeling should be studied in relation to other cellular structures relevant for the transmission of biophysical stimuli to the nucleus. Finally, the integration of experimental research with computational models of the actin cytoskeleton behaviour is a helpful tool to converge towards an in-depth understanding of actin-related biological processes. These lines of research are further illustrated below.

Studying actin cytoskeleton remodeling in 3D environments

The results obtained in this thesis come from investigations of the actin cytoskeleton on 2D substrates (chapter 2 and 3). 2D environments are often chosen as favourable experimental settings since controlling the biophysical cues is relatively easy and imaging of sub-cellular structures can be performed by standard confocal microscopy. Future development in the study of the actin cytoskeleton remodeling should aim at a deeper understanding in 3D, more *in vivo*-like, environments. These substrates are of special interest because they mimic more closely the physiological environment of tissue cells. There are preliminary data showing that, in 3D, analogues of actin cap-LINC complex interconnections exist. The presence of such nuclear-bound actin filaments in a more physiological context adds value to our results and those obtained in similar studies performed in 2D⁵². This also opens up the doors for the translation of findings obtained on 2D substrates to the 3D environment. Moreover, if absence of interconnection between the actin fibers and the nucleus would be found in laminopathy cells in 3D environments, a clearer explanation for the observed lack of cellular alignment and impaired response to strain would be provided⁵³. The major challenges in this kind of studies are related to the difficulty of imaging the actin cytoskeleton and quantifying the actin organization as well the changes in the actin structure.

Despite recent advances, imaging individual actin filaments have not been resolved in cells by optical means, including super-resolution methods^{54,55}, due to the small diameter and high packing density of actin filaments. To this end STED (Stimulated Emission Depletion) microscopy is suggested to provide a valuable tool as it provides fast and direct super-resolution.

Studying actin remodeling by live-cell imaging, using vital probes

To address issues on how cells integrate, transduce and respond to physical signals, it is crucial to develop live imaging techniques to analyse the responses of the structural components at the subcellular level with high spatial and temporal resolutions. Live imaging of actin cytoskeleton remodeling can provide crucial information about actin-related cellular processes and can overcome the fixation artifacts that can occur when working with fixed specimens⁵⁶. Actin-related cellular processes however can occur in fractions of a second, therefore the image acquisition speed need to be adapted to these time frames²⁸. The development and use of spinning disk confocal microscopy has allowed to simultaneously illuminating and collect light from across the entire sample in a highly time resolved manner. However this should be combined with good image quality, which is often a problem as scattered or emitted light by structures residing in regions removed from the focal plane can still reach the detector by travelling through adjacent pinholes and create artefacts⁵⁷. Moreover, for live actin cytoskeleton observations by fluorescent microscopy, appropriate fluorescent probes that do not interfere with the normal actin dynamic should be employed. The recent development of a new generation of far-red fluorescent probes for live-cell imaging based on a novel cell-permeable silicon rhodamine (SiR) dye has shown to represent a promising powerful approach. These probes are suitable for live super-resolution microscopy of actin cytoskeleton remodeling as they are permeable and biocompatible, bright and photostable, fluorogenic, and show little toxicity^{58,59}.

Studying the roles of structural and biochemical mechanotransduction pathways in actin cytoskeleton remodelling

The transduction of signals from the extracellular environment to the nucleus and the vice versa does not only occur via the structural mechanotransduction pathway⁶⁰, which has extensively been addressed in this thesis. Mechanotransduction occurs also via an intricate network of biochemical signals such as GTPase^{61,62}. While the model system used in this thesis is capable of dissecting topographical cues and cyclic strain stimulation, the concurrent biochemical cues were not blocked. Thus, it remains to be investigated to which extent the structural and mechanotransduction pathways cooperate in mixed pathways for the physiological functioning of the cell. It is also relevant to understand i) whether the two pathways result activated depending from the stimuli to which cells are exposed⁶³, ii) whether biochemical signalling could compensate the lack or the malformation of (part of) the structural mechanotransduction pathway and iii) to which extent the biophysical cues of the environment also invoke a biochemical signalling. From our results it seems that the signalling cascade invoked by topographical cues is independent from the formation of a complete structural mechanotransduction pathway. In another study, instead, it has been suggested that the nuclear translocation and downstream signalling of transcription factors pivotal for cardiac development (biochemical signalling), such as such MLK¹⁰, is dependent on the presence of a functional actin cytoskeleton, which is compromised in cells with of mutations in lamins. The complexity of this system can be illustrated by examining the function of focal adhesion kinase (FAK) that does not only phosphorylate other proteins but also makes a physical connection to the

sarcomeres upon phosphorylation. Investigations of these aspects of cellular mechanotransduction will not only advance our understanding of the relevance of the structural connections in the cellular mechanoreponse, but will also help to elucidate whether diseases/disorders of mechanotransduction arising from mutations of proteins mediating the structural pathway (such as LINC-associated proteins and lamins) primarily result from structural defects or impaired biochemical signalling.

Linking actin remodeling to other sub-cellular structures

The results of the studies of this thesis point out the relevance of the completeness of the nucleocytoskeletal connection for correct strain avoidance response to cyclic uniaxial strain (chapter 2 and 3). However the actin cytoskeleton is only one part of the structural mechanotransduction pathway connecting the cellular exterior with the inner part of the nucleus⁶⁴. Analyzing the response of the actin cytoskeleton to separate and combined biophysical cues concurrently with the study of the behaviour of other structures, can provide valuable insights in the mechanisms underlying cell response to biophysical cues⁶⁵. Therefore, a major integration for future experimental studies would be to take into consideration other sub-cellular components of the structural mechanotransduction pathway. For instance, it may be relevant to investigate the role of focal adhesions. These are the outer most components interacting with the surrounding cellular environment, thus the starting place for mechanotransductive events. At the same time, focal adhesions are critical for actin cytoskeleton anchorage. Knockout cells could represent a valuable tool for investigating the effects of the absence of sub-cellular structures. This research will help to integrate mechanics into our understanding of molecular basis of disease and eventually elucidate the onset of several diseases where defects in mechanotransduction are implicated⁶⁶.

Studying actin remodeling with the support of computational models

Computational modelling should be combined with experimental research to achieve an in-depth understanding of actin cytoskeleton remodeling. Actin cytoskeleton remodeling models will produce novel insights into sub-cellular mechanics, reduce the number of experiments, and provide a powerful predictive tool for tissue regenerative strategies. Our findings could be incorporate in computational models describing actin cytoskeleton response to topographical cues and cyclic strain. To our knowledge, such a model must still be implemented, while computational models describing actin cytoskeleton orientation response to separate topographical cues⁶⁷ and cyclic uniaxial straining are already available⁶⁸⁻⁷⁰.

Conclusion

The presented work describes our efforts to understand actin cytoskeleton remodeling induced by biophysical cues in healthy and diseased cells in 2D environments. Overall the results of this work demonstrate that dedicated model systems must be developed to unravel the influence of combined biophysical cues on the actin cytoskeleton behaviour. Moreover, accurate analysis of sub-cellular structures such as actin cap and basal actin fibers is of fundamental importance to understand overall cell response. Our results pointed out that competition between topographical cues and cyclic uniaxial strain for actin cytoskeleton orientation response arise from distinct orientation

responses of cap and basal actin fibers, respectively. Our findings also show that cells with an aberrant cytoskeletal conformation have inadequate orientation response to cyclic strain. This suggests that an intact actin cytoskeleton, thus an intact structural mechanotransduction pathway, is crucial in the control of normal cellular mechanoresponse. Lastly, we demonstrate that cells with reduced structural integrity, thus cells with impaired mechanotransduction can be protected from mechanical instability and loss of structural integrity by using soft substrates, i.e. by imposing low cytoskeletal tension.

This research opens up the way to rational designs of strategies for guiding and controlling cellular orientation such as the biomaterial-based regenerative approaches that need to mimic native cellular organization to achieve proper tissue functioning. In addition, valuable knowledge is gathered for understanding the onset of diseases of the mechanotransduction.

Key challenges for the future translation of our results to the clinical research are: a) investigating actin cytoskeleton behaviour by live-cell imaging in more *in vivo*-like 3D environments, b) understand the interplay between the structural mechanotransduction pathway and biochemical signalling in the transduction of biophysical signals c) link actin cytoskeleton response to relevant structures for the transmission of biophysical signals, such as focal adhesions and d) integrate the experimental knowledge with computational model of the actin cytoskeleton mechanoresponse.

References

1. Pollard,T.D., Blanchoin,L., & Mullins,R.D. Molecular mechanisms controlling actin filament dynamics in nonmuscle cells. *Annu. Rev. Biophys. Biomol. Struct.* **29**, 545-576 (2000).
2. Khatau,S.B. *et al.* A perinuclear actin cap regulates nuclear shape. *Proc. Natl. Acad. Sci. U. S. A* **106**, 19017-19022 (2009).
3. Kim,D.H., Cho,S., & Wirtz,D. Tight coupling between nucleus and cell migration through the perinuclear actin cap. *J. Cell Sci.* **127**, 2528-2541 (2014).
4. Versaevel,M., Grevesse,T., & Gabriele,S. Spatial coordination between cell and nuclear shape within micropatterned endothelial cells. *Nat. Commun.* **3**, 671 (2012).
5. Li,Q., Kumar,A., Makhija,E., & Shivashankar,G.V. The regulation of dynamic mechanical coupling between actin cytoskeleton and nucleus by matrix geometry. *Biomaterials* **35**, 961-969 (2014).
6. Zhu,J.H. *et al.* Cyclic stretch stimulates vascular smooth muscle cell alignment by redox-dependent activation of Notch3. *Am. J. Physiol Heart Circ. Physiol* **300**, H1770-H1780 (2011).
7. Chambliss,A.B. *et al.* The LINC-anchored actin cap connects the extracellular milieu to the nucleus for ultrafast mechanotransduction. *Sci. Rep.* **3**, 1087 (2013).
8. Nagayama,K., Yamazaki,S., Yahiro,Y., & Matsumoto,T. Estimation of the mechanical connection between apical stress fibers and the nucleus in vascular smooth muscle cells cultured on a substrate. *J. Biomech.* **47**, 1422-1429 (2014).
9. Natale,C.F., Ventre,M., & Netti,P.A. Tuning the material-cytoskeleton crosstalk via nanoconfinement of focal adhesions. *Biomaterials* **35**, 2743-2751 (2014).
10. Ho,C.Y., Jaalouk,D.E., Vartiainen,M.K., & Lammerding,J. Lamin A/C and emerin regulate MKL1-SRF activity by modulating actin dynamics. *Nature* **497**, 507-511 (2013).
11. Frey,M.T., Tsai,I.Y., Russell,T.P., Hanks,S.K., & Wang,Y.L. Cellular responses to substrate topography: role of myosin II and focal adhesion kinase. *Biophys. J.* **90**, 3774-3782 (2006).
12. Frey,M.T., Tsai,I.Y., Russell,T.P., Hanks,S.K., & Wang,Y.L. Cellular responses to substrate topography: role of myosin II and focal adhesion kinase. *Biophys. J.* **90**, 3774-3782 (2006).
13. Lenz-Bohme,B. *et al.* Insertional mutation of the *Drosophila* nuclear lamin Dm0 gene results in defective nuclear envelopes, clustering of nuclear pore complexes, and accumulation of annulate lamellae. *J. Cell Biol.* **137**, 1001-1016 (1997).
14. Fidzianska,A. *et al.* Obliteration of cardiomyocyte nuclear architecture in a patient with LMNA gene mutation. *J. Neurol. Sci.* **271**, 91-96 (2008).
15. Gupta,P. *et al.* Genetic and ultrastructural studies in dilated cardiomyopathy patients: a large deletion in the lamin A/C gene is associated with cardiomyocyte nuclear envelope disruption. *Basic Res. Cardiol.* **105**, 365-377 (2010).
16. Ostlund,C., Bonne,G., Schwartz,K., & Worman,H.J. Properties of lamin A mutants found in Emery-Dreifuss muscular dystrophy, cardiomyopathy and Dunnigan-type partial lipodystrophy. *J. Cell Sci.* **114**, 4435-4445 (2001).
17. Scharner,J., Lu,H.C., Fraternali,F., Ellis,J.A., & Zammit,P.S. Mapping disease-related missense mutations in the immunoglobulin-like fold domain of lamin A/C reveals novel genotype-phenotype associations for laminopathies. *Proteins* **82**, 904-915 (2014).
18. Kim,D.H., Chambliss,A.B., & Wirtz,D. The multi-faceted role of the actin cap in cellular mechanosensation and mechanotransduction. *Soft. Matter* **9**, 5516-5523 (2013).

19. Tamiello, C. *et al.* Soft substrates normalize nuclear morphology and prevent nuclear rupture in fibroblasts from a laminopathy patient with compound heterozygous LMNA mutations. *Nucleus*. **4**, 61-73 (2013).
20. Fedorchak, G.R., Kaminski, A., & Lammerding, J. Cellular mechanosensing: getting to the nucleus of it all. *Prog. Biophys. Mol. Biol.* **115**, 76-92 (2014).
21. Saez, A., Ghibaudo, M., Buguin, A., Silberzan, P., & Ladoux, B. Rigidity-driven growth and migration of epithelial cells on microstructured anisotropic substrates. *Proc. Natl. Acad. Sci. U. S. A* **104**, 8281-8286 (2007).
22. Teixeira, A.I., Abrams, G.A., Bertics, P.J., Murphy, C.J., & Nealey, P.F. Epithelial contact guidance on well-defined micro- and nanostructured substrates. *J. Cell Sci.* **116**, 1881-1892 (2003).
23. Teixeira, A.I., Nealey, P.F., & Murphy, C.J. Responses of human keratocytes to micro- and nanostructured substrates. *J. Biomed. Mater. Res. A* **71**, 369-376 (2004).
24. Dreier, B. *et al.* Early responses of vascular endothelial cells to topographic cues. *Am. J. Physiol Cell Physiol* **305**, C290-C298 (2013).
25. Tan, J.L. *et al.* Cells lying on a bed of microneedles: an approach to isolate mechanical force. *Proc. Natl. Acad. Sci. U. S. A* **100**, 1484-1489 (2003).
26. Shao, Y., Mann, J.M., Chen, W., & Fu, J. Global architecture of the F-actin cytoskeleton regulates cell shape-dependent endothelial mechanotransduction. *Integr. Biol. (Camb.)* **6**, 300-311 (2014).
27. van, H.H. *et al.* The nanoscale architecture of force-bearing focal adhesions. *Nano. Lett.* **14**, 4257-4262 (2014).
28. McKay, K.K. & Simpson, J.C. Actin in action: imaging approaches to study cytoskeleton structure and function. *Cells* **2**, 715-731 (2013).
29. Rino, J., Braga, J., Henriques, R., & Carmo-Fonseca, M. Frontiers in fluorescence microscopy. *Int. J. Dev. Biol.* **53**, 1569-1579 (2009).
30. Foolen, J., Deshpande, V.S., Kanters, F.M., & Baaijens, F.P. The influence of matrix integrity on stress-fiber remodeling in 3D. *Biomaterials* **33**, 7508-7518 (2012).
31. Ghibaudo, M. *et al.* Traction forces and rigidity sensing regulate cell functions. *Soft Matter* **4**, 1836-1843 (2008).
32. Fu, J. *et al.* Mechanical regulation of cell function with geometrically modulated elastomeric substrates. *Nat. Methods* **7**, 733-736 (2010).
33. Sochol, R.D., Higa, A.T., Janairo, R.R.R., Li, S., & Lin, L.W. Unidirectional mechanical cellular stimuli via micropost array gradients. *Soft Matter* **7**, 4606-4609 (2011).
34. Faust, U. *et al.* Cyclic stress at mHz frequencies aligns fibroblasts in direction of zero strain. *PLoS. One.* **6**, e28963 (2011).
35. Trappmann, B. *et al.* Extracellular-matrix tethering regulates stem-cell fate. *Nature Materials* **11**, 642-649 (2012).
36. Chaudhuri, O. & Mooney, D.J. Stem-Cell Differentiation Anchoring Cell-Fate Cues. *Nature Materials* **11**, 568-569 (2012).
37. Chaudhuri, O. *et al.* Extracellular matrix stiffness and composition jointly regulate the induction of malignant phenotypes in mammary epithelium. *Nature Materials* **13**, 970-978 (2014).
38. Wen, J.H. *et al.* Interplay of matrix stiffness and protein tethering in stem cell differentiation. *Nature Materials* **13**, 979-987 (2014).
39. Kumar, S. Cellular Mechanotransduction Stiffness Does Matter. *Nature Materials* **13**, 918-920 (2014).
40. Evans, N.D. & Gentleman, E. The role of material structure and mechanical properties in cell-matrix interactions. *Journal of Materials Chemistry B* **2**, 2345-2356 (2014).

41. Hinz,B. The myofibroblast: paradigm for a mechanically active cell. *J. Biomech.* **43**, 146-155 (2010).
42. Tomasek,J.J., Gabbiani,G., Hinz,B., Chaponnier,C., & Brown,R.A. Myofibroblasts and mechano-regulation of connective tissue remodelling. *Nat. Rev. Mol. Cell Biol.* **3**, 349-363 (2002).
43. Mol,A. *et al.* The relevance of large strains in functional tissue engineering of heart valves. *Thorac. Cardiovasc. Surg.* **51**, 78-83 (2003).
44. Schnell,A.M. *et al.* Optimal cell source for cardiovascular tissue engineering: venous vs. aortic human myofibroblasts. *Thorac. Cardiovasc. Surg.* **49**, 221-225 (2001).
45. Mol,A. *et al.* Autologous human tissue-engineered heart valves: prospects for systemic application. *Circulation* **114**, 1152-1158 (2006).
46. van Geemen,D. *et al.* Decreased mechanical properties of heart valve tissue constructs cultured in platelet lysate as compared to fetal bovine serum. *Tissue Eng Part C. Methods* **17**, 607-617 (2011).
47. Verstraeten,V.L. *et al.* Compound heterozygosity for mutations in LMNA causes a progeria syndrome without prelamin A accumulation. *Hum. Mol. Genet.* **15**, 2509-2522 (2006).
48. Argento,G. *et al.* Modeling the impact of scaffold architecture and mechanical loading on collagen turnover in engineered cardiovascular tissues. *Biomech. Model. Mechanobiol.*(2014).
49. Mol,A. *et al.* Tissue engineering of human heart valve leaflets: a novel bioreactor for a strain-based conditioning approach. *Ann. Biomed. Eng* **33**, 1778-1788 (2005).
50. Cattin,M.E., Muchir,A., & Bonne,G. 'State-of-the-heart' of cardiac laminopathies. *Curr. Opin. Cardiol.* **28**, 297-304 (2013).
51. Broers,J.L. *et al.* Decreased mechanical stiffness in LMNA-/- cells is caused by defective nucleo-cytoskeletal integrity: implications for the development of laminopathies. *Hum. Mol. Genet.* **13**, 2567-2580 (2004).
52. Khatau,S.B. *et al.* The distinct roles of the nucleus and nucleus-cytoskeleton connections in three-dimensional cell migration. *Sci. Rep.* **2**, 488 (2012).
53. Bertrand,A.T. *et al.* Cellular microenvironments reveal defective mechanosensing responses and elevated YAP signaling in LMNA-mutated muscle precursors. *J. Cell Sci.* **127**, 2873-2884 (2014).
54. Betzig,E. *et al.* Imaging intracellular fluorescent proteins at nanometer resolution. *Science* **313**, 1642-1645 (2006).
55. Gould,T.J. *et al.* Nanoscale imaging of molecular positions and anisotropies. *Nat. Methods* **5**, 1027-1030 (2008).
56. Schnell,U., Dijk,F., Sjollem,K.A., & Giepmans,B.N. Immunolabeling artifacts and the need for live-cell imaging. *Nat. Methods* **9**, 152-158 (2012).
57. Stehbens,S., Pemble,H., Murrow,L., & Wittmann,T. Imaging intracellular protein dynamics by spinning disk confocal microscopy. *Methods Enzymol.* **504**, 293-313 (2012).
58. Lukinavicius,G. *et al.* Fluorogenic probes for live-cell imaging of the cytoskeleton. *Nat. Methods* **11**, 731-733 (2014).
59. Lukinavicius,G. *et al.* A near-infrared fluorophore for live-cell super-resolution microscopy of cellular proteins. *Nat. Chem.* **5**, 132-139 (2013).
60. Wang,N., Tytell,J.D., & Ingber,D.E. Mechanotransduction at a distance: mechanically coupling the extracellular matrix with the nucleus. *Nat. Rev. Mol. Cell Biol.* **10**, 75-82 (2009).
61. Das,T. *et al.* A molecular mechanotransduction pathway regulates collective migration of epithelial cells. *Nature Cell Biology* **17**, 276-+ (2015).

62. Vogel,V. Mechanotransduction involving multimodular proteins: converting force into biochemical signals. *Annu. Rev. Biophys. Biomol. Struct.* **35**, 459-488 (2006).
63. Stachowiak,M.R. *et al.* A mechanical-biochemical feedback loop regulates remodeling in the actin cytoskeleton. *Proceedings of the National Academy of Sciences of the United States of America* **111**, 17528-17533 (2014).
64. Ingber,D.E. Cellular mechanotransduction: putting all the pieces together again. *FASEB J.* **20**, 811-827 (2006).
65. Dumbauld,D.W. *et al.* How vinculin regulates force transmission. *Proc. Natl. Acad. Sci. U. S. A* **110**, 9788-9793 (2013).
66. Ingber,D.E. Mechanobiology and diseases of mechanotransduction. *Ann. Med.* **35**, 564-577 (2003).
67. Vigliotti,A., McMeeking,R.M., & Deshpande,V.S. Simulation of the cytoskeletal response of cells on grooved or patterned substrates. *J. R. Soc. Interface* **12**, (2015).
68. Livne,A., Bouchbinder,E., & Geiger,B. Cell reorientation under cyclic stretching. *Nat. Commun.* **5**, 3938 (2014).
69. Obbink-Huizer,C. *et al.* Computational model predicts cell orientation in response to a range of mechanical stimuli. *Biomech. Model. Mechanobiol.* **13**, 227-236 (2014).
70. Hsu,H.J., Lee,C.F., & Kaunas,R. A dynamic stochastic model of frequency-dependent stress fiber alignment induced by cyclic stretch. *PLoS. One.* **4**, e4853 (2009).

Acknowledgments

There is no substitute for hard work, nor for the human help that one receives during the journey of a PhD. Without this help, the completion of my 4+ year travel would have been much more difficult. For this, I feel grateful to many people.

First of all, this long and intense educational adventure was made possible by Frank and Carlijn. Thank you for giving me the chance to pursue my PhD degree. Frank, at the beginning, the freedom that you gave me made me feel sometimes unstable. Now, I realize that this opportunity has shaped me into an independent, persistent and mature researcher. Carlijn, your encouragement has been the key of the success, especially in the difficult moments. I have learnt a lot from you both.

Jos, I was very lucky to meet you already during my Master's studies. Merging the engineering expertise with your knowledge as a cellular biologist has made the trip a bit more fascinating every day. Thank you for introducing me to the world of laminopathies and for teaching me microscopy. Miriam, your help with understanding the laminopathy cells has been crucial. Thank you for all the patience and effort in preparing the cells for the experiments and taking (endless) images with the confocal microscope. My trips to Maastricht were always enjoyable, because of the friendly atmosphere I could find at your department.

I would like to thank prof.dr. Gijsje Koenderink, prof.dr. Keita Ito, prof.dr. Vikram Deshpande, prof. dr. Peter Hilbers and dr. Cecilia Sahlgren for diving into my PhD thesis and taking part in the committee of my doctoral defence.

Being part of the NanoNextNL consortium has been an interesting aspect of this journey. I owe my thankfulness to NanoNextNL for creating a great environment for sharing science-related opinions and for the opportunity to enhance my knowledge and skills by attending interesting courses.

Donia and Lynn, you have been two hard-working and interested students. Your work gave inspiring inputs to the work reported in this thesis. I truly enjoyed coaching you. I wish you every success!

A big part of this journey was made of 'life in the lab'. It was pleasant to work in such a good environment, full of talents and positive people. That gave me the energy to continue when the experiments were failing. For this, I want to thank all the members of the Laboratory for Cell and Tissue Engineering and the colleagues of STBE. Moniek deserves a special mention for keeping everything under control, for giving structure and teaching everyone the importance of responsibility. For the microscopy measurements, I would like to acknowledge Mark van Turnhout. Thanks also to all colleagues of MATE that, in one way or another, made the time in between an experiment, a presentation and some statistical analysis more fun (without mentioning my skills at table football ...). Gitta and Tommaso, thanks for being my 'paranymphs'. Working with you, Gitta, is very easy because of your friendly attitude and your passion for science. Tommaso, the discussions we had were very fruitful. Your enthusiasm for the actin cytoskeleton (and life :-)) is contagious. Good luck, focal adhesion and actin crew!

Acknowledgments

I owe special thanks to all my friends in Eindhoven, in Italy and around the world. I treasure and value the strong and genuine bond I have with each of you. Thanks for all the support and the nice moments we spent together. In the daily life of the PhD, inside and outside work, Francesca and Agnese have been the two pillars that helped me remain stable and guided me in the moments of confusions. You know how much you mean to me.

During this adventure in the Netherlands, I have found the love of my life together with a fantastic family. Bedankt familie Nguyen voor jullie steun en interesse in mijn onderzoek. Ik voel me als een dochter bij jullie thuis!

Dear family, mamma, papà, Roberto, grazie a voi! Senza di voi non sarei di certo qui! Il vostro supporto e l'aver accettato scelte a volte difficili, sono per me il motore di tutto. Grazie, grazie, grazie!

Chiara

Curriculum Vitae

Chiara Tamiello was born on September 22, 1985 in Rovigo, Italy. After finishing her secondary education in 2004 at the Liceo Scientifico "P.Paleocapa" in Rovigo (Italy), she started studying Bioengineering at the Università degli Studi di Padova (Italy). She completed her BSc studies in 2007. In 2008 she was awarded a TU/e Talent Scholarship and she moved to the Netherlands to study her MSc in Biomedical Engineering at the Eindhoven University of Technology. She received her MSc degree in 2010 on the subject of mechanobiology of laminopathy cells. After that, she started her PhD project in the Soft Tissue Biomechanics and Engineering group at the Biomedical Engineering Department of the Eindhoven University of Technology. She worked on the biophysical regulation of actin cytoskeleton remodeling in adherent cells. During her PhD she collaborated with the Department of Molecular Cell Biology of Maastricht University. The results of her research are presented in this thesis.

List of publications

Tamiello,C., Kamps,M.A., van den Wijngaard,A., Verstraeten,V.L., Baaijens,F.P., Broers,J.L., & Bouten,C.V. Soft substrates normalize nuclear morphology and prevent nuclear rupture in fibroblasts from a laminopathy patient with compound heterozygous LMNA mutations. *Nucleus*. 4, 61-73 (2013).

Tamiello,C., Bouten,C.V., & Baaijens,F.P. Competition between cap and basal actin fiber orientation in cells subjected to contact guidance and cyclic strain. *Sci. Rep.* 5, 8752 (2015).

Tamiello,C., Kamps,M., Baaijens,F.P., Broers,J.L., & Bouten,C.V. Cellular strain avoidance is regulated by a functional actin cap. *Submitted*.

Tamiello,C., Buskermolen,A.B., Baaijens,F.P., Broers,J.L., & Bouten,C.V. Understanding cellular orientation responses to complex biophysical cues – the need for systematic, combinatorial approaches. *In preparation*.

